MULTIBAND ANTENNA STRUCTURES FOR HETEROGENEOUS WIRELESS SYSTEMS WITH IMPROVED PERFORMANCE

A THESIS

SUBMITTED IN FULFILLMENT OF THE REQUIREMENT
FOR THE AWARD OF DEGREE OF

DOCTOR OF PHILOSOPHY

IN

ELECTRONICS & COMMUNICATION ENGINEERING

BY

Davinder Parkash

Regn. No. 950806004

SUPERVISIOR

Dr. RAJESH KHANNA

PROFESSOR, DEPARTMENT OF ELECTRONICS & COMMUNICATION ENGINEERING, THAPAR UNIVERSITY, PATIALA

DEPARTMENT OF ELECTRONICS & COMMUNICATION ENGINEERING

THAPAR UNIVERSITY

PATIALA-147004 (INDIA)

2014

CERTIFICATE

I, **Davinder Parkash** hereby certify that the thesis entitled "**MULTIBAND ANTENNA STRUCTURES FOR HETEROGENEOUS WIRELESS SYSTEMS WITH IMPROVED PERFORMANCE**" which is being submitted by me to **Department of Electronics & Communication Engineering, Thapar University, Patiala** in fulfillment of the requirements for the award of degree of "Doctor of Philosophy" is a record of bonafide research work carried out under the guidance and supervision of **Prof. (Dr.) Rajesh Khanna**. The matter presented in this thesis does not incorporate without acknowledgment of any material previously published or written by any other person except where due reference is made in the text.

Davinder Parkash

Reg. No. - 950806004 **Dated-: 16/11/2014**

This is to certify that the above statement made by the candidate is correct and true to the best of my knowledge and belief.

18/12/17

Prof. (Dr.) Rajesh Khanna
Department of ECE,
Thapar University, Patiala.

Dated-: 16/11/2014

ABSTRACT

The field of wireless and mobile communication is growing at very fast rate covering many technical areas. With the recent progress and rapid increase in mobile terminals, the design of multiband antennas for small mobile terminals is acquiring great importance. Research on microstrip antenna systems has been a warm topic in current years due to the demands for compact and multiband antennas for next generation heterogeneous wireless communications systems. Wi-Fi/WLAN/WiMAX technologies are most rapidly growing area in the modern wireless communication. This provides greatly increased freedom and flexibility such that user can move around within a broad coverage area and still be connected to the network. There have been growing demands for broadband and multiband antenna with compact size. Devices having internal antennas have appeared to fulfill this need.

In this work, the multiband and compact size microstrip antenna has been proposed to cover operating bandwidth requirements of various wireless standards like Wi-Fi/WLAN/WiMAX and UWB. Analytical models provide a basic understanding of the operation of a patch antenna and they also provide approximate dimensions of a patch antenna for a targeted frequency without using numerical simulations. The objective of this thesis is to provide compact, efficient and multiband microstrip antenna designs for heterogeneous wireless communication devices. All these proposed designs contribute to the development of wireless devices for the fourth generation wireless communication systems. Theoretical analysis and simulation is performed by using IE3D simulator and a photolithography process is used for fabrication of the proposed antenna and prototype antenna is tested with help of vector network analyzer to validate the simulated results. The various antenna characteristics of all the proposed antennas like return loss, current distribution, gain, efficiency and radiation pattern has been analyzed and plotted. Finally, the results are also validated by using HFSS simulator.

In this thesis, the five multiband antennas are proposed for heterogeneous wireless communication systems. In first design, the rectangular shaped multiband antenna embedded with 'hash shaped slots' has been proposed for WLAN/WiMAX applications. The first design is modified by inserting I-shaped slot from the top of the patch to achieve three resonating modes with higher bandwidth. In third design, the design is composed of four vertical monopoles with CPW feed and defects in the ground plane have been proposed to achieve multi-band operation. In the fourth design, antenna based on rectangular shaped ring embedded with three inverted 'S'

and inverted 'C' shaped strips is used to generates the multiband operation. In the fifth design, rectangular shaped ring antenna based on microstrip feed embedded with three vertical strips has been presented. All the proposed antennas provide multiband and wide operating bandwidth with relatively low profile to achieve the thesis objectives and it is suitable for heterogeneous wireless communication systems.

ACKNOWLEDGEMENT

Working on the PhD thesis in the area of multiband microstrip antenna is one of the most valuable and exciting experiences in my education. The knowledge, I learned and the confidence I gained during the study years will be beneficial to the whole of my life. I am greatly indebted to my supervisor, **Prof.(Dr.) Rajesh Khanna**, who takes so much patience and effort in mentoring and helping me in every aspect to complete my thesis on time.

I would like to express my sincere thanks and gratitude towards my thesis supervisor, for continuous encourage, guidance and support through a beautiful year of academic coursework, writing and doing experiments of this thesis. He gave me direction in every step of this work while never forgetting trivial details. It is his insight and wide knowledge that guided me to the completion of this work. Due to his broad research interest, he gave me the opportunity to explore many interesting properties of the microstrip antennas.

I would like to express my sincere gratitude for the entire administration and management of Thapar University, Patiala for supporting me in achieving one of the most important goals of my life. I have great pleasure in expressing thanks to Director, Thapar University for his constant encouragement, timely advice and support throughout. I greatly acknowledge my doctoral research committee members Dr. Kulbir Singh, Associate Professor, ECED, and Dr. Hardeep Singh, Associate Professor, ECED, for closely monitoring and sharing their valuable inputs in completing this work. Their watchful way of analytically promoting and monitoring research activities helped me immensely in completing my assignment.

I express my gratitude to "**Dr. Sanjay Sharma**" Head of the Department, I am also grateful to the support I received from the laboratory assistants in the Electronics and communication department. Also I thank all the teaching and non-teaching staff for their nice cooperation to the students. I would like to thank all whose direct and indirect support helped me in completing my thesis report.

I would also like to thank Mr. Arun Kumar, Ex-colleague at HCTM for his immense helpful suggestions regarding my thesis. I would also like to thank Mr. Lalit Bansal and Mr. Dinesh Trivedi, Scientist-C at DEAL, Dehradoon for their valuable support in the experimental work. Finally, I wish to thank my colleague at HCTM and friends for their kindness, love, support, crucial assistance and fruitful suggestions they gave all the time. Special mention must be made of my parents whose encouragement enabled me to pursue my higher studies. Finally, I dedicate this thesis to my parents and my family especially to my lovely sons named Sanyam and Saksham.

Davinder Parkash

CONTENTS

LIST OF FIGURES

LIST OF TABLES

ACRONYMS AND ABBREVIATIONS

2D	Two Dimensional
3D	Three Dimensional
3G	Third Generation
4G	Fourth Generation
5G	Fifth Generation
ANN	Artificial Neural Network
AM	Amplitude Modulation
AMPS	Advanced Mobile Phone System
CAD	Computer Aided Design
CDMA	Code Division Multiple Access
CPW	Co-Planar Waveguide
DCS	Digital Cellular System
DTV	Digital Television
EBG	Electromagnetic Bandgap
EM	Electromagnetic
FEM	Finite Element Method
FM	Frequency Modulation
GPS	Global Positioning System
GSM	Global System for Mobile
HFSS	High-Frequency Structure Simulator
ICs	Integrated Circuits
IEEE	Institute of Electrical and Electronics Engineering
IMT-2000	International Mobile Telecommunication-2000
ISM	Industrial, Scientific and Medical bands
LAN	Local Area Network
LHCP	Left hand Circular Polarization
LTE	Long Term Evolution
MSA	Microstrip Antenna
PBG	Photonic Band Gap
PCB	Printed Circuit Board

PCS	Personal Communication System
PCN	Personal Communication Network
PIFA	Planar Inverted-F Antenna
PR	Photo Resist
PSO	Particle Swarm Optimization
RF	Radio Frequency
RHCP	Right hand Circular Polarization
RL	Return Loss
RSA	Rectangular Shaped Antenna
RSR	Rectangular Shaped Ring
UMTS	Universal Mobile Telecommunication System
UWB	Ultra-Wide Band
VNA	Vector Network Analyzer
VSWR	Voltage Standing Wave Ratio
WCDMA	Wideband Code Division Multiple Access
Wi-Fi	Wireless Fidelity
Wi-MAX	Worldwide Interoperability for Microwave Access
WLAN	Wireless Local Area Network

LIST OF PUBLICATIONS

International/National Journal

1. Davinder Parkash and Rajesh Khanna, "Design and Development of CPW-Fed Microstrip Antenna for WLAN/WiMAX Applications," International Journal of Progress in Electromagnetics Research C, vol. 17, pp. 17-27, 2010. (Available online)
2. Davinder Parkash and Rajesh Khanna, "A Compact Wideband CPW Fed Hash-Shape Slot Monopole Antenna for Wireless Communication Applications," Journal of Punjab Academy of Sciences, vol. 5 & 6, pp. 5-9, 2010.
3. Davinder Parkash and Rajesh Khanna, "Multiband Antenna Structure for Heterogeneous Wireless Communication Systems using DGS Technique" International Journal of Microwave and Wireless Technologies, vol. 6, Issue-5, pp. 521-526, oct.,2014, Doi: 10.1017/S1759078713001104.
4. Davinder Parkash and Rajesh Khanna, "Multiband Rectangular Shaped Ring Antenna Embedded with Inverted S- and C-Shaped Strips for WLAN/WiMAX/UWB applications," International journal of Microwave and Wireless Technologies, Vol. 7, Issue 1, pp. 81-86, Feb. 2015, Doi: 10.1017/S1759078714000440.
5. Davinder Parkash and Rajesh Khanna, "Triple Band Rectangular Shaped Monopole Antenna for WLAN/WiMAX/UWB Applications" Microwave and optical Technology Letters, volume 56, Issue 9, pp. 2113-2117, September 2014.

International IEEE Conferences

1. Davinder Parkash and Rajesh Khanna, "Design of a Dual Band Monopole Antenna for WLAN/WiMAX Applications," IEEE International Conference on WOCN2010, ISBN No.- 978-1-4244-7202-4 at Colombo, Sri Lanka from 6-8th Sept., 2010. [available online at IEEExplore]
2. Davinder Parkash and Rajesh Khanna, "Design of Planar Monopole Antenna Fed by Asymmetric Coplanar strip for WLAN Applications," IEEE Applied Electromagnetics Conference and Indian Antenna Week, ISBN No.-978-1-4577-1457-3, Calcutta University, Kolkata, Dec., 2011. [available online at IEEExplore]
3. Davinder Parkash and Rajesh Khanna, "Compact Design of Planar Microstrip Patch Antenna Fed by Asymmetric Coplanar strip for Wireless Communication Applications," IEEE International Conference on ICDECOM 2011, ISBN No.-978-1-4244-9190-2 at BIT, Mesra from 24-25th Feb., 2011. [available online at IEEExplore]

CHAPTER-1

INTRODUCTION

1.1 Introduction

Communication has a prime importance to human beings from the time of civilization. Firstly, communication was done through voice and fire. However, as the distance of communication increased; numerous devices were introduced, such as horns, drums, and so forth. With rapid development of microwave and wireless communication systems, much effort has been developed to enhance the performance of communication devices [1, 2]. An economical and a flexible way to transmit and receive information over short or long distances i.e. for communication have been provided by wireless technology. It has become a very common for today's society to exchange information every day by using hand-held pagers, landline phones, smart phones, laptops, various types of other wireless communication devices [2, 3]. Antenna is an integral component of any commonly used wireless communication device and is instrumental in harnessing the electromagnetic spectrum which is mankind's greatest natural resource.

Antenna history starts with Hertz when he proved Maxwell's theoretical prediction of electromagnetic waves by the classical experiments in 1880s. In 1895, the great Indian scientist Sir Jagadish Chandra Bose made a revolutionary attempt to demonstrate radio communication at microwave frequency. Guglielmo Marconi is called the father of the wireless communication, acquired the discoveries of Maxwell and Hertz. In 1897, he demonstrated and established radio communication link between the shore and ships traveling in the English Channel [2, 4]. With this achievement, the scientists and engineers all over the world in field of wireless communication were activated [4, 5].

In the last decade, the research in the field of hand-held device antennas has observed an extraordinary progress. In the early age of wireless communication, the main use of mobile phones was for speech communication which operate at a single frequency band of 900 MHz e.g. global system for mobile (GSM). An external terminal antenna; either a retractable rod, folded antenna was used with these phones. External antenna is replaced by compact internal antenna. Two more frequency bands viz. Digital Communication System (DCS) at 1800 MHz and Personal Communication System (PCS) at 1900 MHz were allocated for wireless communication systems to increase the capacity of systems, thus generating a requirement for dualband antennas in mid 90’s. The first mobile phone was launched in the market in late 1997 with dualband capability. In order to meet the requirements of global roaming, the triple band antennas at 900/1800/1900 MHz frequencies were proposed. A separate internal antenna was used for Bluetooth module in the mobile phones around the same time. The new mobile network called third generation (3G) or Universal Mobile Telecommunication System (UMTS) having a separate frequency band, started in early 2003. Thus, wireless systems are transformed from one system and one band to multiple systems and multiband in about 5 to 6 years time span [6, 7].

The increasing demand of mobile user to provide nonstop connection anytime, anywhere has led to our current efforts towards integrations of different wireless technologies. A network formed with integration of different wired and wireless technologies is known as heterogeneous network [8].In future heterogeneous wireless communication systems, the antenna will play an important role and it should be carefully designed to meet all requirements of broadband and multiband operation. In order to provide the various services like speech and video calling, video and audio streaming, gaming, data traffic has show the way to integrate the various wireless technologies [9]. There is a requirement of mobile devices to be equipped with multiband antenna and will be the key feature of the upcoming 4G and 5G wireless communication systems. Thus, the most important task is to propose a novel multiband antenna designs that can integrate the various frequency standards like Bluetooth, WLAN, Wi-Fi, WiMAX, and UWB in one antenna design to be used in the next generation wireless communication systems. The bandwidths requirements of major standards used in wireless applications are presented in the Table-1.1.

In the recent years, beside the multiband antennas for mobile handsets, there is the major requirement for a compact hand-held device. The size of antenna is a most important factor that limits the handset miniaturization. To meet these miniaturization requirements, internal antennas are employed in mobile phones to be fit in the mobile circuit board. The microstrip antenna has become one of the biggest components used in the portable devices. The performance of antenna is closely linked to the size of antenna and performance can be degrades with reduction in size of antenna. Miniaturization has direct impact on antenna performances like gain, efficiency and bandwidth. Antenna miniaturization is an important issue for the design of patch antennas for multiband applications [10]. In the recent years, innovative geometries based on the Planar Inverted-F Antenna (PIFA), Monopole Antenna, Fractal Antenna, Microstrip Antennas (MSA), Slot Antenna and planar antenna has been very popular for personal communication devices because these antennas have compact size and can be inserted into the handheld terminal.

Table 1.1: Bandwidth of Wireless Standards

Wireless Standards	Frequency Bands(MHz)	Bandwidth (MHz)
GSM 900	890-960	70 (7.6 %)
DCS-1800	1710-1880	170 (10.6 %)
PCS-1900	1850-1990	140 (7.3 %)
IMT-2000	1885-2200	315 (15.5 %)
UMTS	1920-2170	250 (13 %)
WLAN	2400-2484 5150-5350 5725-5825	84 (3.4 %) 700 (13.6 %)
Bluetooth	2400-2500	100 (4.1 %)
Wi-Fi	2400-2500	100 (4.1 %)
WiMAX	2500-2600 3400-3700 5250-5850	100 (4 %) 300 (8.25 %) 600 (16 %)
RFID	902-928	26 (2.88 %)

The demand of multiband antenna with compact size has been increased due to personal communication handsets. The possible solutions are metallic patches with multiple resonances [11]. The world has witnessed an amazing growth in modern wireless communication technology with the introduction of Wi-Fi, WLAN, WiMAX and UWB technology and multiband antennas fulfils the requirement of these standards. In present world wireless communication applications, the circularly polarized microstrip antennas provide more flexibility for the mobile phone and portable wireless devices from the device orientation or multipath effects [12]. Multiband internal antenna design with compact size for mobile applications is an active area of research.

1.2 Research Motivation

Communication industry is going through a developmental era. Today, Wireless technology is one of the main areas of research in the world of communication systems. Now a day's, our lifestyle has undergone a major transformation with the advent of wireless communication. The amazing expansion of cellular mobile communications in the late '80s and early '90s is a typical example of large scale market development. The significance of mobile phones has increased rapidly in last few years; it has become a necessity to a human life. Moreover, the rapid growth in mobile communication systems has led to a great demand for the development of internal antennas with the multiband and broadband operations. A variety of antennas have been designed and fabricated for these applications. In order to meet such challenging requirement, a comprehensive research is required for developing such antenna [13]. In a multi-channel system, signals more than one is handled by the system. In a multiple subject system, signals from more than one subject are transmitted and received [14]. The challenging task of the microwave scientists and engineers is to device compact printed radiating antennas having multi-band behavior, together with good efficiency.

Fast development in field of wireless communication and with increasing requirements for personal and mobile communications has stipulated the design of multiband antenna with compact size. The commercial requirements for compact, light weight, low cost and mass production solutions have dictated the increased use of monolithic technology [15]. Mobile convergence is a rising trend in the wireless applications. Future multi-functional smart phones are required to provide a variety of services like speech, video, data, multimedia and internet contents without sacrificing the performance [16, 17]. The demand of compact and multifunctional handsets design is a dynamic area of research.

The main aim of our thesis work is to design, simulate, fabricate and test, the various antennas for heterogeneous wireless communication systems. It focuses on the design of rectangular shaped geometries, suitable for multifunctional and multi-standard antennas.

1.3 Objectives of Thesis Work

The following research objectives have been proposed based on the identified gaps in the study of heterogeneous wireless communication systems:

1. To review and study the existing dualband, triple band and multiband antenna designs.

2. To design and simulate the triple-band antennas.
3. To design and simulate the multiband antennas.
4. Performance evaluation of the proposed antenna designs.

1.4 Basic Operation of an Antenna

Antenna is a device used to transmit and receive the electromagnetic waves [13]. A typical antenna structure is depicted in Fig. 1.1. It acts as a transducer which converts the electromagnetic wave propagating in free space into electrical energy [3]. Antennas are like electronic eyes and ears for wireless communication device that acts as interface between free space and circuitry. A brief review of various antenna parameters studied in this thesis is given in the next section.

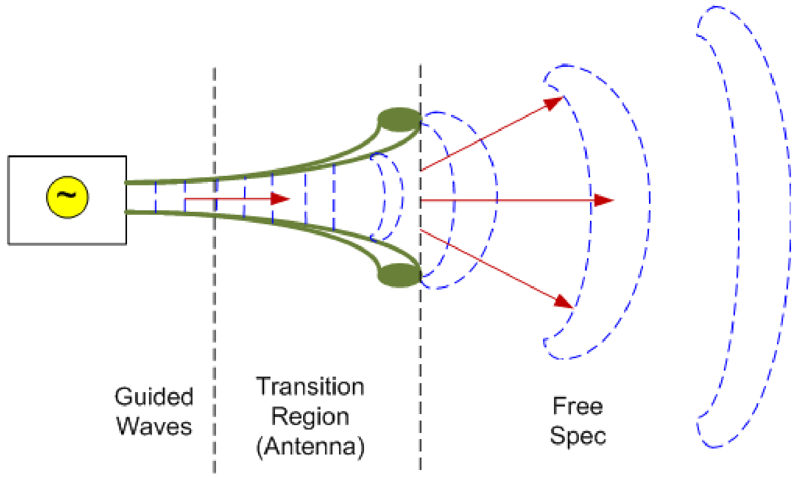

Fig. 1.1 Basic Operation of Antenna

1.4.1 Antenna Parameters

The performance of an antenna can be described by the various antenna parameters. An antenna is chosen for operation in a particular application according to its physical and electrical characteristics. A brief overview of antenna parameters considered for various proposed designs in this thesis work are given below.

1.4.1.1Return Loss

The return loss is the loss of signal power due to reflection caused at a discontinuity in a transmission line. The wave is reflected due to a mismatch in the terminating load with a device embedded in the line [18, 19]. When the load is mismatched the total power is not delivered and there is a loss of the power in the form of reflected power and that is measured in terms of return loss. It is usually expressed in decibels (dB).

1.4.1.2 Voltage Standing Wave Ratio

VSWR is defined as the ratio of the maximum voltage to the minimum voltage [21]. A standing wave is formed when power is reflected from a load. The maximum power is transferred between the transmitter and antenna when the load is matched and antenna operates efficiently. An ideal value of SWR is 1.0 when all the power reaching destination and no power is reflected back. The complete wave reflection represents the infinite value of SWR which means all the power is reflected back down the transmission line [20, 22].

1.4.1.3 Radiation Pattern

The radiation pattern is defined as: “A mathematical function or a graphical representation of the radiation properties of the antenna as a function of space coordinates. In most of the cases, the radiation pattern is determined in the far-field region and is represented as a function of the directional coordinates.” Antenna does not radiate energy uniformly in all the directions [21].

Radiation Pattern Lobes

The different components of the radiation pattern are called lobes. The different types of lobes are classified as major or main lobe, minor lobe and back lobe as shown in Fig 1.2. The direction of maximum radiation is referred to as main lobe and other lobes are called minor lobe [19, 23]. Back lobes are in opposite side of the main lobe. In most of the wireless systems, minor lobes are an undesired lobe that contains the wasted energy and it is should be minimized to reduce the loss of energy. Omni-directional radiation patterns are normally desirable in mobile and hand-held systems.

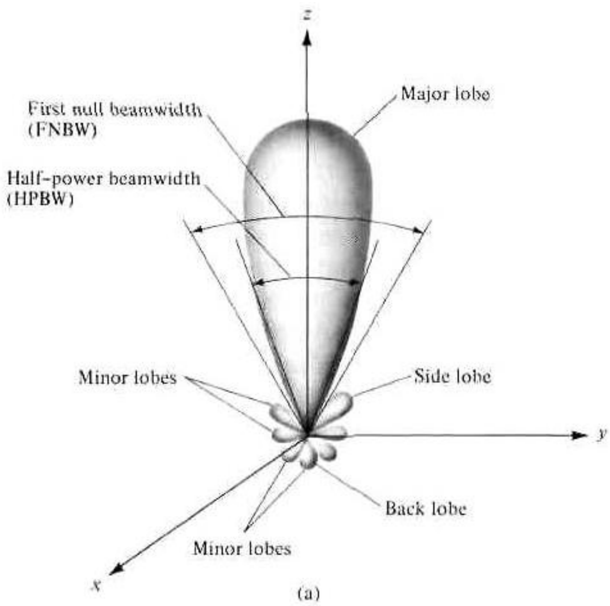

Fig. 1.2 Radiation Lobes of Antenna [19]

1.4.1.4 Bandwidth

Antenna bandwidth is defined as the range of working frequencies within which the performance of the antenna, with respect to some characteristic is matched to a specified standard [19, 21].

1.4.1.5 Gain

The ratio of maximum radiation intensity from test antenna to the maximum radiation intensity from reference antenna with the same input power is called gain. The gain is the ability of a patch antenna to focus the radiated power in a particular direction [19, 21]. Gain is a property by which, we can find out the figure of merit and this can be expressed in dBi.

1.4.1.6 Input Impedance

The input impedance of patch antenna is complex in nature. Both the real and imaginary parts of the impedance vary as a function of frequency. Ideally, both the resistance and reactance has similar curve about the resonant frequency [19, 20, and 21]. The antenna impedance can be categorized into three types: terminal impedance, characteristic impedance and wave impedance.

Due to rising demand of wireless and microwave communication systems, there is a need of more efficient antenna compatible with integrated circuits; with easy installation and fabrication. These are the most stringent requirements of an antenna for an antenna designer [19, 20]. Microstrip antennas (MSAs) received great attention in wireless communication systems due to their various characteristics like compact size and low volume and multiband operation. The basic concept of microstrip antenna is discussed in the next section:

1.5 Microstrip Antenna

In 1953, Deschamps has proposed a new concept of microstrip antenna (MSA) [24]. In the early 1970s, first practical implementation of microstrip patch antennas was done by Howell [25] and Munson [26]. The microstrip antenna consists of four major parts: the conductive patch, the dielectric substrate, ground plane, and the feedline as presented in Fig. 1.3. The same material is used for fabrication of the radiating element and ground plane. For determining the resonance frequency and characteristics of the antenna, the width, length and thickness of the patch play a major role. The material of the substrate and its thickness are also an important. The conducting element of the patch is generally made of copper or gold that can take any type of shape [19, 27].

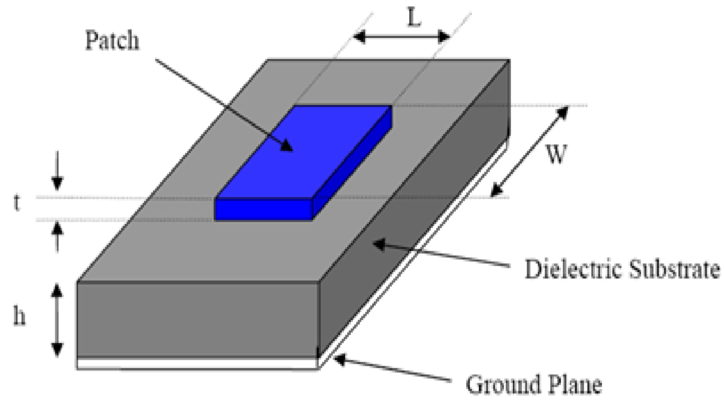

Fig. 1.3 Geometry of Microstrip Patch Antenna [19]

The different configurations of the metallic radiating element can be square, dipole, rectangular, circular, elliptical, triangular, circular ring, and ring sector etc. [19, 20]. Although, the radiating element can acquire any possible shape but the most desirable designs are rectangular and circular configurations. A microstrip antenna is characterized by different antenna parameters like bandwidth, resonant frequency, VSWR, return loss, and radiation pattern.

1.5.1 History of Microstrip Antenna

The concept of microstrip antennas was conceived by Deschamp's in 1953. In 1955, Gluton and Bassinot [28] patented a flat aerial that can be used in the UHF region. Lewin [29], studied the radiation from discontinuities in strip line. However, serious attention was given to this element only in the early 1970s. Howell, designed basic rectangular and circular micros trip patches in 1972. Munson, demonstrated a new classes of microstrip wrap around antenna suitable for missiles using microstrip radiator and microstrip feed networks on the same substrate in 1974. Weinschel [30], reported a practical pentagonal antenna in 1975.

Various types of mathematical models were developed for analysis of patch antenna. Mathematical modeling of microstrip antenna was first proposed by Munson and Derneryd [31] by applying transmission line analogy. This gives an approximate explanation of the radiation mechanism and provides the expressions for the radiation fields, radiation resistance, and input impedance. Agarwall and Bailey [32], suggested the wire grid model for the evaluation of microstrip antenna characteristics.

Newman et al. [33], proposed the method of moments for the analysis of microstrip antenna. They used Richmond reaction method in connection with the method of moments for the calculation of unknown surface currents flowing on the walls forming the microstrip patch, ground plane and magnetic walls. A more accurate mathematical cavity model for analysis of patch was suggested by Lo et. al. [34]. In this model, the upper patch and the section of the ground plane located below it are joined by a magnetic wall. The antenna parameters for different geometries with arbitrary feed points can be calculated by using this model.

Caver and Coffey [35], proposed the expansion model, which is similar to cavity model. The patch is considered as a thin cavity with leaky magnetic walls. Hammer et. al. [36], developed an aperture model for radiation field calculations of the microstrip antenna. This method accounts radiation from all the edges of the patch and gives the radiation fields and radiation resistance of any mode in the microstrip resonator antenna. Microstrip disc has been analyzed by Derneryd for calculating the radiation conductance, antenna efficiency and quality factor associated with circular disc antenna.

The circular microstrip antenna was rigorously treated by Butler [37]. He solved the problem of central fed circular microstrip antenna by treating patch as a radiating annular slot, in which the radius of the outer ring is very large. Mink [38], developed a circular microstrip antenna, which operates at a low frequency compared to a circular patch antenna of the same size. Shen [39], analyzed the elliptical microstrip patch and proved that the radiation pattern from this antenna is circularly polarized in a narrow band when eccentricity of the ellipse is small. R. Chadha and K.C. Gupta [40], developed Green’s function of circular sector and annular sector shaped antennas. Microstrip antenna covered with a dielectric later was proposed by Bahl et. al.. They suggested an appropriate correction for the calculation of resonant frequency of a microstrip antenna coated with protective dielectric layer.

1.5.2 Feeding Techniques

The various types of feeding techniques are used in the microstrip antenna. Microstrip antennas have radiating element on front side of a substrate and thus, it may be feed by different methods. These feeding techniques can be categorized as contacting and non-contacting. In contacting feeding technique, the radio frequency power is directly connected to the patch through microstrip line. The radio frequency power is transferred between the feedline and the radiating element by using electromagnetic coupling is called non-contacting feeding technique [19, 41, 42, and 44]. The most commonly used feeding techniques are:

- Microstrip line feed (contacting or direct schemes)
- Coaxial probe feed (contacting or direct schemes)
- Coplanar waveguide feed (contacting or direct schemes)
- Aperture coupled feed (non-contacting or indirect schemes)
- Proximity coupled feed (non-contacting or indirect schemes)

There are various factors responsible for selection of the feeding techniques. The most important factor is the impedance matching between the radiating element and feeding structure. A brief overview of various feeding techniques is given in next paragraph.

1.5.2.1 Microstrip Line Feed

In transmission line feeding technique, the edge of the microstrip patch is connected directly to a conducting strip as presented in Fig. 1.4. The width of feed strip is designed to match the impedance of the patch. The advantage of microstrip line feed arrangement is that it provide a planar structure [19, 41, 44]. The position of the inset can be properly controlled to match the impedance of the patch.

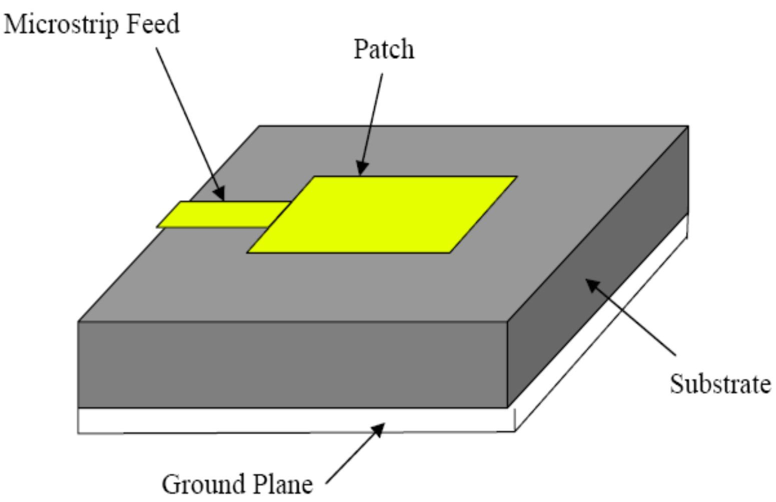

Fig. 1.4 Microstrip Line Feed [44]

1.5.2.2 Coaxial Feed

The Coaxial feed is also known as probe feed. The typical diagram of coaxial feed is depicted in Fig. 1.5. The interior part of conductor is soldered to the radiating patch after passing through the dielectric substrate but the outer part of conductor is soldered to the ground plane. The coaxial feed is more beneficial as it provides the freedom to place at any convenient position to match the impedance of the patch. The disadvantages of this feed technique are small bandwidth and difficult to model [19, 43]. The indirect or non-contacting feed techniques are used to solve these issues.

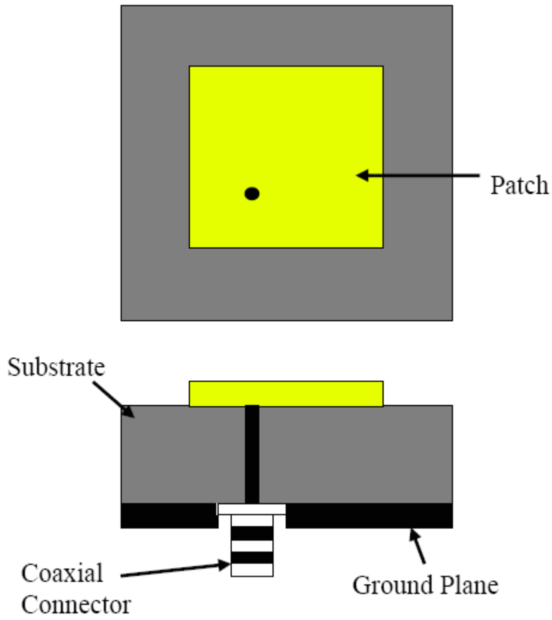

Fig. 1.5 Coaxial or Probe Feed [44]

1.5.2.3 Aperture Coupled Feed

The slot or aperture is used in the ground plane to couple the feedline with the patch in aperture coupled feed as depicted in Fig. 1.6. The ground plane separates the radiating patch and the feedline. The shape, size and location of the aperture or slot are responsible for the quantity of coupling between the microstrip line and the radiating element [19, 43, and 44]. The main disadvantage of aperture coupled feedline technique is that it is difficult to make a prototype of multi-layers structures.

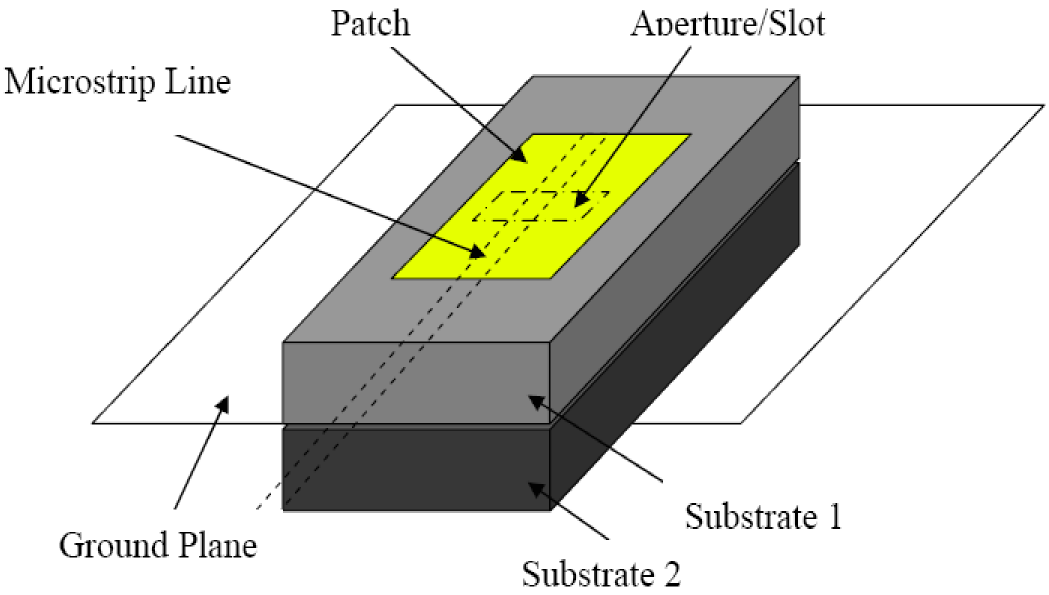

Fig. 1.6 Aperture Coupled Feed[44]

1.5.2.4 Proximity Coupled Feed

The electromagnetic coupling scheme uses two dielectric substrates in a way that the feed line is lies in between the two substrates and radiating patch is on the top of the upper substrate as depicted in Fig. 1.7. The major advantage of this feed technique is to provide wide bandwidth and it also eliminates spurious feed radiation [19, 45]. This feeding scheme is complicated to manufacture since it needs a proper alignment between the two dielectric layers.

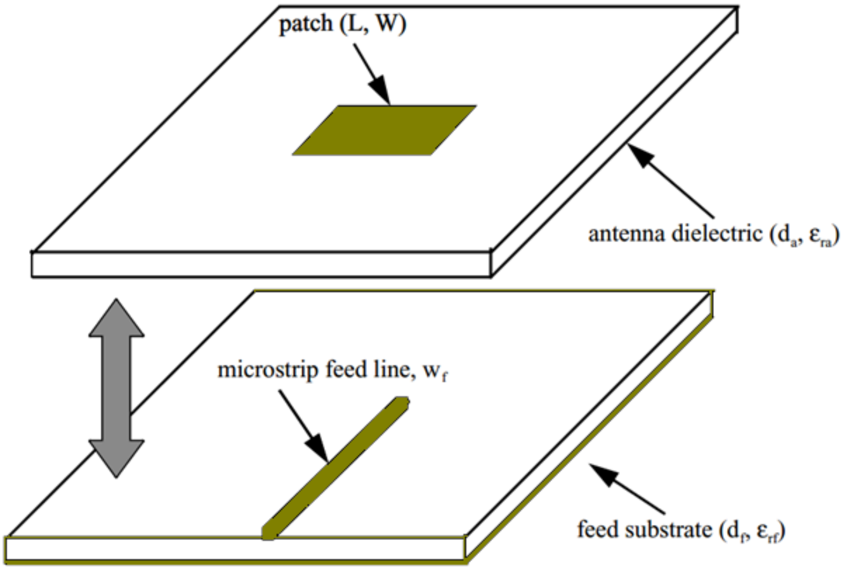

Fig. 1.7 Proximity Coupled Feed[44]

1.5.2.5 Coplanar Waveguide Feed

The conventional CPW feed consisting of a central signal strip conductor and two semi-infinite ground planes on both sides of the signal strip is presented by Wen in Fig. 1.8 [45]. The full-wave analysis and quasi-static approximation are used to study the CPW waveguide structure. This feeding technique has number of advantages such as broad bandwidth, lower radiation leakage, better impedance matching, light weight, and easy incorporation with microwave monolithic integrated circuits (MMICs) etc. [46].

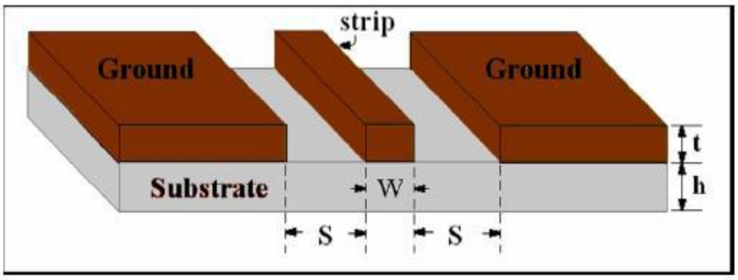

Fig. 1.8 Coplanar Waveguide Feed [45]

1.5.3 Methods of Analysis

The method of analysis is used to calculate the radiation characteristics of the patch like radiation pattern, gain, input impedance, bandwidth, and antenna efficiency. The analytical analysis of microstrip antennas becomes complex due to the presence of in-homogeneity of dielectric substrate and other configurations [19, 20 and 41].

The analysis of the microstrip antenna is done by dividing the patch into two regions viz: interior and exterior. The interior region is shaped by the radiating conductor, the parts of the ground plane under the patch, and the walls are formed by the projection of the patch periphery onto the ground plane. In the transmission line model, the fields in the interior region can be modeled as a transmission line section whereas in the cavity model, it is considered as cavity. The exterior region is the remainder of the dielectric, and the top of the patch conducting surface [19]. The fields in the exterior region contain the radiation fields, surface waves, and fringing fields. The three main analytical techniques are listed as follows:

- Transmission line model
- Cavity model
- Multiport network model (MNM)

The types of the numerical methods used for analyzing microstrip antennas are given below:

- Method of Moments (MOM)
- Finite-Element Method (FEM)
- Finite-Difference Time Domain (FDTD) Method

1.5.3.1 Transmission Line Model

It is a method based on integral equation. In this model, one important assumption has been made that the dielectric substrate and the ground plane are infinite in the extent. The rectangular patch antenna is modeled by two slots [47, 48]. This model is used for any generalized patch shapes but, initially developed for rectangular shaped patch. The microstrip radiator element provides no transverse field variation means the field varies only along the length and the open circuited end radiates the fringing fields.

Based on the field variation along their length, the four edges of the patch are categorized as radiating type or non-radiating type. The slow field variation along its length is referred to as radiating type edge. The non-radiating edge should have an integral multiple of half-wave variations along the edge [19, 47].

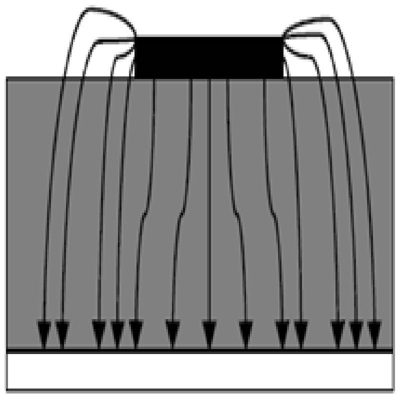

Fig. 1.9 Electric Field Lines [47]

The patch antenna has non-homogeneous structure made of two dielectrics viz substrate and air. The electric field lines mostly reside on the substrate and some parts of lines in air is depicted in Fig. 1.9. The effective dielectric constant is calculated in order to answer for the fringing field surrounding the boundary of the patch antenna and mathematical relation is given in next section on research methodology.

1.5.3.2 Cavity Model

Lo et. al. suggested the accurate mathematical cavity model for the analysis of microstrip antennas. It is based on modeling the patch and the ground plane beneath it as a cavity resonator and having these two layers treated as electric walls, while the four side substrate planes are considered as magnetic walls. The fringing fields around the periphery are taken into consideration by lengthening the patch boundary outward so that the effective dimensions are larger than the physical dimensions of the patch [49]. In the cavity model, various types of losses, such as dielectric loss, conductor loss and radiation loss, are taken into account by defining an effective loss tangent [19, 47].

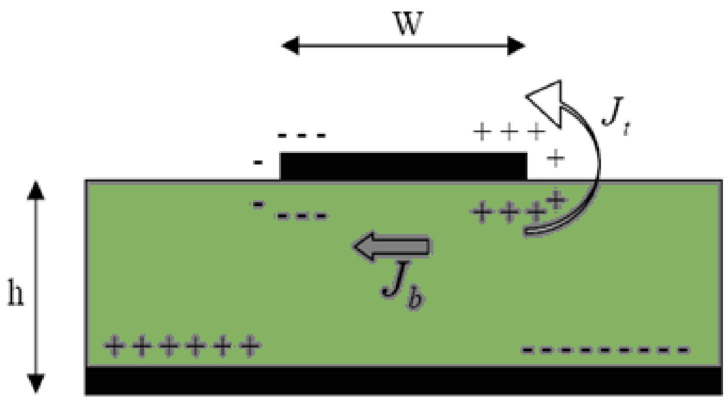

Fig. 1.10 Charge Distributions on the Microstrip Antenna [47]

When the power is supplied to the microstrip antenna, a charge distribution is observed on surfaces of the patch and the ground plane as represented in Fig. 1.10. There are two types of charge distribution mechanisms on the microstrip patch viz attractive mechanism and repulsive mechanism. The attractive and repulsive mechanisms of charge distribution will create various transverse magnetic (TM) field modes. The current flows at the surface of the patch due to movement of charge [19, 47].

1.5.3.3 Multiport Network Model

Multiport Network Model (MNM) used for analyzing the MSA is an expansion of the cavity model. In this method, the electromagnetic fields at bottom of the patch and exterior parts of the patch are modeled separately. Then segmentation method is used to calculate the overall impedance matrix [19, 50]. The fringing fields along the periphery and the radiated fields are incorporated by adding an equivalent edge admittance network. The radiated fields are obtained from the voltage distribution around the periphery.

1.5.3.4 Full-Wave Solutions

Full-wave electromagnetic model was used to solve the Maxwell's equations constrained by appropriate boundary conditions. The MOM model is based on the integral equations whereas the FEM and FDTD model are based on differential equations.

1.5.3.4.1 Method of Moment (MOM)

The Green's function is used in the MOM based model to account for the dielectric substrate. It is assumed that there is infinite extent of the substrate. The electric currents on the metal patch and feed network elements are solved by this model. The current expansion equation is substituted in the integral equations which include the Green's function. The testing of the integral equation with sub-domain testing functions is done by using set of linear equations. The numerical method is used to solve the resulting matrix. The MOM can be very computationally efficient [19, 27, 42]. The accuracy of the model is sensitive to the basis and testing functions. Zeland IE3D simulator is based on MOM method.

1.5.3.4.2 Finite-Element Method

Finite-Element Method (FEM) is a common method used for calculating partial differential equations in the frequency domain whereas the MOM solves the integral equations. This method is used to analyze the planar or volumetric structures, the region of interest can be broken into any number of finite surfaces or volume elements. The FEM is suitable for volumetric configurations. These discretized units are generally referred to as finite elements can be of any well-defined geometrical shapes such as triangular elements, tetrahedral and prismatic elements and therefore also suitable for curved geometry. It involves the integration of certain basis functions over the whole conducting patch, which is divided into a number of subsections [19, 27, 42].

1.5.3.4.3 Finite-Difference Time Domain Method

FDTD method is based on differential equations can be solved with leapfrog algorithm. In this method, the discretisation scheme is used and solution of the Maxwell's curls equations is directly obtained in the time domain. The discretisation scheme is orthogonal and the magnetic and the electric fields are specified every-where. The electric fields and the magnetic fields both are solved and the value of an E field point depends on its past value and the surrounding H fields. The same method is applied for the H fields. The spatial discretizations along three Cartesian coordinates are taken to be same. The volume is discretised in tetrahedra shape; the shape of the antenna can be more accurately represented in the FEM [19, 27, 42]. Hence, the FDTD method was favored over FEM.

1.6 Research Methodology

The search for knowledge is called research. To answer the questions or problems a process is used called research by collecting, analyzing and interpreting the information. The scientific and systematic search for significant information on a specific topic is called research [51]. The systematic observation classification and interpretation of data comes under the scientific research method. The systematic approach concerning generalization and the formulation of a theory is also called research. The research methodology is used to find out the hidden truth and to provide the new findings.

1.6.1 Flow Graph of Research Methodology

In this thesis work, step by step flow graph of the research methodology is presented in Fig. 1.11. First, we model an idea and calculate the parameters of the design problems by using standard equation available in the literature for microstrip antenna. The proposed design is simulated by using EM simulator like Zeland IE3D. If the simulated results obtained from simulator is matches with the requirements of the designer then the prototype of antenna design are fabricated by using photolithography technique otherwise it goes back to the previous stage. The prototype of the fabricated design is measured by using Agilent VNA. If the measured results do not satisfy the requirements of the designer then goes back to the simulation stage. The possible difference in both results is because of errors in dimensions of antenna parameters and impact of glue used during the fabrication process and also loss due to SMA connector. The proposed design is modified to remove these discrepancies. Then, the modified prototype is manufactured and the process continues until the desired antenna requirements are satisfied by the prototype.

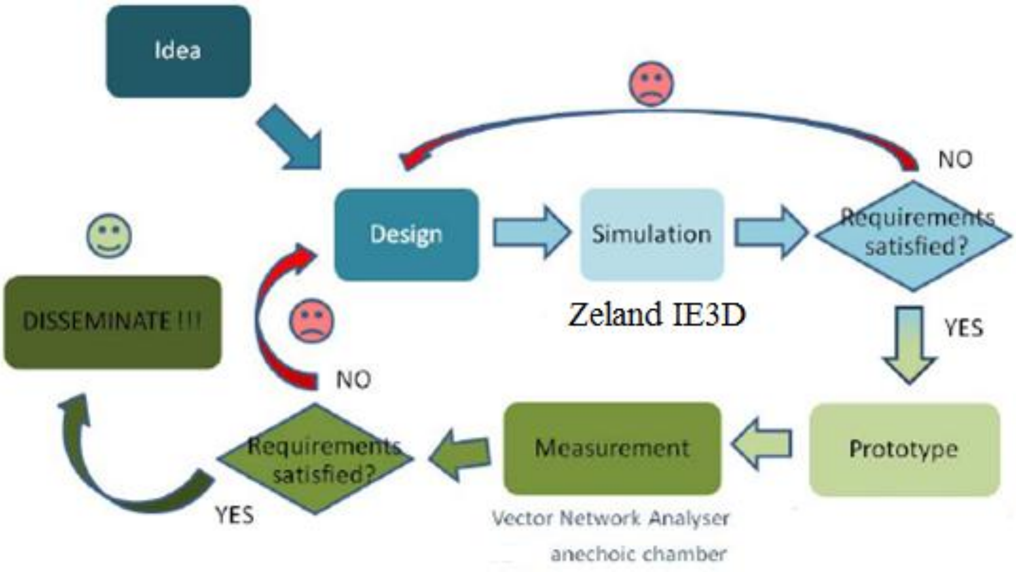

Fig. 1.11 Flow Diagram of the Research Methodology

1.6.2 Design Procedure

This subsection contains the calculation of various parameters required for designing the microstrip antennas at desired frequencies. Equations pertaining to rectangular antenna design are presented. The antenna size is designed based on the formulation of length, width of microstrip rectangular patch for a given dielectric constant and resonant frequency. The design procedure for calculation of various parameters of rectangular microstrip patch antenna is given below:

(a) Selection of Substrate

The selection of substrate plays a very important role in antenna design. Low loss substrates are very useful. The loss tangent of the substrate material used is slightly increased as frequency of operation increases. The strength and power handling capability of the antenna depends on the substrate materials. A variety of substrate materials are available in the market. The selection of dielectric material of the substrate depends on the application of the antenna and the radiation characteristics specifications [19, 27].

The relative dielectric constant and loss tangent of the substrate are major electrical properties to be considered for selection of material. To achieve the miniaturization of the patch, a higher dielectric constant is used but it also reduces the bandwidth of the antenna. The commonly used substrates are FR-2, FR-4, RT-Duroid, Silicon and BT resin. In this thesis work, the low cost FR4 substrate is selected because of easy availability in the market and small tangent loss [19]. Table 1.2 shows the specification of FR-4 substrate used in the fabrication of proposed antenna.

Table 1.2: FR4 Substrate Specification

Property	Value
Relative Dielectric Constant	4.4
Substrate Thickness (mm)	1.6
Loss Tangent	0.02
Dielectric Strength	20 MV/m

(b) Calculation of Width

The following equation is used to calculate the width of the patch antenna:

$$W = \frac{c}{2 f_0 \sqrt{\frac{(\varepsilon_r + 1)}{2}}} \tag{1.1}$$

where W is width of the patch,

f_o is the resonant frequency,

ε_r is the dielectric constant,

C is speed of light.

(c) Calculation of Effective Dielectric Constant

This equation is used to calculate the effective dielectric constant of the patch:

$$\varepsilon_{reff} = \frac{\varepsilon_r + 1}{2} + \frac{\varepsilon_r - 1}{2} \left[1 + 12 \frac{h}{W} \right]^{-\frac{1}{2}} \tag{1.2}$$

where h is thickness of the substrate.

(d) Calculation of the Effective Length

The following equation is used to calculate the length of the patch antenna

$$L_{eff} = \frac{c}{2 f_0 \sqrt{\varepsilon_{reff}}} \tag{1.3}$$

(e) Calculation of the Length Extension (ΔL)

To calculate the length extension of the patch antenna the following equation is used:

$$\Delta L = 0.412h \frac{\left(\varepsilon_{reff} + 0.3\right)\left(\frac{W}{h} + 0.264\right)}{\left(\varepsilon_{reff} - 0.258\right)\left(\frac{W}{h} + 0.8\right)} \tag{1.4}$$

(f) **Calculation of Actual Length of Patch**

The actual length of the patch is obtained by using equation given below:

$$L = L_{eff} - \Delta L \tag{1.5}$$

(g) **Calculation of the Ground Plane Diemensions**

The infinite ground plane is assumed in the transmission line model but for practical considerations a finite ground plane is used. However, the practical size of ground plane is approximately six times the substrate thickness plus the patch diemensions. The ground plane dimensions are calculated as given below:

$$Lg = 6h + L \tag{1.6}$$

$$Wg = 6h + W \tag{1.7}$$

where h = substrate thickness,

Lg =length of ground,

Wg =width of ground.

For the design of complex RF printed microwave circuit, antennas, high speed digital circuits and other electronic components, simulation tools are used based on electromagnetic simulation. A brief overview of various simulation tools used in this thesis are given below:

1.6.3 Zeland IE3D Simulator

Zeland IE3D simulator is an integrated full wave EM simulation tool based on Method of Moment (MOM). The layout editor is used for construction of geometry and then simulates the given geometry. With help of post processor, different parameters of antenna can be calculated and displayed. This simulator has inbuilt optimization package for the study and design of 3-dimensional microstrip designs, high frequency printed circuits etc. [52]. This tool has been accepted as an industrial standard for antenna structures.

1.6.4 Ansoft HFSS Simulator

HFSS simulator based on FEM is used to calculate the behavior of high-frequency components and antennas [53]. The parameters like S, Y, and Z can be analyzed with the help of this simulator. It can also be used to visualize 3D electromagnetic fields, and optimize design performance. Various types of port schemes are available in the simulator e.g. lumped port, wave port, incident etc. The wave port scheme is used for the simulation of CPW and microstrip line feed structure. This simulator uses the optimization algorithm to optimize the dimensions of the proposed antenna. The various types of boundary schemes are available in the simulator.

In the simulation process, first step is to define the geometry of the proposed structure by providing the material properties and defining the boundaries for 2D and 3D elements. For simulation a radiation boundary filled with air, surrounding the structure is defined [53]. Finally, the scattering parameters, current distributions and far field radiation pattern can be obtained by using this simulator. In this thesis work, HFSS simulator is used to validate the proposed design.

1.6.5 Fabrication Method

Photolithography process is used for fabrication of proposed antenna. A good accuracy can be achieved by using this method to create the patterns on the substrate. The steps used in the fabrication process are briefly described below:

- Fix the simulated microstrip antenna in Zeland IE3D main window. Press file icon and then go to Export option to generate the DXF format file.
- Auto-CAD software can be used to read the DXF file. This software is used to take the print out on a transparency paper or butter paper for making a negative mask of the geometry to be generated.
- After this, the printed transparency is placed on top of the substrate and the layout is aligned with the substrate. First, the substrate is cleaned with soap and then with acetone solution. Any dust or impurities on it can produce small discontinuity on the copper traces etched on the substrate.
- Dry the cleaned substrate in a microwave oven at 100 degrees for 10 minutes.
- In a dark room, uniformly apply negative photo resist solution on the dry substrate and spin controller is used to spread the photo resist throughout the surface area.
- Dry the substrate again in a microwave oven. The substrate should be exposed to UV radiation for 2-2.5 minutes.
- After exposing the substrate to the ultra-violet light, the substrate is soaked in developer solution.
- The pure water is used to clean the substrate to dispose of the developer solution and then the board is soaked in hot etching solution ($FeCl_3$). This solution is required to

generate the antenna pattern on the copper plate. After the photolithography, wet etching is done and the substrate is cleaned and dried.

- The 50 ohm SMA connector is used to connect the measuring instruments with the prototype of the fabricated antenna.

1.6.6 Measurement Setup

The microstrip antenna characteristics e.g. return loss, VSWR and radiation pattern are measured by using vector network analyzer (VNA) and anechoic chamber. The following section gives the description about measurement procedures:

1.6.6.1 Vector Network Analyzer

This is a popular instrument used to measure the return loss and VSWR parameters. The sophisticated VNA has time domain and frequency domain operation capability. The two port network parameter such as S_{11}, S_{12}, S_{21} and S_{22} can be measured very accurately by using VNA [54]. The VNA instrument based on signal processing algorithm is used to transmit and receive the data and the measured results are displayed and saved in many graph formats.

1.6.6.2 Measurement Procedure

The experimental procedures followed to determine the antenna characteristics are discussed. For experimental work, the coaxial cables and connectors are used to connect the VNA and cable losses are high at microwave frequency. To obtain accurate scattering parameter the instrument used in the experimental work should be calibrated with known standards of open, short and matched loads. The various method used for the calibration of VNA instrument are single port, full two ports and TRL method. The single port calibration method is used to characterize the different antenna parameters like return loss, VSWR and input impedance [54].

1.6.6.3 Measurement of Return Loss

The VNA is used in S_{11}/S_{22} mode to measure the S_{11} parameter of the antenna and any one of port of network analyzer is used to connect the proposed antenna. The calibration of the port is done by using the standard methods for the desired frequency range. The antenna under test (AUT) is connected to the port of calibrated instrument including port cable. The frequency for which the return loss value is minimum can be considered as resonant frequency of the antenna. The series of frequencies for which the value of return loss is within the 10dB points is usually treated as the bandwidth of the antenna.

1.6.6.4 Anechoic Chamber

The anechoic chamber provides a ‘quite zone', free from all types of electro-magnetic (EM) distortions. An anechoic chamber is used to avoid reflections from nearby objects for characterizations of antenna. The microwave absorbers are fixed on the walls, roof and the floor to avoid the EM reflection. At microwave frequencies, the absorbers fixed on the walls are highly lossy. The tapered absorber shapes are used to achieve good impedance matching at the microwave power [54]. The aluminum sheets are used in the chamber to cover all the walls and the roof to avoid the surrounding EM interferences.

1.6.6.5 2D Radiation Pattern Measurement

An anechoic chamber is used to conduct the measurement of radiation pattern. AUT is placed on a rotating table in the quite zone of the chamber and connected to first port of the network analyzer. The horn antenna is connected to the second port of the VNA which acts as a transmitter. The instrument required for measurement of radiation pattern is signal generator, transmitting antenna, a rotating motor and a spectrum analyzer. The manual procedure is used for measurement of radiation pattern.

The network analyzer is kept in S_{21}/S_{12} mode to compute the radiation pattern of the microstrip antenna. The numbers of frequency points are set according to the convenience. Now, the THRU calibration is performed for the specified frequency band and saved in the CAL set. One can manually perform the radiation pattern measurement by using this setup and then compare experimental results with the simulated results.

1.7 Organization of Thesis

The research proposed in the present thesis has addressed the several aspects in the domain of multiband antenna engineering. In this work, we study, analyze, design, fabricate and test the different structures of rectangular patch antennas to achieve triple band and multiband capability to cover Wi-Fi, WLAN, WiMAX and UWB standards. This thesis comprises of seven chapters and their brief description is given below:

Chapter 1: First chapter provides a brief introduction about multiband microstrip antenna and their applications, problems associated with multiband antenna and their potential solutions, motivation and objectives of the thesis. This chapter also describes the antenna parameters, concept and history of microstrip antenna. It also explains different feeding techniques and various methods for analyzing the microstrip antenna. It also gives a brief description about the research methodology used in this thesis.

Chapter 2: This chapter covers a comprehensive literature survey of the various research contributions reported in the area of multiband microstrip antenna using different techniques and methods. It presents the various geometry descriptions, simulation and fabrication of the multiband antenna structures with their application. The number of designs reported by various researchers related to the Wi-Fi, WLAN, WiMAX and UWB standards have been referred and summarized in this chapter. It also studies the gaps which are present in the works reported so far.

Chapter 3: Chapter 3 is the concerned with design and construction of the dualband or triple-band rectangular shaped microstrip antenna. A hash shaped slot is embedded in the rectangular shaped antenna to provide two resonant modes suitable for WLAN/WiMAX standards. The simulated results and their comparison with measured results show a good conformity. The effect of slot length parameters L_3, L_4 and L_5 of the proposed design in terms of return loss has been investigated. The proposed antenna structure has been modified by inserting I-shaped slot to improve the parameters of antenna. It provides triple resonant modes which is suitable for WLAN/WiMAX wireless communication systems.

Chapter 4: This chapter illustrates the design of a CPW fed multiband microstrip antenna based on defected ground structure (DGS) technique to provide the wide impedance bandwidth to cover all the bands of Wi-Fi/WLAN/ WiMAX applications. The radiating part of proposed antenna is composed of four vertical monopoles made up of a number of rectangular bricks of equal size. The few rectangular horizontal strips are used to join the vertical monopoles to improve the return loss. The parametric study was performed to understand the characteristics of monopole antenna. To validate the simulated design concept, a physical model of antenna is constructed and tested. The simulated and measured results show a satisfactory agreement.

Chapter 5: This chapter presents a research work related to microstrip-fed multiband antenna for WLAN, WiMAX and UWB applications. The rectangular shaped ring (RSR) antenna loaded with the inverted ‘S’ and ‘C’ shaped strips to generate five resonant modes to achieve multiband operation. The parametric study is conducted to understand the working of different parameters of the proposed design. The prototype of the fabricated antenna is also tested to validate the proposed concept. The simulated results and their comparison with measured results show a good conformity.

Chapter 6: This chapter elaborates a microstrip-fed rectangular shaped ring (RSR) antenna for WLAN, WiMAX and UWB standards. The rectangular shaped ring antenna loaded with three vertical strips to produce the triple band operation. It is designed and fabricated on substrate and then experimentally characterized to validate the design concept. The comparisons between simulated and measured results show a good agreement.

Chapter 7: Finally, this chapter presents the summary of conclusions drawn from research work reported in this thesis. The ideas for future work in the area of multiband antenna structures for heterogeneous wireless communication systems are also suggested.

In the next chapter, a brief review of the work, done by various researchers in the field of multiband antennas has been presented.

CHAPTER-2

LITERATURE SURVEY

2.1 Introduction

To start the design of multiband and broadband microstrip antenna, it is essential to have a bottomless knowledge of microstrip antenna and presented in the literature survey. In the recent years, there is a very fast progress in the area of wireless communications as the mobile entities are shrinking rapidly. To meet the never dying miniaturization requirement, compact antennas are needed to be designed. Planar printed antennas have the advantages like small size, low profile and multiband operation. For these reason, many antenna researchers are trying to design the planar antennas to satisfy the bandwidth requirements of current day mobile communication systems e.g. Wi-Fi systems at the 2.4 GHz and WLAN system at the 5.2 GHz /5.8 GHz bands, WiMAX standard at the 2.5/ 3.5/5.5 GHz bands and UWB standard at 3.1 GHz to 10.6 GHz band and have been published in the open literature. A brief review of various standards considered in this thesis is discussed in the next section.

2.2 IEEE Standard 802.11x for WLAN

IEEE 802.11x is the standard for wireless Local Area Network under Institutes of Electrical and Electronic Engineers. A wireless LAN is a local network without wires. Wireless LANs use electromagnetic waves (radio and infrared) as transmission media, for sending network traffic over the air and it is an alternate to wired technology such as twisted wires, coaxial cable or fiber optics. The carrier wave is used to modulate the data and voice traffic which is demodulated at the receiving end. The different frequencies are used for transmitting the multiple carriers in the same space [55].

IEEE 802.11 comprises a series of seven standards known as IEEE 802.11x. The development of WLAN standard was started in the late 1980s by the IEEE 802.11 working group and finally got launched in market in 1997 [56]. WLAN standard gives a high data rate of approximately 11 Mbps. The IEEE 802.11a standard was accepted in 1999 and operating at 5 GHz ISM band. WLAN standard provides high-speed data transfer rate which increase the popularity of the system and the requirement of multiband antenna. There are three various wireless standards like 802.11a, 802.11b and 802.11g. WLAN standard operates at three frequency bands viz. 2.4 GHz, 5.2 GHz and 5.8 GHz.

2.2.1 IEEE 802.11a

IEEE 802.11a standard has specifications for physical layer for Wi-Fi system and operates at 5 GHz band. The data transfer rate of this standard is upto five times faster than IEEE 802.11b for improving the quality of steaming media [57]. Although, solving interference problem and provides better security at 5 GHz. For the same coverage area 802.11a requires more access points than 802.11b to maintain the same quality [58].

2.2.2 IEEE 802.11b

In year 1999, IEEE 802.11b standard was accepted and which works at 2.4 GHz band. 802.11b standard provide a data rates of approximately 11 Mbps and range of approximately 100 meters [59]. However, Wi-Fi networks will remain vulnerable to other sources of radio frequency interference, such as a microwave oven operating in the same frequency or a nearby Wi-Fi network under the management of different company. Interference will become severe in the future as the density of the Wi-Fi network gets increased.

2.2.3 IEEE 802.11g

The 802.11g standard gives higher data rates upto 54 Mbps and is backward compatible with 802.11b. IEEE 802.11g is the latest wireless LAN standard ratified by the IEEE standard association's board on 12 June, 2003. This standard is three to five time faster than 802.11b version. IEEE 802.11g standard also comes with three advantages: lower power consumption, better penetration and longer range [60].

2.2.4 IEEE 802.11n

IEEE 802.11n-2009, commonly shortened to **802.11n**, is a wireless networking standard that uses numerous antennas to increase data rates upto 600 Mbit/s by using beam forming and diversity technique. The commonly used IEEE standards are 802.11a, 802.11b, 802.11g, 802.11n, and 802.11ac versions which provide wireless connectivity in homes and businesses. The initial development of 802.11n was begun in 2002. Its objective is to improve network throughput over the two previous standards: 802.11a and 802.11g. The frequency bands 2.4 GHz or 5GHz is used in this standard. The demand of IEEE 802.11n has been driven primarily by users connecting notebook computers to networks at work and to the Internet at home as well as at coffee, shops, airports, hotels etc.. 802.11n provides backward compatibility for devices using earlier versions of Wi-Fi standard like 802.11g, 802.11b, and 802.11a.

2.3 IEEE Standard 802.16 for WiMAX

Worldwide interoperability for microwave access (WiMAX) is a telecommunications technology and proposed in June 2001 by WiMAX forum. IEEE 802.16 standard can provide broadband services up to 5–15 km for mobile station and 50 km for fixed station [61, 62]. WiMAX is the future-generation wireless systems which provides high-speed internet access to the variety of devices like smart phones, handsets, notebook PCs, laptop and consumer electronics such as cameras, gaming devices, music players, and many more. WiMAX forum provides three licensed bands at 2.5 GHz, 3.5 GHz and 5.5 GHz. WiMAX revision provides higher data rates upto 40 Mbps. Mobile WiMAX devices typically requires omni-directional antenna [62].

2.4 IEEE standard 802.15.3 for Ultra-Wideband

Robert A. Scholtz et. al. have developed Ultra-Wideband radio technology which is also known as UWB IEEE standard 802.15.3 and was formerly known as "pulse radio". This standard may be used for short-range at a very low energy level, high-bandwidth communications greater than 500MHz. UWB gives a boost for wireless connecting device over short distances and is able to share the spectrum with other users. The main advantages provided by UWB band over Bluetooth are: high data speed approximately 100 times, cheaper and low power consumption device. The data rate supported by UWB device is 110 Mbps for a range of up to 10 meters. UWB is an extension of Bluetooth technology [63]. UWB technology is probably going to lead the home networking market.

Federal Communication Commission (FCC) spectrum for unlicensed UWB communications devices is from 3.1 GHz to 10.6 GHz which has limited the power spectral density (PSD) of the signal to –41.25 dBm/MHz. The FCC spectrum mask for UWB communications devices has been specified for indoor and outdoor UWB operation as shown in Fig. 2.1. To provide additional protection to GPS users, the FCC has also mandated that spurious emissions between 0.96 GHz and 1.61 GHz be limited to -75 dBm/MHz. The reduction of PSD of UWB signal reduces UWB interference on narrowband (NB) systems and keeps UWB signal under the FCC spectral mask.

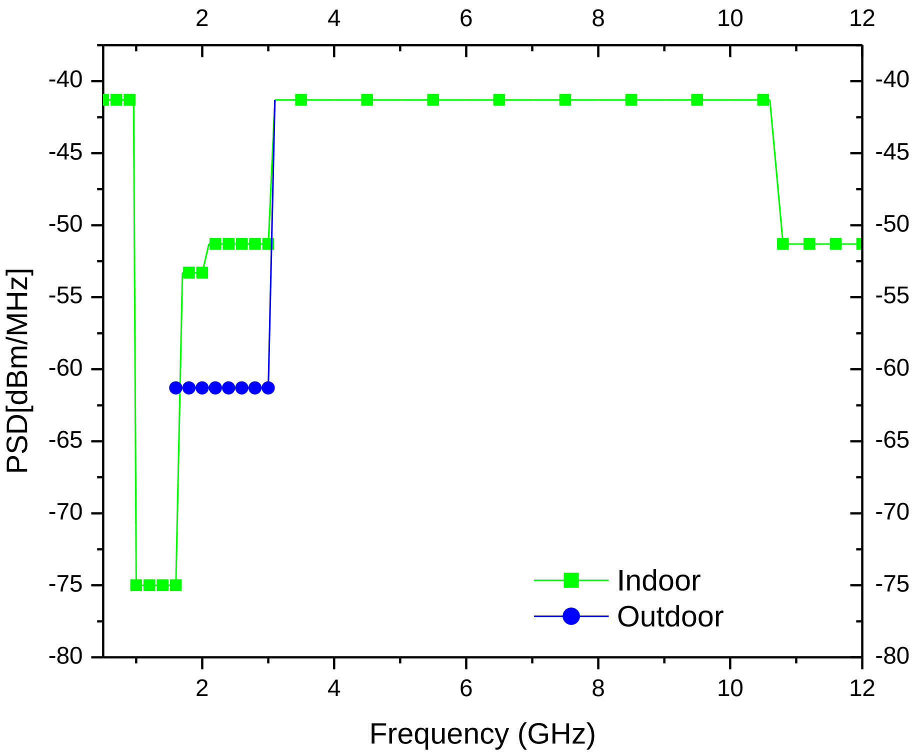

Fig. 2.1 FCC Power Spectrum Mask for UWB Applications

2.5 Bluetooth

Bluetooth is a wireless technology standard for exchanging data over short distances from fixed and mobile devices and building personal area networks (PANs). Invented by telecom vendor Ericsson in 1994. The IEEE standard for Bluetooth as IEEE 802.15.1, but no longer maintains the standard. Bluetooth operates at frequencies between 2400 and 2483.5 MHz. Bluetooth is a standard wire-replacement communications protocol primarily designed for low-power consumption, with a short range based on low-cost transceiver microchips in each device. Bluetooth and Wi-Fi have some similar applications: setting up networks, printing, or transferring files. Wi-Fi is intended as a replacement for high speed cabling for general local area network access in work areas. Bluetooth exists in many products, such as telephones, tablets, media players, robotics systems, handheld, laptops and console gaming equipment, and some high definition headsets, modems, and watches.

2.6 ZigBee

ZigBee is a low-cost, low-power; wireless mesh network standard targeted at wide development of long battery life devices in wireless control and monitoring applications. The technology defined by the ZigBee specification is intended to be simpler and less expensive than other wireless personal area network (WPANs), such as Bluetooth or Wi-Fi. ZigBee technology builds on IEEE standard 802.15.4 which defines the physical and MAC layers. Applications include wireless light switches, electrical meters with in-home-displays, traffic management systems remote control, sensor and other consumer and industrial equipment that require short-range low-rate wireless data transfer. Data rates vary from 20 kbit/s (868 MHz band) to 250 kbit/s (2.4 GHz band). The ZigBee network layer natively supports both star and tree networks, and generic mesh networking. For non-commercial purposes, the ZigBee specification is available free to the general public. The system is specified to operate in one of the three licenses free bands at 2.4 GHz, 915 MHz for North America and 868 MHz for Europe.

The various structure designs on dualband, triple band and multiband antennas are reported by various researchers on Wi-Fi/WLAN/WiMAX and UWB standards and summarized in the next section.

2.7 Literature Survey on Various Multiband Antenna Designs

There are several number of papers published on the design, analysis and optimization of the multiband antenna. The advent of multi-standard mobile devices is significant challenge for antenna designer, to implement multiband antennas with rapidly shrinking volume. The different multiband techniques developed by the antenna designer's across the world have been described in the next section:

2.7.1 Microstrip Antenna Designs for WLAN Applications

In [64], author presented an antenna is composed of a bent monopole, a shorting portion, ground plane and an assembly plate. This design is appropriate for lower frequency band of WLAN standard at 2.4 GHz. The simulated bandwidth of antenna is approximately 195 MHz and is also not capable to cover the upper frequency band of WLAN standard. In [65], researchers have proposed a horse-shoe shaped antenna embedded with multiple L-shaped slots to obtain a dualband operation for WLAN standard at 2.4/5 GHz bands. The measured result shows dualband operation ranges from 2.38 GHz to 2.51 GHz for lower operating band and 5.1 GHz to 5.88 GHz for upper operating band, respectively. It has a small gain of approximately 2 dBi. The author Meng-Ju Chiang et. al. present the circular shaped slot antenna loaded with arc shaped metallic strips in [66]. The multiple arc-shaped metallic strips are inserted into the circular patch to achieve the multiband and wideband operating range which is suitable for all the bands of WLAN standard and ISM applications. The size of this antenna is approximately 1.3 cm^3 which is quite larger than design proposed in this work.

An obtuse pie-shaped radiating antenna feed by a microstrip line is proposed in [67] for WLAN applications. The width of microstrip line feeding is 1.5 mm and its complementary metal structure is connected to the ground plane. The proposed design provides a dualband operation ranging from 2.24 GHz to 2.532 GHz and 4.62 GHz to 6.16 GHz which meets the bandwidth requirements of WLAN standard at 2.4/5.2/5.8 GHz. A compact folded slot antenna based on CPW-feed is examined for WLAN applications in [68]. The folded slot antenna is embedded with a pair of different shaped slots to produce the three resonant modes at 2.4 GHz, 3.6 GHz and 5.5 GHz. The two inverted L-shaped strips are used in the proposed antenna to generate third resonant mode. The complex geometry of the antenna is fabricated on the single sided copper clad.

The author W. Ren presented slot type structure loaded with a square ring slot and a circular ring slot in the ground plane. It is able to cover all the bands of WLAN standard. The L-shaped microstrip feedline is used in the patch by using electromagnetic coupled feeding technique. The simulated impedance bandwidths range from 2.3 GHz to 2.6 GHz which covers the lower frequency band of WLAN standard at 2.4 GHz and 5.15 GHz to 5.9 GHz which covers the upper frequency band of WLAN standard at 5.2/5.8 GHz. The size of proposed structure [69] is 1.6 cm^3 which is larger than design proposed in this work. The proposed monopole antenna composed of two split ring elements and the metallic strips which are used to connect the two rectangular shaped rings in [70]. It covers all the bands of WLAN standard at 2.4/5.2/5.8 GHz. In optimizing the design, the following parameters are important viz: substrate thickness, diemensions of ring, ground plane, microstrip feed and positions of the connecting strips. The G-shaped monopole antenna based on CPW feed has been proposed and optimized by using PSO technique to produce dualband operation in [71]. It is composed of two folded strips L_1 and L_2 and which is folded to form the antenna in 'G' shaped geometry. The measured result has impedance bandwidths ranging from 2.3 GHz to 2.536 GHz for lower operating band and 3.92 GHz to 6.62 GHz for upper operating band, respectively. The measured impedance bandwidths are capable to cover all the bands of WLAN standard at 2.4/5.2/5.8 GHz.

A novel monopole antenna consists of a meandered strip as a radiating element and a rectangular patch on the back side of the substrate has been presented in [72]. These elements are connected through via hole of radius 0.4 mm. The rectangular patch below the radiating element can resonate at the higher frequency band of WLAN standard at 5.2/5.8 GHz bands. The meandered strip width of 1 mm can resonate very close to a quarter wavelengths at 2.4

GHz of WLAN standard. The simulated antenna gain is small in the lower frequency band. A compact CPW fed planar antenna with modified feedline is investigated in [73] for WLAN communication systems. The modified feedline uses two short strips each with a diemensions of Ls and Ws and these strips are horizontally and symmetrically loaded from the left and right sides of the feeding line. The measured impedance bandwidth ranges from 2.23 GHz to 2.96 GHz and 4.6 GHz to 7.62 GHz. In upper frequency band, the two resonant modes are excited at close frequency to form a single wideband operation by merging the two frequency bands. The two L-shaped strips have impact on the return loss of an upper frequency band. The measured result shows that it is suitable for all the bands of WLAN standard.

A compact multiband microstrip line feed antenna is composed of four bent radiating arms with a partial ground and a linear structure as presented in [74] and is suitable for WLAN systems. The meandered radiating patch along with a partial ground plane is used to achieve the miniaturization of the proposed antenna. The partial ground plane is also helpful to achieve good return loss. The rectangular shaped slot is cut in the ground plane to reduce the size of the patch and also to enhance the current path in the ground plane. A compact CPW fed modified sierpinksi gasket antenna is proposed by Xiaodi Song for WLAN applications in [75]. The pentagon shaped antenna is cut in trapezium shape at the top of the monopole antenna with a view to create a hollow trapezium. The bottom of monopole antenna is loaded with triangular shaped slot at center. To achieve the miniaturization, we can reduce the height of the bottom triangle of the proposed design. The measured result provides three resonant bands. The complete size of the proposed antenna is 40 mm× 100 mm× 0.81 mm which is comparatively large in size.

A compact multiband microstrip antenna is presented for WLAN systems in [76]. A combination of both the C-shaped strip and the straight strip are used to achieve multiband operation. The two separate resonant paths of different dimensions have been chosen close to the quarter wavelengths at 2.4 GHz and 5 GHz. The proposed antenna has impendence bandwidth ranging from 2.38 GHz to 2.52 GHz for lower resonant band and 4.86 GHz to 6.87 GHz for upper resonant band, respectively. It can well satisfy all the bands of WLAN standard at 2.4/5.2/5.8 GHz. It has large size of approximately equal to 2.24 cm^3 which is quite large in size. A compact dualband antenna has been proposed in [77] to meet the requirements of WLAN application. This design is composed of spiral strip formed by two strips and an inverted L-strip. The simulated result shows that the spiral strip is responsible for generating two operating modes at 2.4 GHz and 5 GHz bands but cannot fully covers the

WLAN standard at 5 GHz band. It provides three resonant modes at 2.5 GHz, 4.66 GHz and 5.86 GHz frequencies. The measured peak gain is 1.3 dBi in the lower band.

The multiband design is constructed of two radiating rectangular shaped arms perpendicular to each other and these arms are short circuited by using shorting strips at the corners in [78]. These radiating arms are loaded with L-shaped slot to produce a dualband operation suitable for WLAN applications. The measured result has an impedance bandwidths ranging from 2.28 GHz to 2.569 GHz for lower band and 5.15 GHz to 5.622 GHz for upper band, respectively. It covers the WLAN standard at 2.4 GHz and 5.2 GHz bands but is not able to cover the WLAN standard at 5.8 GHz band. The location and shape of slot has an impact on the return loss of the proposed design. A compact tapered CPW fed triangular microstrip antenna is investigated in [79]. It has a wide impedance bandwidth ranging from 4.14 GHz to 9.84 GHz which covers the upper frequency bands of WLAN standard.

A CPW fed T-shaped slot loop type antenna is presented in [80] for WLAN standard at 2.45 GHz. It is composed of rectangular radiating element and T-shaped feeding strip. The slots are etched on the same side of the substrate in ground plane of the proposed design. The dumbbell shaped DGS is inserted into the ground plane to reject the harmonic radiation. The size of this antenna is 2.28 cm^3 and its quite large size as compared to this work. A novel dual band antenna based on microstrip line feed consisting of four half wavelength dipoles and two pairs of dipoles are placed back to back in [81]. Two dipoles are formed of two parts; one part is connected to the microstrip feedline and other part is connected to the ground plane vias hole. The good omni-directional radiation pattern is obtained by using small rectangular ground plane. It fulfills the bandwidth requirements for WLAN applications at all frequency bands. The measured impedance bandwidths are about 120 MHz from 2.38 to 2.50 GHz for lower band, 1750 MHz from 4.4 GHz to 6.15 GHz for upper band, respectively. The small gain is observed in the lower frequency band.

A CPW feed rectangular shaped monopole antenna is presented in [82]. The L-shaped strips are attached to the antenna to generate dualband operation. A triangular shaped geometry is placed on the top of the rectangular shaped structure to achieve a wideband operation. A compact multiband slot antenna consisting of a C-shaped slot and a vertical strip has been presented in [83]. The C shaped slot has impact on the lower resonant mode at 2.4 GHz band. The impedance bandwidth of upper frequency bands of WLAN standard has been improved by cutting slot of L-shaped strip around the vertical strip. It is clear from the simulated result that the lower resonant band ranges from 2.38 GHz to 2.52 GHz and upper resonant band ranges from 5.08 GHz to 6.7 GHz. Thus, covering all the bands of WLAN communication systems at 2.4/5.2/5.8 GHz.

In [84], author proposed a multiband antenna with three resonant patches to cover all the bands of WLAN application by inserting the two L-shaped slits. Two square shaped slits are cut in the second L-shaped slit to increase the average current path to cover the lower frequency band. The shorting wall is used to improve the impedance bandwidth. The width of the shorting wall has impact on the return loss. The dimensions of L-shaped slits and the shorting wall can be properly adjusted to achieve the desired bandwidth. A compact multiband monopole antenna has hook shaped strips on both sides of the horizontal strip, and a T-shaped strip is placed on the top of hook shaped strips to achieve the wideband operation in [85]. It is suitable for all the bands of WLAN systems. The symmetrical hook shaped strips are responsible for generating the lower resonant mode. The impedance bandwidths of the dual band antenna range from 2.1 GHz-2.52 GHz and 5.07 GHz-6.62 GHz for lower and upper frequency band, respectively. The peak antenna gain is 1.95 dBi in the lower resonant mode.

In [86], a CPW fed rectangular shaped antenna is loaded with a cross shaped slot which is capable of producing dual band operation suitable for WLAN standard. The current distribution shows that a longer current path is produced at the lower resonant mode and cross slot has small current distribution at upper frequency band. The simulated and measured results show a good agreement. The simulated result has impedance bandwidths of 13.7% at the lower frequency band and 28.3% at the upper frequency band, respectively. The volumetric size of the antenna is 2.92 cm^3 and it's quite large in size as compared to this work. A novel compact annular ring slot antenna has been presented in [87] for WLAN communication systems. The miniaturization of approximately 50% of the slot area is achieved by embedding a pair of symmetric Y-shaped like slots in the centre of circular patch. The ring shaped slot was etched in the rectangular shaped ground plane. The proposed slot antenna provides three resonant modes. The diemensions of Y shaped slots incorporated in the circular patch have impact on the first and second resonant mode but third resonant mode has neglible effect. The measured result shows a dualband operation ranging from 2.4 GHz to 2.5 GHz and 5 GHz to 6.6 GHz and suitable for covering all the bands of WLAN standard. The pair of slots is embedded in the center of the patch antenna to excite three resonant modes. In [88], author use skew-F shaped DGS in microstrip antenna to achieve dual band operation at microwave frequencies. A stacked microstrip patch antenna (SMPA) has been designed for broadband behavior.

A dualband annular-ring slot antenna is presented in [89] which are suitable for all the bands of WLAN standard at 2.4/5 GHz. The inner circular patch is connected to the ground plane by using a meandered strip. It provides three resonant modes with a meandered ground strip embedded in the ring slot. This meandered ground strip can generate one extra resonant mode as compared to generated by an annular ring antenna without meandered strip. The size of the proposed antenna is decreased by 53% as compared to the area of conventional microstrip line feed antenna. The wideband operation is obtained at the upper operating band by merging the second and third resonant modes by using a pair of notches properly etched in the inner circular patch. The objective of the design presented in [90] is to fabricate a polyester substrate based on metamaterials loaded with a rectangular microstrip antenna for WLAN applications. The square shaped patch is embedded with square ring resonators for better impedance matching. The small shift in the location of square SRR provides shift in the resonant frequency. The slots are inserted into the radiating element to reduce the bending effect of wearable antenna. The volumetric size of the antenna is approximately 2.88 cm^3.

It is clear from the literature survey that the antenna designs presented in [64, 65] cover only the lower frequency band at 2.4 GHz and are not able to cover the required bandwidth of upper frequency bands of WLAN standard. It is clear from the result that antenna proposed in [75], covers only the lower frequency band of WLAN standard and upper frequency bands are partially covered by the proposed design. In [76], an antenna was discussed that cover all the bands of WLAN standard but with poor return loss and small bandwidth in the lower frequency band. The designs proposed in [77, 80], covers only the lower frequency band of WLAN standard but it is not able to cover the upper frequency band of WLAN standard at 5.8 GHz. The entire antenna designs presented above by various authors cover only the WLAN standard but are not able to cover the wireless standards like WLAN/WiMAX.

2.7.2 Microstrip Antenna Designs for WiMAX Applications

A compact design of rectangular monopole antenna loaded with a meandered slit is presented in [91] to obtain a wideband operation suitable for WiMAX application. Two small I-shaped slots are inserted into the CPW feedline to suppress the band from 3.96 GHz to 4.9 GHz. It provides three operating bands ranging from 2.3 GHz to 2.99 GHz, 3.2 GHz to 4 GHz and 5.2 GHz to 6 GHz, which meets the bandwidth requirements of the WiMAX communication devices. The volumetric size of the proposed antenna is approximately 2.52 cm^3. The proposed rectangular shaped antenna incorporates two rectangular shaped slots to improve the impedance bandwidth by exciting the three resonant modes [92]. The shorter slot in the proposed antenna provides a resonant mode at 5 GHz band and the longer slot provides the two resonant modes at close frequencies gets merged together to provide a wider operating band in the lower frequency range. The proposed design is able to cover all the bands of WiMAX application at 2.5/3.5/5.5 GHz. A compact design of planar slot antenna embedded with C- shaped strip and inverted L-shaped slot has been presented in [93]for WiMAX communication systems. The C-shaped slot is embedded in the ground plane at a half wavelength resonant geometry to produce the operating modes at 2.5 GHz and 5.5 GHz frequencies. In order to obtain the wideband operation in lower frequency band, a horizontal slot is inserted into the ground plane which excites the second resonant mode at 2.7 GHz. The inverted L-shaped slot is inserted into the ground plane to generate the middle resonant mode at 3.5 GHz to provide wideband operation. The length and width of the T-shaped microstrip feeding has been adjusted to obtain the characteristic impedance which provides better impedance matching across the operating bands. It has been observed that three resonant bands are obtained to cover all the bands of WiMAX standard.

A compact CPW fed rhomb shaped patch has been proposed and investigated for WiMAX communication devices in [94]. A pair of inverted L-shaped slits is inserted into rhomb shaped radiating element to achieve a broadband operation. The notches and pair of slits are also inserted into the ground plane. The proposed antenna provides three operating bands ranging from 2.25 GHz - 2.9 GHz, 3.3 GHz - 3.9 GHz and 5.1 GHz - 6 GHz. A triple band CPW fed rectangular shaped antenna is presented in [95] which satisfy the bandwidth requirements of WiMAX operation. The proposed rectangular shaped antenna is loaded with a pair of narrow slit on both sides of the radiating patch to obtain the band reject frequency. In order to obtain the desired suppression of frequency, the dimensions of the slits are adjusted. The effect of coupling and interference between lower band and the middle band can be significantly reduced with the use of narrow slits in the patch. The author Nang Chang presented a compact CPW fed slot antenna suitable for WiMAX application at 2.5 GHz in [96]. The central conductor strip of the CPW is blended into a semi-circular shaped patch and two ground planes are extensively connected to form a closed loop. The width of the closed loop is tuned to achieve the desired frequency band.

The antenna design presented in [95] covers only the frequency band at 2.5/5.5 GHz but partially covered the required impedance bandwidth of 3.5 GHz band of WiMAX standard. The design presented in [96], covers only the lower frequency band of WiMAX standard and is not able to cover upper frequency bands at 3.5/5.5 GHz of WiMAX standard. All the antenna designs discussed above can cover only the WiMAX standard and is not able to cover heterogeneous wireless communication systems like WLAN/WiMAX applications.

2.7.3 Multiband Antenna Designs for Heterogeneous Wireless Systems for WLAN/WiMAX Applications

The increasing demand of mobile user to have uninterrupted connection anytime, anywhere has led to our current efforts towards integrations of different wireless technologies. A network formed with integration of different wired and wireless technologies is known as heterogeneous network. The fundamental idea of wireless communications is to provide a communication while the mobile user is moving through the different coverage area. To provide the access to wireless communication there should be integration and convergence of technologies is required to form a heterogeneous network. Fig. 2.2 depicts a heterogeneous wireless environment including Wi-Fi, WiMAX and WLAN technologies. A mobile user is moving in the train is initially connected to WLAN network at home. The user may choose between his home Wi-Fi network and the other network of his cellular operator. To start a voice call, the user selects a Wi-Fi access due to the lower service cost.

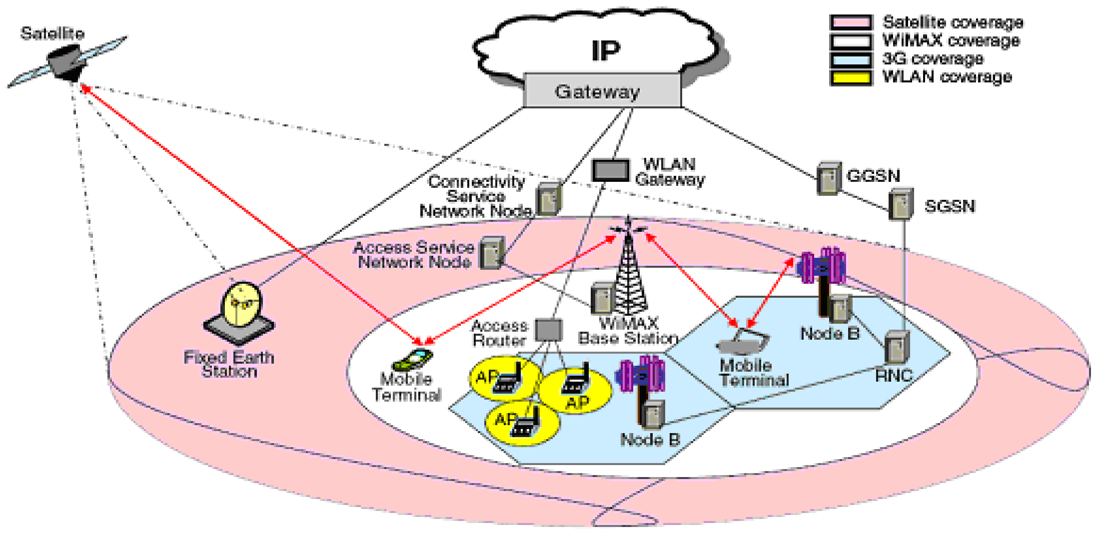

Fig. 2.2 Heterogeneous Wireless Network Scenario

In [97], the DGS is adopted in the design of ground plane of the microstrip antenna in order to achieve the multibanding, small size and high gain characteristics. A series of curved cylindrical antennas with DGS is used which is smaller in size and have wider radiation beam. The proposed antenna is suitable for WLAN systems in different radiation environments. Firstly, the planar microstrip antenna with DGS on the limited ground plane is studied. A compact wideband antenna based on CPW feed has been proposed in [98]. It comprises of a triangular shaped monopole and U-shaped monopole antenna to cover all the bands of WLAN/WiMAX applications. The U shaped element is responsible for producing the lower resonant mode at 2.5 GHz of WiMAX standard. The triangular shaped monopole is responsible for generating the resonant mode at 3.6 GHz of WiMAX standard. Due to the coupling effect of two monopoles, the two upper resonant modes are merged to generate wideband operation for upper frequency band which cover all the higher frequency bands of WLAN/WiMAX applications.

A triple-band slot antenna applied to WLAN/WiMAX applications is investigated in [99]. It consists of a microstrip feed line, a substrate, and a ground plane. The rectangular and trapezoid shaped slots are used to obtained dual broadband operation at high frequency. In [100], the proposed antenna is constructed of a rectangular shaped ring and two inverted L-shaped strips. These strips are attached to a rectangular shaped ring to provide the triple band operation. It is suitable to cover all the bands of WLAN/WiMAX applications. The proposed antenna has three impedance bands ranging from 2.39 GHz - 2.51 GHz, 3.26 GHz - 4.15 GHz and 5 GHz -6.43 GHz. It satisfies the bandwidth requirements of WLAN standard at 2.4/5.2/5.8 GHz and WiMAX standard at 3.5/5.5 GHz. The width and length of the two inverted L-shaped strips are varied in the proposed antenna to achieve better impedance matching. The proposed rectangular ring antenna is responsible for generating single wideband operation ranging from 3 GHz - 4.49 GHz. The rectangular shaped ring and upper inverted L-shaped strip produces the dualband operation from 2.39 GHz - 2.56 GHz and 3.37 GHz -5.19 GHz. The inverted L-shaped strip is inserted inside the rectangular shaped ring to achieve the triple band operation.

A compact microstrip line fed slot antenna is investigated in [101] for WLAN/WiMAX communication systems. The proposed antenna is composed of a circular shaped radiator embedded with trapezoid and ellipse shaped slots in the ground plane. Two similar inverted L-shaped strips and an elliptical arc shaped stub is incorporated in the proposed antenna to produce two separate resonant modes at 3.5 GHz and 5.5 GHz bands. The strong current distribution is mainly along trapezoid and ellipse shaped slots shows that it is responsible to generate the lower frequency band at 2.5GHz. The surface current is concentrated along the elliptical-arc shaped stub indicates that it is responsible for producing the middle frequency band at 3.5GHz. There are strong current distributions around a pair of inverted L-shaped strips which acts as a resonator for the upper frequency bands at 5.5 GHz.

A miniaturized multiband circular ring shaped antenna with a Y shaped arc strip has been proposed in [102] for WLAN/WiMAX applications. The circular ring and ground plane are responsible for generating single band from 2.71 GHz to 3.6 GHz. The circular shaped ring antenna is joined with a Y shaped arc strip, to excite the two resonant modes but the second operating band has a poor return loss. In the proposed design, an isosceles triangular defect is cut in the ground plane to achieve good return loss in the desired band. The return loss of the proposed antenna has three operating band ranging from 2.4 GHz – 2.7 GHz for lower band, 3.1 GHz – 4.15 GHz for middle band and 4.93 GHz - 5.89 GHz for upper band, respectively. The width of the arc shaped strip has a negligible effect on the performance of the proposed antenna. A microstrip line fed sectoral fractal antenna has been presented for Wi-Fi/WLAN/WiMAX communication systems in [103]. It has better results as compared to sierpinski fractal antenna and triangle shaped fractal antenna. It has been observed that by increasing the number of iteration upto second iteration, the resonant frequency is shifted towards the lower frequency band and the bandwidth also gets improved. The antenna covers numerous wireless bands like WiMAX at 3.5 GHz, Wi-Fi 802.11y at 3.6–3.7 GHz, and WLAN 802.11 at 5.2 and 5.8 GHz, respectively.

A novel CPW-fed triband planar monopole antenna has been presented in [104] for WLAN/WiMAX applications. The compact radiator is inserted with two inverted-L shaped slots to achieve three radiating elements with a view to produce three resonant modes for triband operation. The measured impedance bandwidth has three resonant bands ranging from 2.39 GHz – 2.51 GHz, 3.38 GHz - 3.72 GHz and 4.79 GHz - 6.24 GHz. A CPW fed modified triangular shaped multiband antenna is presented for wireless communication systems in [105]. The modified triangular shaped geometry is utilized as basic radiating patch. The ground plane is also modified to achieve the wideband operation. The trapezoidal shaped slot is cut from the triangular shaped radiating element. A cross shaped strip is inserted inside the trapezoidal shaped slot of the radiating patch. The two small horizontal strips are connected near the ground plane to improve the return loss. The triangular shaped slit is inserted in the triangular shaped patch to produce the resonant frequency at 5 GHz. A compact CPW fed slot antenna has been investigated in [106] for WLAN/WiMAX/WCDMA applications. It is composed of a T-shaped signal strip and U-shaped conducting strip placed on the top of a T-shaped signal strip. The gap between T-shaped strip and U-shaped strip is adjusted to obtain a better impedance matching. The measured result indicates that the proposed antenna covers the lower frequency band from 1.90 GHz to 2.75 GHz and upper frequency band from 3.65 GHz to 6.75 GHz, respectively.

A CPW fed modified Koch fractal printed slot antenna with dual wideband operation has been proposed in [107] and is well suitable for WLAN/WiMAX applications. For creating the fractal geometry, side of equilateral triangle is used to create slot in the basic geometry and repeated iterations are carried out to achieve the optimized design. The proposed antenna provides wideband performance ranging from 2.38 GHz–3.95 GHz for lower frequency band and 4.95 GHz – 6.05 GHz for upper frequency band, respectively. A rectangular shaped patch antenna with multiband and low profile characteristic has been proposed in [108]. These characteristics of the antenna are achieved by incorporating the seven slots in the patch. It has impedance bandwidth in the frequency range of 2-8 GHz which is appropriate for many applications such as WLAN, Mobile WiMAX, and WCDMA. The impact of the ground plane on the antenna performance is studied by mounting the proposed antenna structure either on a conventional perfect electrical conductor (PEC) ground plane or on a DGS ground plane.

A compact CPW fed rectangular patch embedded with two types of slots has been presented in [109] for achieving dualband operations. The prototype of the proposed antenna is fabricated on substrate and its measured results provide a 10 dB return loss for lower frequency band ranging from 2.49 to 5.5 GHz. It is able to cover the required bandwidth of all bands of WLAN standard and the C-band of satellite communication. A modified T-shaped monopole antenna based on microstrip line feed is incorporated in the metallic patch in [110]. The radiant patch is etched by three inverted U-shaped slots to achieve the multiband operations. The measurement results show that it provides four resonating bands ranging from 2.25–2.7 GHz, 3.25–3.6 GHz, 4.95–6.2 GHz, and 7-8 GHz. It covers all the bands of WLAN, Bluetooth, WiMAX and X-band of satellite communication systems.

In [111], the proposed dualband antenna has rectangular shaped radiating element printed on the front side of the substrate and a trapezoid conductor on the back side of substrate with a semi-ground plane. The rectangular shaped radiating element is electrically coupled to the trapezoidal conductor backed plane to improve the impedance bandwidth of the proposed antenna and it is responsible for generating the higher frequency bands. The proposed antenna has dual wideband operation to satisfy all the bands of WLAN/WiMAX applications. A CPW fed antenna is composed of Y shaped radiator loaded with a meandering split ring slot and a pair of equal sized inverted L shaped strips in [112] for WLAN/WiMAX applications. The Y shaped radiating element is embedded with a modified rectangular shaped slot; and the ground plane is extended to form slot type antenna. The measured impedance bandwidths of the proposed antenna are 430 MHz, 730 MHz and 310 MHz. It has been observed from the current distribution that current mainly flows around a pair of inverted L strips and responsible for generating an upper resonant mode at 5.8 GHz frequency. The meandered split ring slot provides a band notched frequency at 3 GHz.

A compact printed slot antenna incorporates with a slotted structure and an inverted L shaped slot to cover all the bands of WLAN/WiMAX communication systems in [113]. The slot length used in the ground plane has an impact on its impedance bandwidth. It has four resonant modes at 2.62 GHz, 3.97 GHz, and 5.42 GHz and 5.8 GHz frequencies. A new design based on CPW feed printed antenna has been proposed in [114] and linear tapering is used for matching the impedance bandwidth. The angle of tapering has impact on the impedance bandwidth. The measured impedance bandwidth of the prototype antenna is 3.31 GHz ranging from 4.27–7.58 GHz which covers all the bands of WLAN/WiMAX applications.

The geometry of the proposed antenna is a combination of rectangular shaped ring and a rectangular monopole as presented in [115]. It is suitable for wireless communication systems. The rectangular shaped ring is responsible for generating the lower frequency band at 2.9 GHz whereas the rectangular patch is used to produce the higher frequency band at 4.4 GHz. It has been observed that the dimensions of the ground plane have effect on the resonant frequencies. The proposed antenna can produce two wide resonant bands at 3 GHz and 6 GHz. It covers all the bands of WLAN standard at 2.4/5.2/5.8 GHz and all the bands of WiMAX standard at 2.5/3.5/5.5GHz. A compact monopole antenna comprises of horizontal H-shaped patch, an inverted L-shaped stub and a deformed T-shaped strip has been presented in [116]. The horizontal H-shaped patch is constructed to produce the higher frequency band. The second configuration has horizontal H-shaped strip and inserted L-shaped strip which provides the dualband operation. The triple band operation can be achieved by adding z-shaped slot in the L and H-shaped patches. The simulated operating bands of the proposed antenna range from 2.4 GHz - 2.7 GHz, 3.4 GHz - 3.72 GHz and 5.1 GHz -5.85 GHz.

A CPW fed planar monopole antenna consisting of pentagonal shaped radiating element loaded with a pair of inverted U-shaped thin slots to produce triple band operation for WLAN/WiMAX communication systems in [117]. The thin bent slots are etched on the radiating element in order to achieve the dual band reject frequencies at 3 GHz and 4.5 GHz. The operating bands of the proposed antenna range from 2.14 GHz – 2.85 GHz, 3.29 GHz – 4.1 GHz and 5.1 GHz – 6.09 GHz. A novel CPW fed planar antenna has been proposed and investigated in [118]. It is composed of a pair of rectangular shaped rings embedded with an inverted T-shaped strip. The proposed antenna produces three resonant bands of the desired frequency bands of wireless communication systems. The outer large rectangular ring is responsible for generating the lower frequency band at 2.4 GHz whereas the small rectangular ring provides a resonant frequency mode at higher frequency band at 3.5/5 GHz. The inverted T-shaped strip is used inside the small rectangular ring to divide an upper frequency band into two bands. The proposed antenna covers all the frequency bands of both WLAN and WiMAX standards. The simulated result has impedance bandwidth ranging from 2.38 GHz to 2.82 GHz, 3.32 GHz to 3.88 GHz and 5.13 GHz to 6.53 GHz.

A compact printed antenna composed of an 'ear' type geometry which is formed by three circular arc shaped strips to generate triple band operation has been presented in [119]. It is suitable for all bands of WLAN/WiMAX standards. The location and sizes of these arc-shaped strips have impact on the resonant modes of the proposed antenna. The width of the arc-shaped strips has influence on the impedance bandwidth. The proposed antenna provides three separate impedance bandwidths of 400 MHz for lower frequency band, 480 MHz for middle frequency band and 1000 MHz for upper frequency band, respectively. A miniaturized CPW fed printed antenna composed of a T-shaped radiating patch with a pair of parasitic strips and trapeziform ground plane is investigated in [120]. The impedance bandwidth of the proposed antenna has been improved by using trapeziform ground plane as compared to the conventional rectangular ground plane. The proposed antenna has triple band operation to cover all the bands of WLAN/WiMAX applications. In order to achieve the wideband operation, the pairs of parasitic strips are attached to both sides of T shaped monopole in the bend form.

A compact CPW-fed triple band printed antenna is proposed for WLAN/WiMAX communication systems in [121]. The proposed antenna has a meandered rectangular ring embedded with inverted T-shaped strip and T-shaped strip. The meandered ring is responsible for generating a lower resonant mode at 2.4 GHz frequency. The inverted T-shaped strip is loaded in meandered ring to excite a higher resonant mode at 5.5 GHz. The rectangular ring is embedded with T-shaped strip to generate a resonant mode at 3.5 GHz.

The measured impedance bandwidth ranges from 2.36 GHz - 2.58 GHz for the lower band, from 3.36 GHz - 3.83 GHz for middle band and from 4.83 GHz - 629 GHz for upper band, respectively.

The proposed antenna design presented in [104] covers some of the frequency bands of WLAN/WiMAX standards but it is not able to cover the required impedance bandwidth of 2.5 GHz frequency band of WiMAX standard. The design discussed in [105], covers only the lower frequency band of WiMAX standard at 3.5 GHz and all the bands of WLAN standard and it is not able to cover frequency bands of WiMAX standard at 2.5 GHz/5.5 GHz. Similarly in [113], the proposed design covers all the lower frequency bands of WLAN/WiMAX standards and it is not able to cover the upper frequency bands of WLAN/WiMAX standards. In all the antenna design discussed above some bands of the WiMAX and WLAN standard are covered but not able to cover all the bands of Wi-Fi/WLAN/WiMAX standard.

2.7.4 Multiband Antenna Designs for Heterogeneous Wireless Systems for WLAN, WiMAX and UWB applications

A compact CPW-fed rectangular microstrip slot antenna with diamond shaped radiator is presented for UWB applications in [122]. The diamond shaped patch is connected to a feedline which excites a resonant mode. The width and length of the rectangular slot has impact on the impedance bandwidth. The distance between the diamond patch and CPW feed line also affects the impedance bandwidth. A compact microstrip fed printed elliptical shaped monopole structure with a modified ground plane has been presented and investigated in [123] for UWB application. The two narrow slits are embedded in the lower edge of the radiating element to lower the resonant frequency. It has been observed from result that it has three resonant frequencies at 3 GHz, 6 GHz, and 9 GHz.

A compact CPW fed monopole antenna is examined for UWB application in [124]. The two inverted L-shaped strip radiators are attached to rectangular patch and ground plane has been extended vertically to the both sides of the radiator. The proposed compact multi-band antenna consisting of two combined radiating elements: a half disc and a rectangular patch element in [125]. It provides resonant modes at different frequency bands, namely, 3.9 GHz, 4.48 GHz, 6.6 GHz, 9.6 GHz, 11.42 GHz, 13 GHz and an UWB standard ranging from 14 GHz to 18 GHz. Thus, making it suitable for several wireless applications. The proposed antenna is a good candidate for the existing and the emerging wireless and mobile handsets targeting multiband, multi-standards technologies, and applications.

In [126], a compact CPW-fed single-layer printed antenna with an UWB rectangular monopole radiator etched with a half-elliptical slot The etching of the half-elliptical slot on the axis of the original small-sized rectangular patch brings in continuously tunable electrical resonance lengths for different wavelengths, especially for the intermediate and higher frequencies in the operating bandwidth. A compact CPW-fed hexagonal monopole antenna is investigated for UWB applications in [127]. The effect of feed gap on bandwidth of hexagonal shaped geometry with two different feed configurations has been studied. The proposed hexagonal shaped monopole antenna has been fabricated on a single sided copper clad PCB. The simulated and measured results show that there is satisfactory agreement. A CPW-fed planar inverted cone antenna (PICA) for UWB communication applications has been presented in [128]. The top part of the circular disc antenna is trimmed to the shape of a planar inverted cone. The radiating element is backed with a finite ground plane, and its total height is about $\lambda/4$, where λ denotes a wavelength at the lowest operating frequency.

A novel compact rectangular shaped antenna is proposed in [129] for WLAN/UWB communication systems. The microstrip fed monopole antenna is composed of a rectangular radiating patch embedded with an inverted L-shaped slit to generate two radiating arms which provide the two fundamental resonant modes at 2.45 GHz and 3.5 GHz. A narrow slot is cut in the ground plane of the proposed antenna just below the microstrip line feed to improve the impedance matching for higher frequency band. The length and width of the radiating patch should be designed very carefully to merge the higher order modes to generate wideband operation for UWB systems. A compact CPW-fed rectangular patch antenna with open stub has been designed for WLAN/UWB applications in [130]. The proposed rectangular shaped radiating element with open meandered stub, and three stepping are used in lower part of rectangular patch for impedance matching. A novel trapezoidal patch antenna loaded with H and U shaped slots has been proposed for PCS/WLAN/UWB communication systems in [131]. The trapezoidal patch with a stub is responsible for generating the UWB band. The radiating patch is embedded with H and U-shaped slots to excite the PCS and WLAN band, respectively.

A novel compact diamond shaped patch (DSP) is investigated for UWB applications in [132]. The several narrow strips are inserted into the diamond shaped patch to obtain multiband operation. The central part of the DSP patch antenna embedded with notched region and quarter wavelength strips are added to achieve the multiband operation which covers the frequency bands of GSM/WLAN and UWB communication systems. The two strip monopole antenna has been modified to achieve the significant improvement in impedance bandwidth thereby making it suitable for Wi-Fi and Mobile WiMAX applications in [133] and fabricated on substrate. The front side has a double T-shaped strip with a width of Ws and connected to an edge launch SMA connector. A compact CPW-fed egg curved slot antenna has been investigated which satisfies the bandwidth requirements of WLAN and UWB applications in [134]. The egg shaped radiating element is obtained from the standard equation of an ellipse. The size of the ground plane and egg curved slot size has significant impact on the impedance bandwidth of the proposed antenna.

A microstrip feed planar antenna for Bluetooth and UWB application has been proposed in [135]. The proposed antenna is composed of rhomboidal geometry and inverted L shaped strip. The rhomboidal radiating element provides UWB band ranging from the 3.1 GHz to 10.6 GHz. The inverted L shaped strip is also termed as Bluetooth element. The radiator patch consisting of a fork shaped stub on the front side of the substrate is presented in [136]. The dimensions of the fork shaped patch are designed carefully to get the required bandwidth so as to cover all the standards like Bluetooth, WiMAX, WLAN and ITU. The ground plane of the proposed antenna contains the elliptical shaped slot loaded with T-shaped and L- shaped slots to achieve multiband operation. The width of slots has impact on the impedance bandwidth of the proposed antenna. A modified tapered monopole antenna for UWB communication system has been investigated in [137]. The proposed antenna also covers all the bands of WLAN/WiMAX applications. It is based on truncated ground plane and a pair of tapered radiating element separated by a slot with different shapes. The effect of inserting a modified inverted T-shaped slot in the first tapered patch has been investigated.

A compact multiband antenna structure fed by proximity coupling has been proposed for WLAN/WiMAX and UWB communication systems in [138]. The proposed antenna is designed by connecting each of the multiple radiating elements in the figure of eight shapes by means of short metallic strips. The main radiating structure can be varied from a digit zero to digit nine by connecting the required arms to form the figure. The double layered FR4 substrate is used in the fabrication process of the proposed antenna. The multiband characteristics of the proposed antenna can be achieved by connecting the main radiating structure with help of short metallic strips. The variation in resonant frequencies is observed from 3.69 GHz to 13.51 GHz, covering the WLAN standard at 5.2 GHz and 5.8 GHz, WiMAX standard at 3.3 GHz, UWB band at 3.1 GHz–10.6 GHz part of WMAN fixed wireless, ranging from 2–11 GHz and 802.16eWMAN mobile wireless, ranging from 2–6 GHz.

The design proposed in [129], covers the lower frequency band of WLAN standard at 2.4 GHz and UWB standard but is not able to cover the upper frequency bands of the WLAN standard. The antenna proposed in [135], covers both the Bluetooth standard and UWB standard but it is not able to cover the lower and upper frequency bands of the WLAN/WiMAX standards. In [137], the proposed structure covers all the upper frequency bands of WLAN/WiMAX standards and UWB standard but it is not able to cover the lower frequency bands of WLAN/WiMAX standards. In all the antenna designs discussed above cover some bands of WiMAX and WLAN standards and are not able cover all the bands of WLAN/WiMAX standards and UWB standard.

Conclusion

In future heterogeneous wireless communication systems, the antenna should be carefully designed to integrate the various wireless communication technologies. A mobile device is needed to be equipped with compact size and multiband internal antenna for wireless terminal is an interesting issue of research. A multipurpose mobile phone will be the key feature of the upcoming 4G and 5G wireless communication system. Thus, the most important task is to propose antenna design that covers non-cellular frequency bands like Bluetooth, WLAN, Wi-Fi, WiMAX, and UWB standards in one antenna design. The next chapter presents a new printed antenna structure for WLAN/WiMAX applications.

CHAPTER-3

RECTANGULAR SHAPED ANTENNA WITH HASH SHAPED SLOT

3.1 Introduction

The purpose of this chapter is to present two new CPW-fed rectangular shaped monopole antennas suitable for WLAN and WiMAX standards. There are various methods like shorting pins, shorting wall and plate, slits, slots and notches, used for the patch antenna to achieve the wide band and multiband operation. One of the easy and efficient methods used in this design is slots of different shapes and sizes in the microstrip antenna to achieve multiband capability. The length and position of the slots can be modified to obtain the multiband operation. WLAN standards are very popular due to their capability to provide high-speed data transfer. WiMAX is the future-generation of wireless systems which provides high-speed mobile internet access to the variety of devices. These heterogeneous wireless standards are relatively inexpensive and can provide wireless connectivity at restaurants, airports, cafes, railway stations, bars and other public areas. Integration of all these standards into handheld devices has led to development of multiband antennas. A CPW fed rectangular shaped antenna (RSA) embedded with hash shaped slot has been proposed for WLAN/WiMAX applications. In this chapter, the new designs are illustrated in the next section:

3.2 Antenna Design and Geometry

The geometry of CPW fed rectangular shaped antenna (RSA) for WLAN/WiMAX applications is depicted in Fig. 3.1 with its optimized parameters. The conventional FR4 substrate with thickness h=1.6 mm and dielectric constant of 4.4 is used for fabrication of the proposed antenna. The copper metal of uniform thickness approximately 0.02 mm is deposited on substrate. The basic radiating structure consists of the rectangular shaped antenna which has dimensions of length L and width W. A CPW feedline consisting of a signal strip of width W_f and two equal finite ground planes, each with dimensions of length Lg and width Wg on both sides of signal strip, is used for feeding the antenna. The overall size of this antenna is 26.4 mm × 35.24 mm × 1.6 mm with total volumetric size of antenna is 1.49 cm^3. The simulation tool IE3D is used for this study.

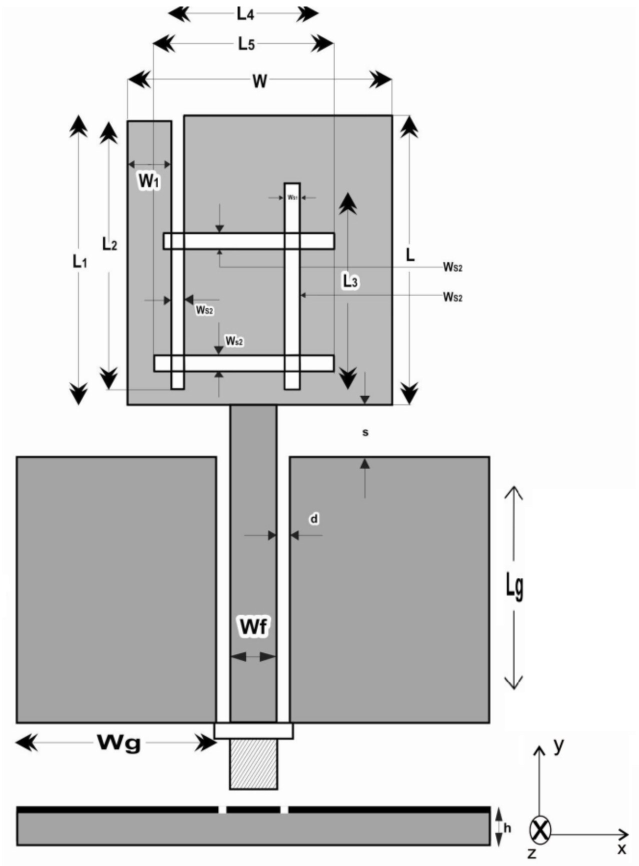

Fig. 3.1 Geometry of the Rectangular Shaped Antenna (RSA)

3.3 Parametric Study

The effect of parametric study has been investigated for the proposed antenna. The variation of parameters has influence on return loss and impedance bandwidth of the proposed antenna and is given in the following section:

3.3.1 Effects of Rectangular Shape

The simulated return loss with respect to frequency for rectangular shape antenna only and compared with proposed antenna is presented in Fig. 3.2. It has been observed from the simulation study that effect of only rectangular shape is generating a single lower band with poor return loss.

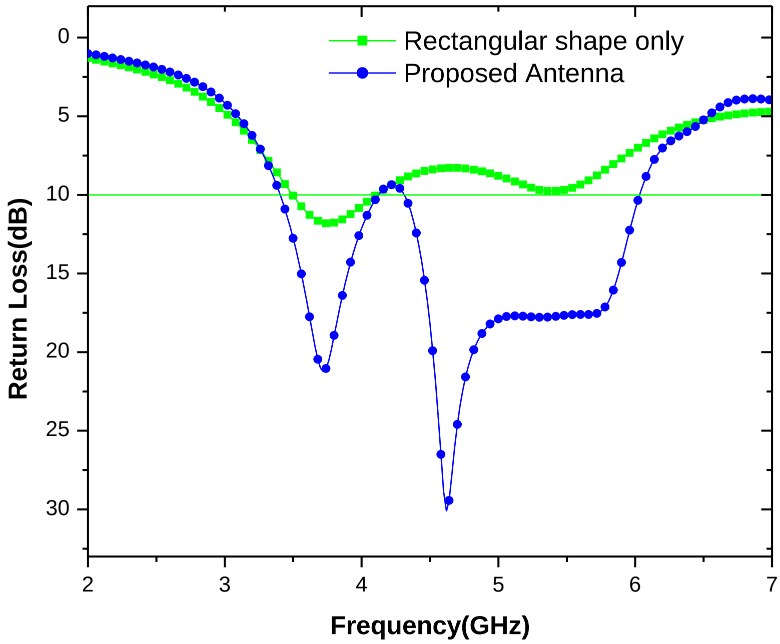

Fig. 3.2 Effects of Rectangular Shape on Impedance Bandwidth

3.3.2 Effects of Varying Slot Length L_3

Effects of variation of slot length L_3 along positive y-axis (top of the patch) of proposed antenna on return loss is shown in Fig. 3.3. The optimum value of slot length L_3 is 14.63 mm. This figure reveals that as the slot length (L_3) is decreased from the optimum value; the impedance bandwidth of lower frequency band is increased by significant amount while the upper frequency band gets decreased by small amount. Further, increase in the slot length (L_3) from 14.63 mm to 16.23 mm, the bandwidth of lower-band is decreased approximately by 40% whereas that of the upper frequency band is increased by small amount as compared to optimized impedance bandwidth.

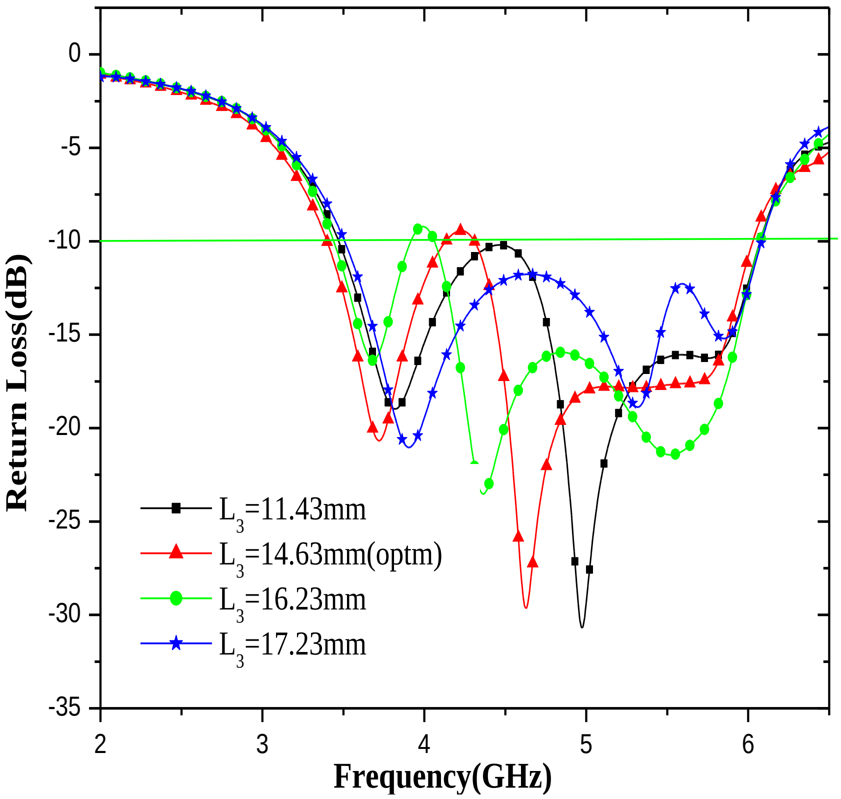

Fig. 3.3 Effects of Variation of Slot Length L_3 on Impedance Bandwidth

3.3.3 Effects of Varying Slot Length L_4

The simulated return loss with respect to frequency of the proposed antenna for different values of slot length L_4 along the positive x-axis (right-side of the patch) is presented in Fig. 3.4. The optimal performance has been obtained for L_4 = 12.75 mm. It has been observed from the simulation study that the slot length (L_4) is decreased from optimal value of slot length, the two bands get merged together into a single wide-band and the overall bandwidth also gets slightly increased. It has also been examined that by increasing the slot length (L_4) from the optimal value, the frequency moves towards the lower side with a loss in the impedance bandwidth approximately by 50% from the optimized value of bandwidth and impedance bandwidth in upper frequency band is increased by a small amount.

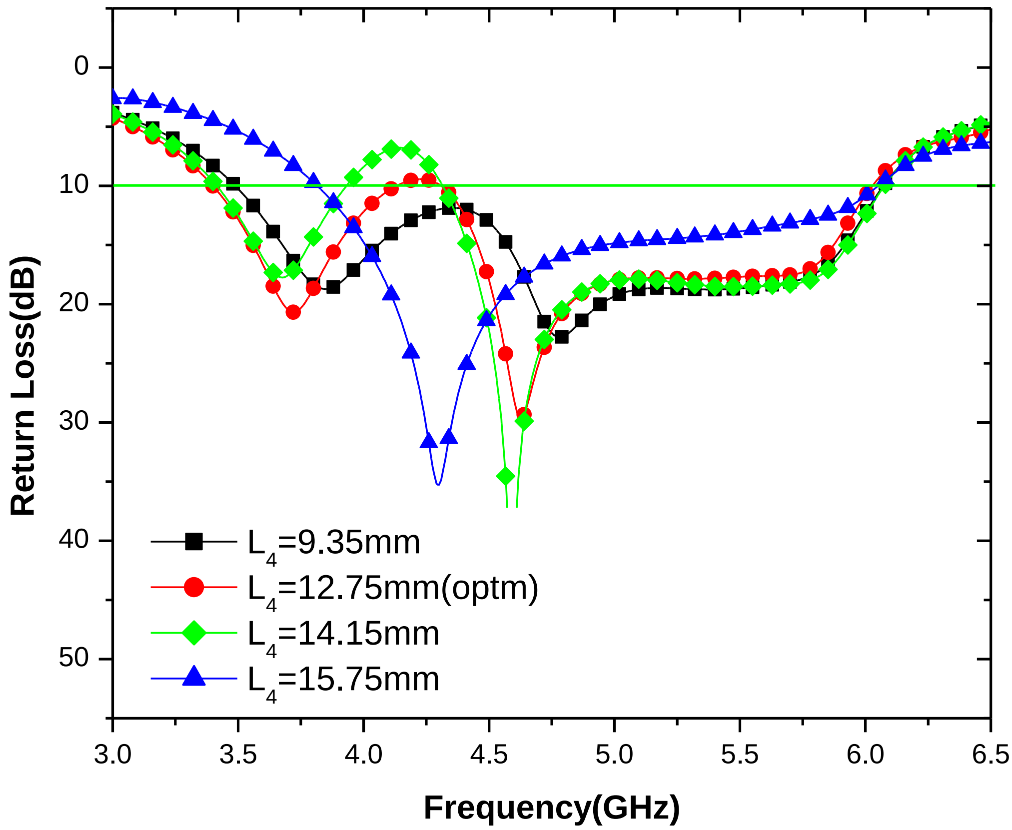

Fig. 3.4 Effects of Variation of Slot Length L_4 on Impedance Bandwidth

3.3.4 Effects of Varying Slot Length L_5

The simulated return loss with respect to frequency of the proposed antenna for different values of slot length L_5 along the positive x-axis (right-side of the patch) is presented in Fig. 3.5. The optimal performance is found at slot length L_5=14.2 mm. It has been examined from the graph that by decreasing the slot length (L_5) from the optimal value, the upper-band shift towards the higher frequency with a small decrease in the bandwidth. By increasing the slot length L_5 from the optimal value, the two bands are merged together to form a single wideband and there is shift in frequency towards the lower frequency with loss in the impedance bandwidth. The lower frequency band remains unaffected even increase in slot length (L_5) up to 15.6 mm. Further, increase in the slot length (L_5) beyond 15.6 mm results in loss in bandwidth of lower operating band.

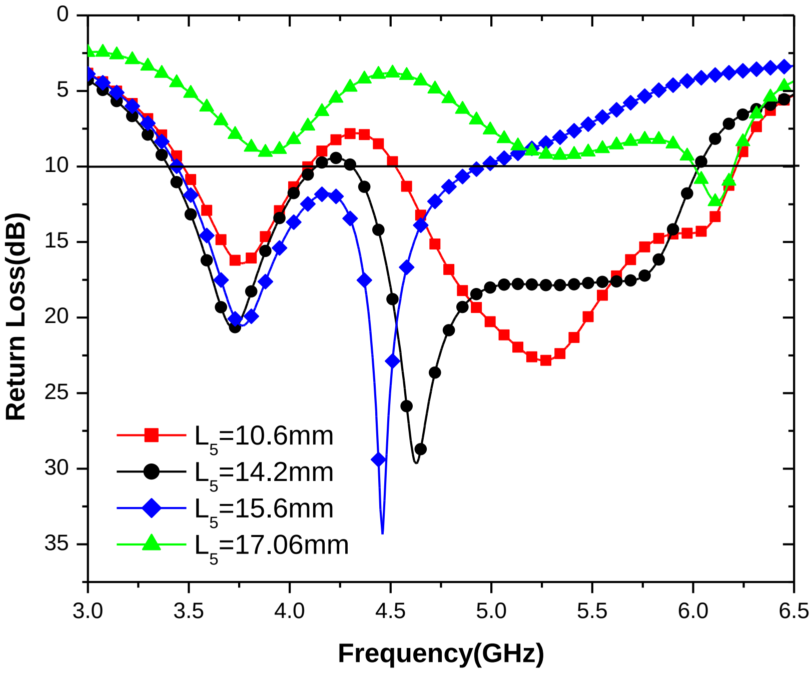

Fig. 3.5 Effects of Variaition of Slot Length L_5 on Impedance Bandwidth

3.3.5 Effects of Slot Length L_2

Effects on return loss of proposed antenna due to only slot length L_2 is shown in Fig. 3.6. The optimum value of slot length L_2 is 17.57 mm. It has been observed from graph that with only slot length (L_2), the two bands gets merged together to provide a single wideband with small overall impedance bandwidth with very poor return loss.

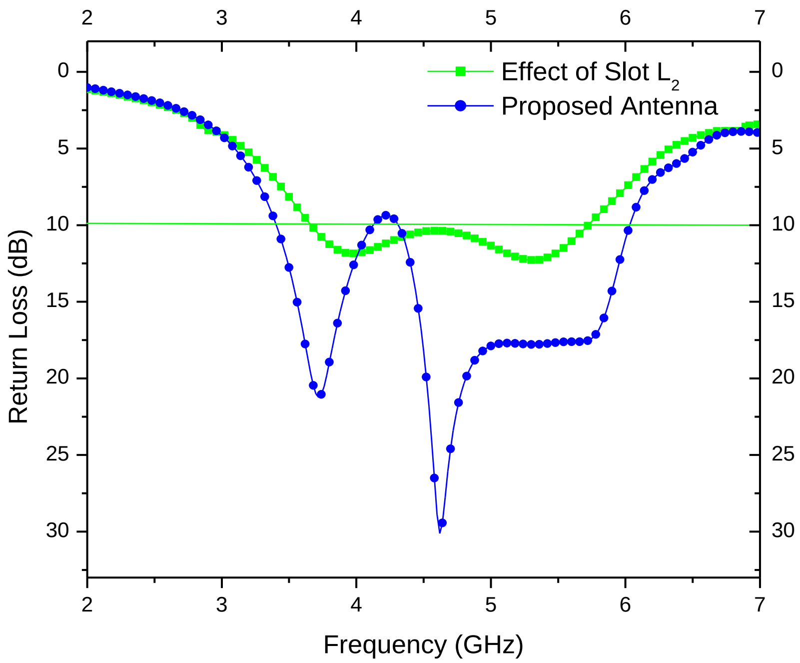

Fig. 3.6 Effects of Slot Length L_2 on Impedance Bandwidth

3.3.6 Effects of Slot Length L_3

Effects of slot length L_3 only (along positive y-axis) on return loss of proposed antenna is shown in Fig. 3.7. It has been seen from figure that slot length (L_3) generate a single wide-band and the overall impedance bandwidth also gets decreased with very poor return loss as compared with proposed antenna.

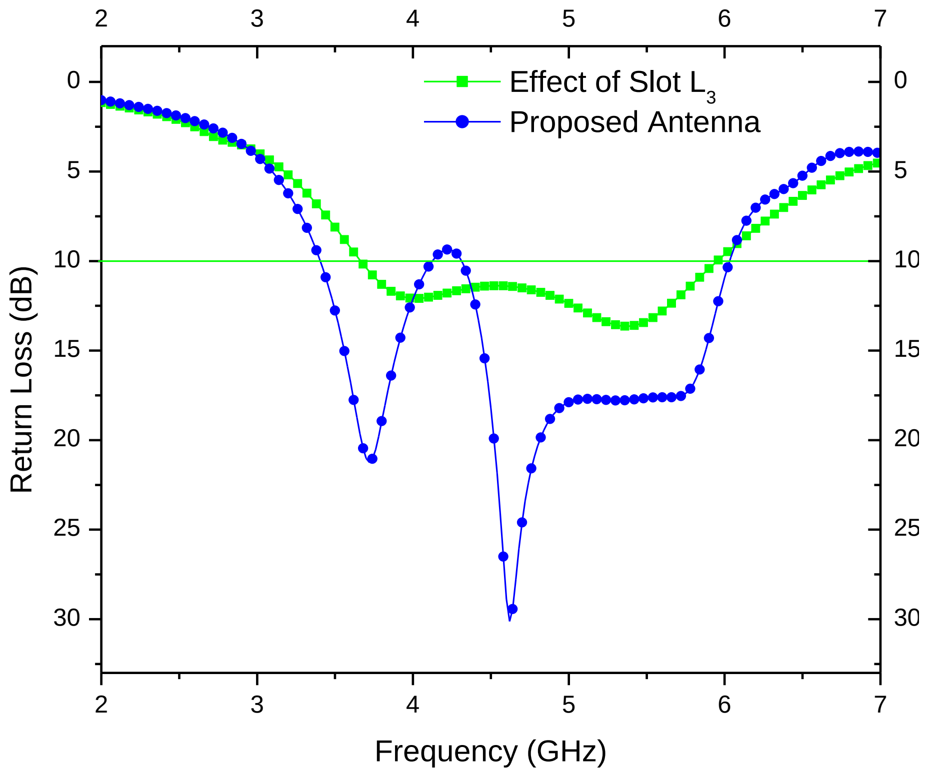

Fig. 3.7 Effects of Slot Length L_3 on Impedance Bandwidth

3.3.7 Effects of Slot Length L_4

Effects of slot length L_4 only (along positive y-axis) on return loss of proposed antenna is shown in Fig. 3.8. It has also been examined that slot length (L_4) produces only lower frequency band with a small impedance bandwidth and no upper frequency band with poor return loss.

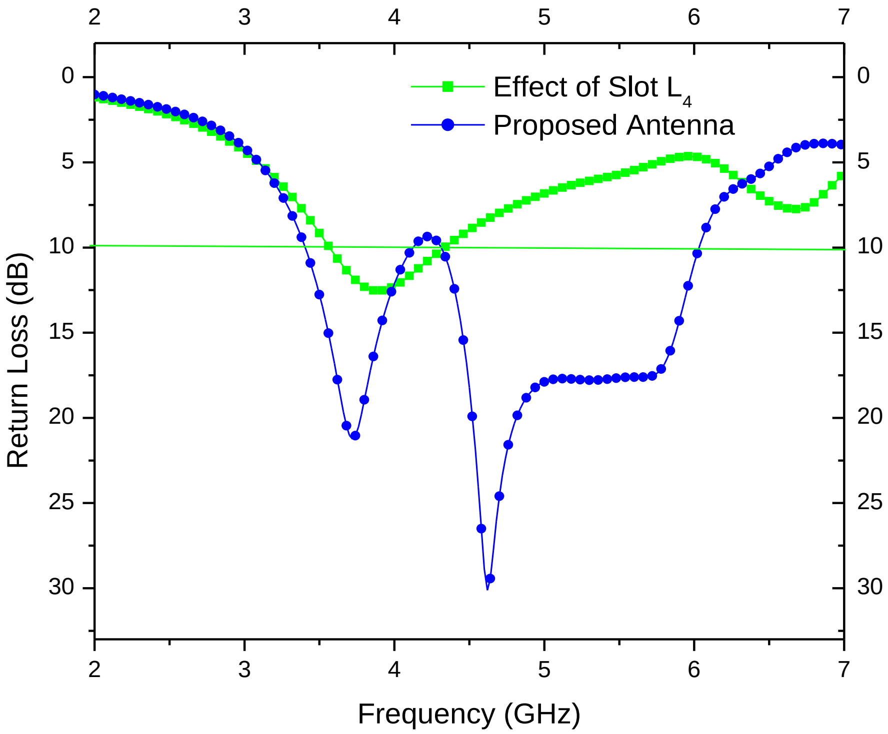

Fig. 3.8 Effects of Slot Length L_4 on Impedance Bandwidth

The final optimized geometric parameters of the proposed antenna are presented in Table 3.1.

Table 3.1: Optimized Parameters of RSA Antenna

Parameters	Diemensions (mm)
L	18.71
W	19.9
L_g	15
W_g	11.2
W_f	2.8
L_f	16.53
L_2	17.57
L_3	14.63
L_4	12.75
L_5	14.2
L_1	18.22
W_1	4.92
s	1.53
d	0.7
W_{s2}	1.2

W_{s1}	1

3.4 Simulated Return Loss

This section represents the simulated return loss for the optimized antenna shown in Fig. 3.9. The result shows that proposed antenna has two resonant frequencies with wideband operation. It is clear from the graph that impedance bandwidth of the antenna ranges from 3.4 GHz to 4.132 GHz and 4.312 GHz to 6.028 GHz. It covers all the upper frequency bands of WLAN standard at 5.2/5.8 GHz and WiMAX standard at 3.5/5.5 GHz.

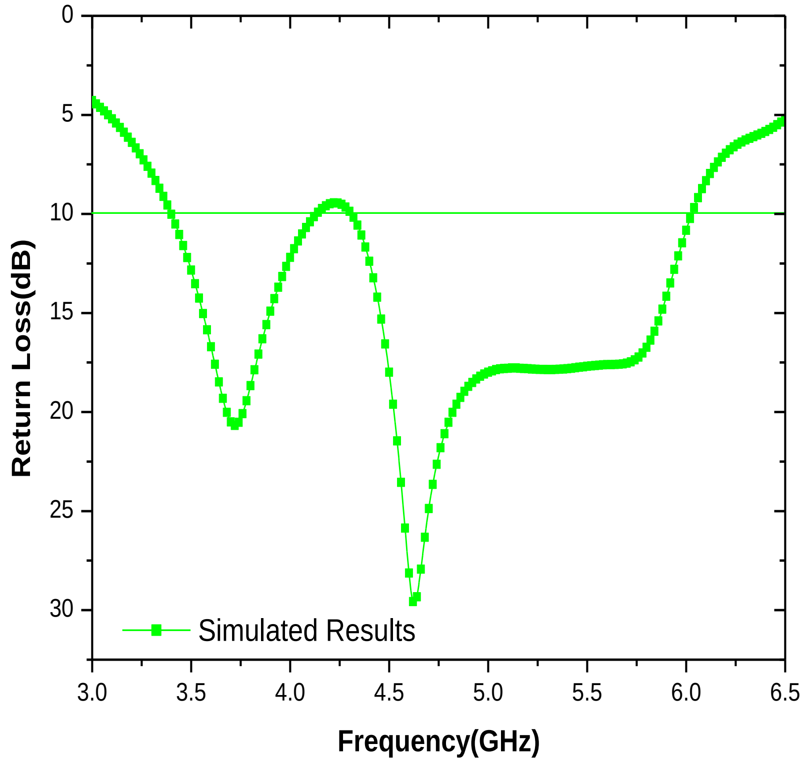

Fig. 3.9 Simulated Return Loss of the RSA Antenna

The research methodology discussed in section 1.6.5 and 1.6.6 is used for the fabrication and measurement of the proposed antenna, respectively. The measured results obtained are given in the following section.

3.5 Measured Return Loss

The FR4 substrate is used for fabrication of the proposed antenna with optimal dimensions. For fabrication of the proposed antenna, a photolithography process is used to craft the antenna model on the substrate. The photograph of the fabricated antenna is depicted in Fig. 3.10.

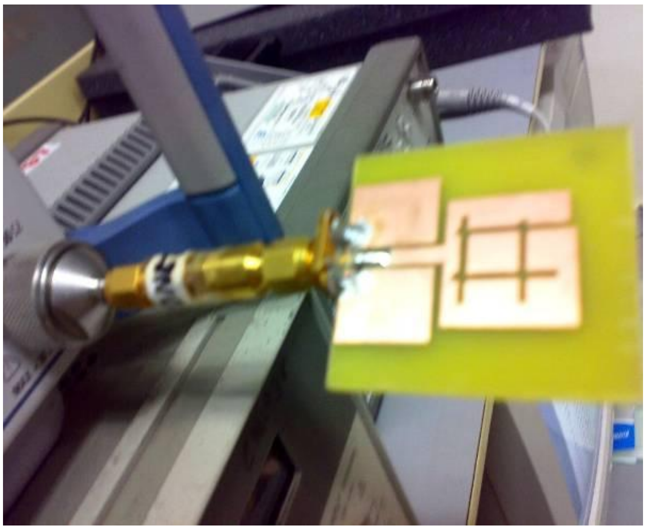

Fig. 3.10 Prototype of the Fabricated Antenna

After the fabrication process, the measurement of the return loss parameter has been brought out by using Agilent VNA N5071. Before starting the measurement process, the Agilent VNA is calibrated for insertion loss and electrical length of the coaxial probe. The comparison between the measured and simulated return loss of the antenna has been presented in Fig. 3.11. From the measured results, it is clear that a single wideband with total impedance bandwidth of 2.85 GHz is obtained This antenna covers the WLAN standard at 5.2 GHz, and 5.8 GHz bands, and WiMAX standard at 3.5 GHz, and 5.5 GHz bands of heterogeneous wireless communication systems. The measured and simulated results have the satisfactory agreement over the entire operating band. By comparing the simulated and measured results, it is observed that there is a slight shift of peak resonant frequency towards higher side in the higher operating band. The reason for the shift in peak resonant frequency is due to the small dimensional inaccuracy during the fabrication process. In the simulation process, SMA connector loading is not considered but it provides a variable reactance when used in the experiment.

3.6 Simulated Gain

The simulated antenna gain with respect to different values of frequencies is presented in Fig. 3.12. In the lower operating band, the simulated gain of antenna ranging from 2.2-3.1 dBi, while in upper operating band ranging from 2.4–5.51 dBi with small gain variation across operating band is observed. The optimum simulated gain of antenna is 5.51dBi at 4.6 GHz frequency. It satisfies the gain requirements of WLAN and WiMAX applications within the operating bands.

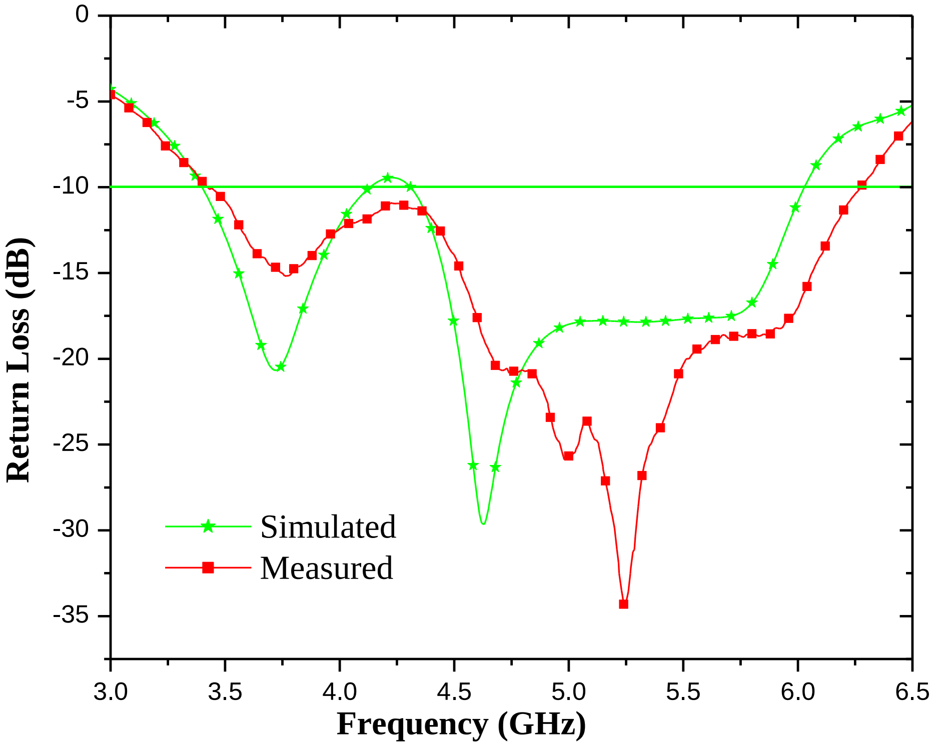

Fig. 3.11 Comparison of Simulated and Measured Return Loss

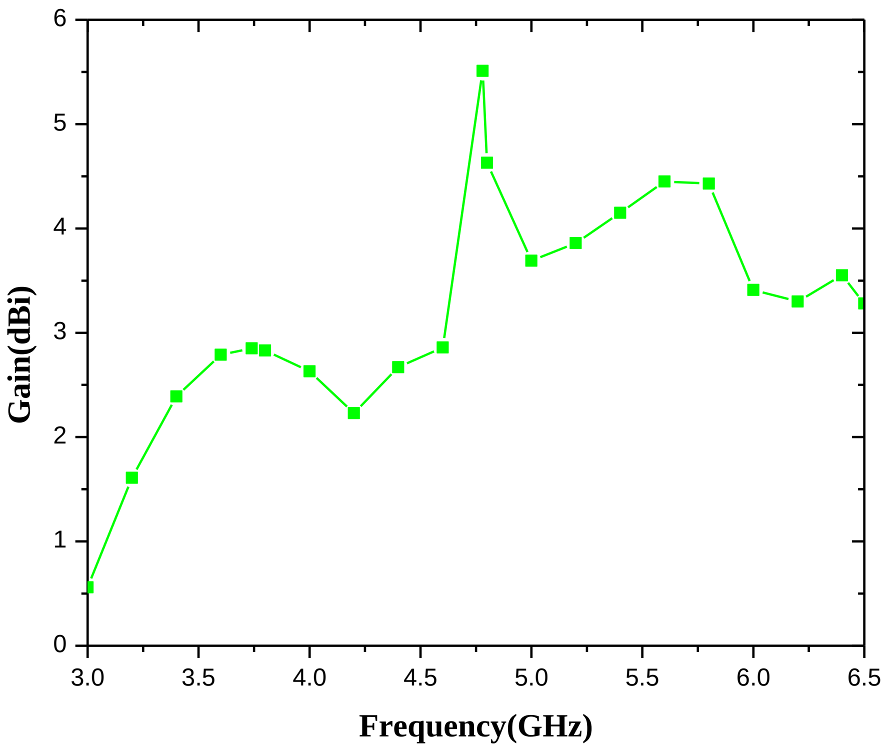

Fig. 3.12 Simulated Gain against Frequency of Antenna

3.7 Current Distributions

The current distributions of the proposed antenna at two frequencies are revealed in Fig. 3.13 (a) and (b). The flow of surface current is indicated by the arrows. The red colour represents the strong current density whereas blue colour represents the weak current density. It has been observed from the Fig. 3.9 (a) that there is strong current distribution near the edge of slot length L_5, along feed line and at top edges of slot lengths L_3 and L_4 at 3.74 GHz frequency. The current distribution indicates that embedded hash shaped slot increase the electrical current path for generating the lower resonant mode. For higher resonant mode at 5.42 GHz, the surface currents mainly flows along the edges of slot length L_1, feed-line and over the edges of the slot lengths L_3, L_4 and L_5 as shown in Fig 3.9 (b).

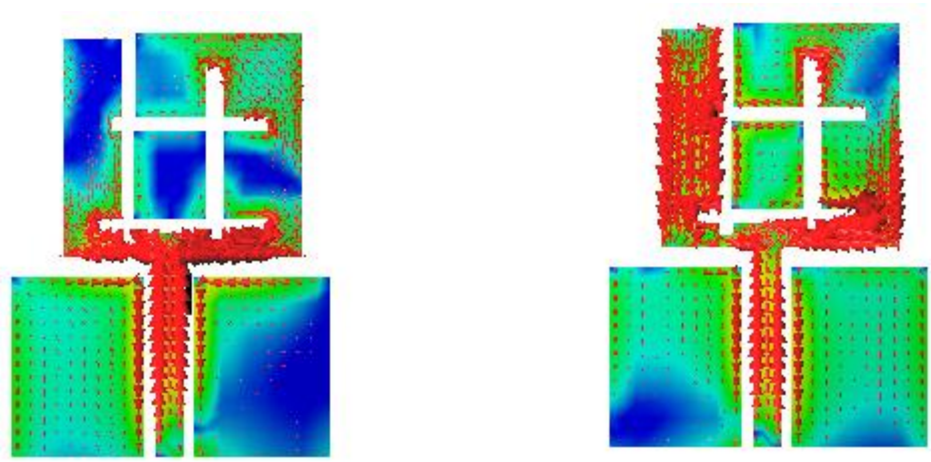

Fig. 3.13 Current Distributions at (a) 3.74 GHz (b) 5.42 GHz

3.8 2D Radiation Pattern

The simulated radiation patterns of the proposed antenna are represented in Fig. 3.14 for different values of frequencies. The simulated radiation patterns of the antenna in the azimuthal plane (x-y) and the elevation plane (y-z) are displayed in Fig. 3.14 (a) for lower frequency at 3.6 GHz and Fig. 3.14 (b) for higher frequency at 5.5 GHz, respectively. The azimuthal plane shows that radiation pattern close to omni-directional antenna at the frequency of 3.6 GHz but a little bit directional radiation patterns has been observed at a frequency of 5.5GHz. The radiation pattern in elevation plane is similar to figure of eight at both the frequencies. The maximum antenna radiation efficiency of approximately 90% is observed from the simulated result.

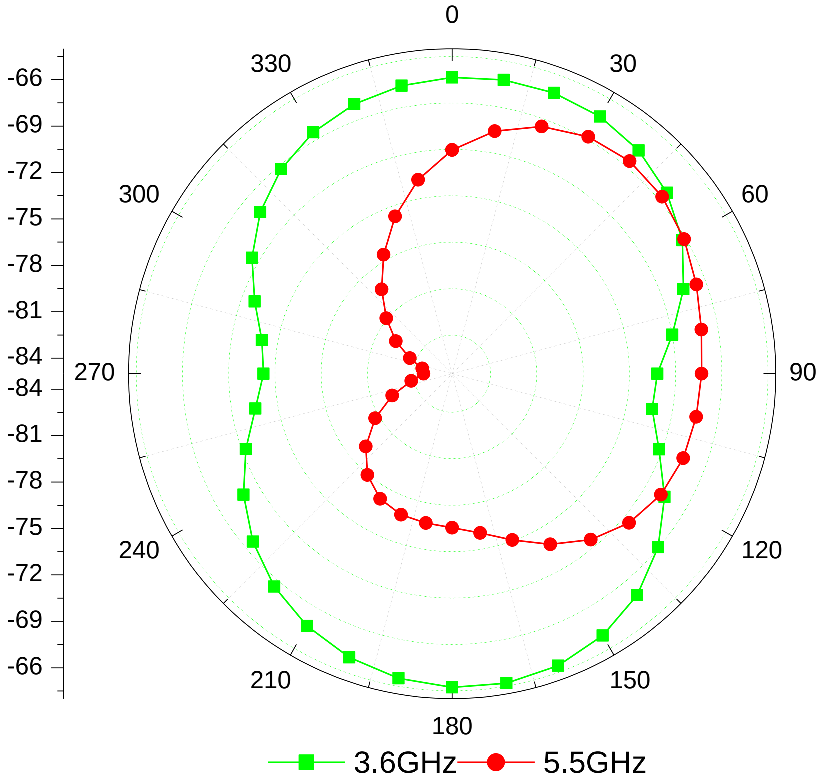

(a) Azimuthal Plane

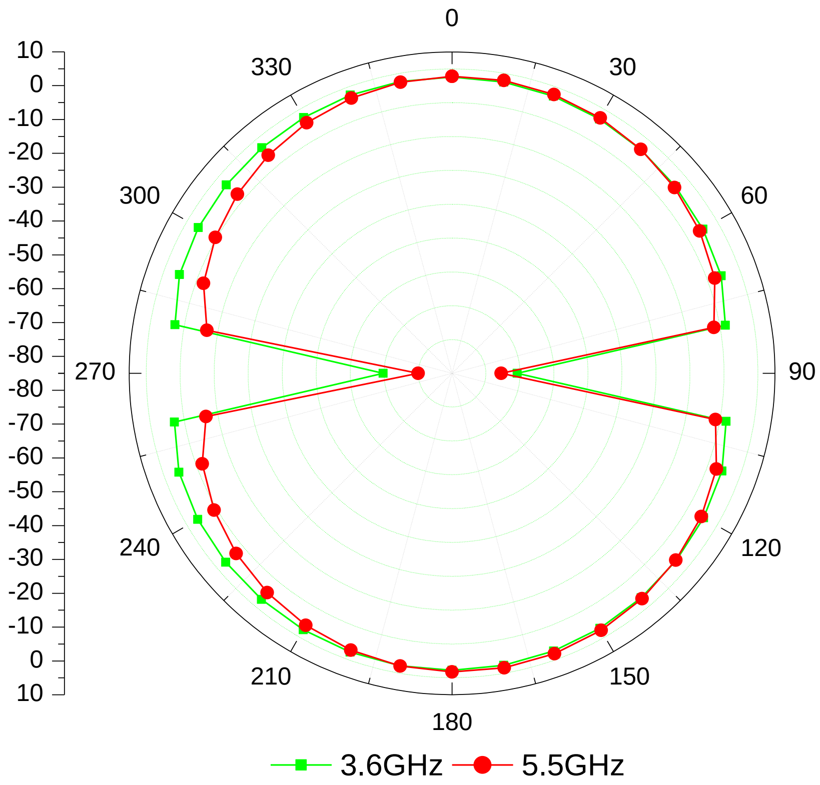

(b) Elevation Plane

Fig. 3.14 2D Radiation Pattern at 3.6 GHz and 5.5 GHz

3.9 Geometry of Modified Antenna Structure

The proposed antenna is modified by inserting a vertical I-shaped slot from the top of the rectangular patch in addition to hash shaped slot used in the previous optimized design. The geometry of modified proposed antenna is demonstrated in Fig. 3.15. This slight modified antenna structure is used to achieve three resonant modes with good return loss. The modified antenna design provides higher bandwidth and small volume as compared to the earlier geometry presented in Fig. 3.1. The vertical I-shaped slot is embedded in the geometry to increase the current path for reduction of antenna size. The prototype of the modified antenna has been designed and fabricated on FR4 substrate. The whole size of the antenna is 20.12 mm × 35.2 mm × 1.6 mm including the finite ground plane. The volumetric size of the modified design is 1.13 cm^3 which is small as compared to the previous design.

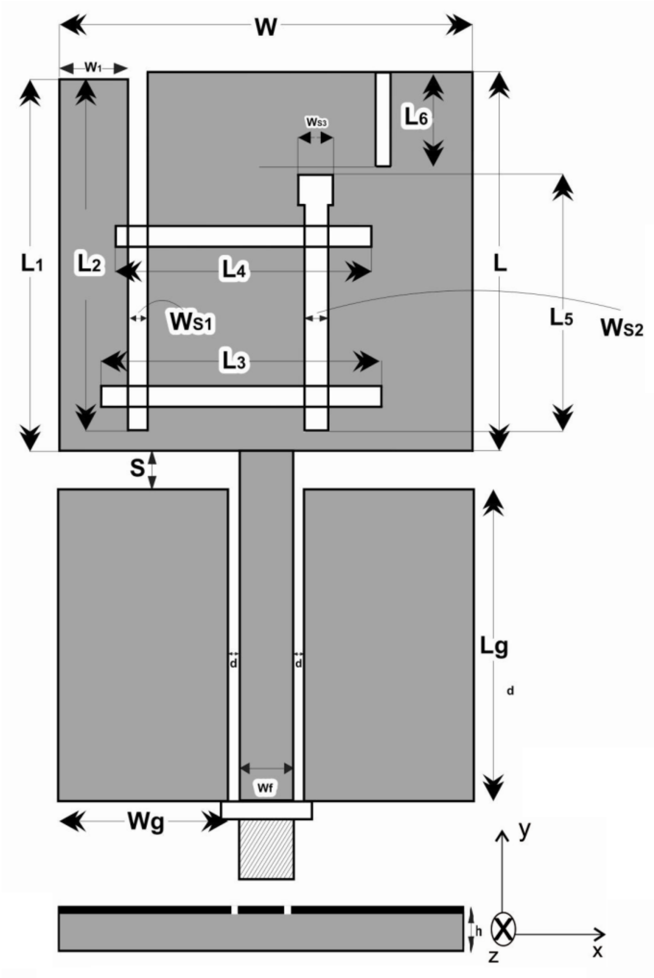

Fig. 3.15 Geometry of the Modified Structure

3.10 Parametric Study

The parametric study of the proposed antenna has been done to achieve the optimum results. In this parametric study, we are varying the values of single parameter while keeping other parameters as a constant. The effects of different parameters are presented in the following section:

3.10.1 Effects of Varying Slot Length L_1

Fig. 3.16 shows the simulated return loss of the proposed antenna as a function of frequency for different values of slot length L_1. It has been observed from the graph that with the decrease in slot length L_1 from the optimum value, there is decrease in bandwidth with slight shift of upper operating band towards the lower side and lower operating band shift towards the higher frequency. It is also observed from result that by increasing the slot length, there is increase in the bandwidth.

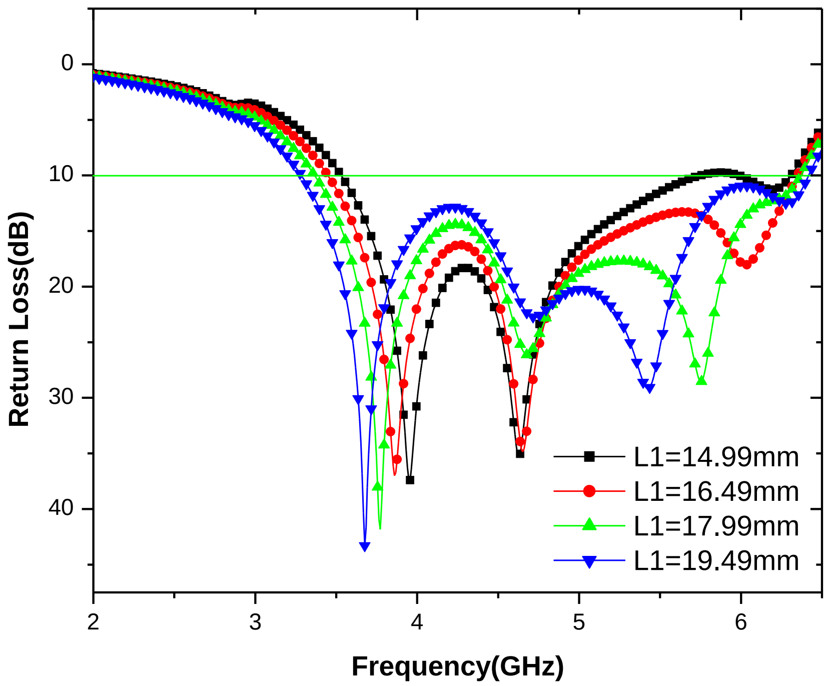

Fig. 3.16 Effects of Variation of Slot Length L_1 on Impedance Bandwidth

3.10.2Effects of Varying Slot Length L_3

Effects of length L_3 on proposed antenna return loss with respect to frequency is represented in Fig. 3.17. It can be seen from the figure that as the slot length (L_3) decreases, there is decrease in bandwidth with a slight shift in frequency towards lower frequency. It is also observed that by increasing the slot length L_3, the bandwidth decreases approximately by 65%. The most of bandwidth loss occur at the upper frequency.

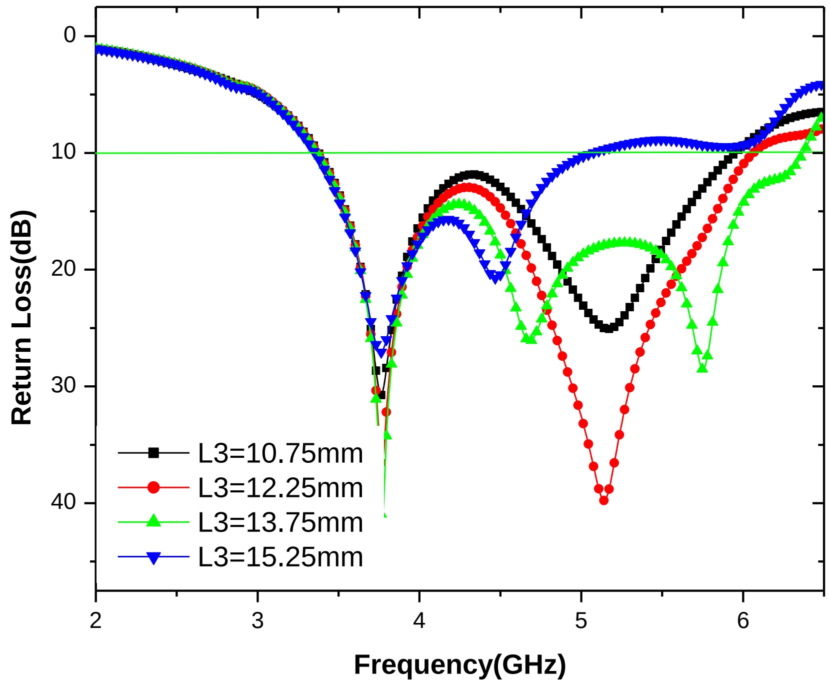

Fig. 3.17 Effects of L_3 Parameter on Impedance Bandwidth

3.10.3 Effects of Varying Slot Length L_6

Effects of slot length L_6 on the proposed antenna performance is shown in Fig. 3.18. It has been observed from the results that by decreasing the slot length (L_6), there is a small loss in the bandwidth with slight shift in frequency toward lower frequency. It is also observed that by increasing the slot length, there is a small loss in bandwidth.

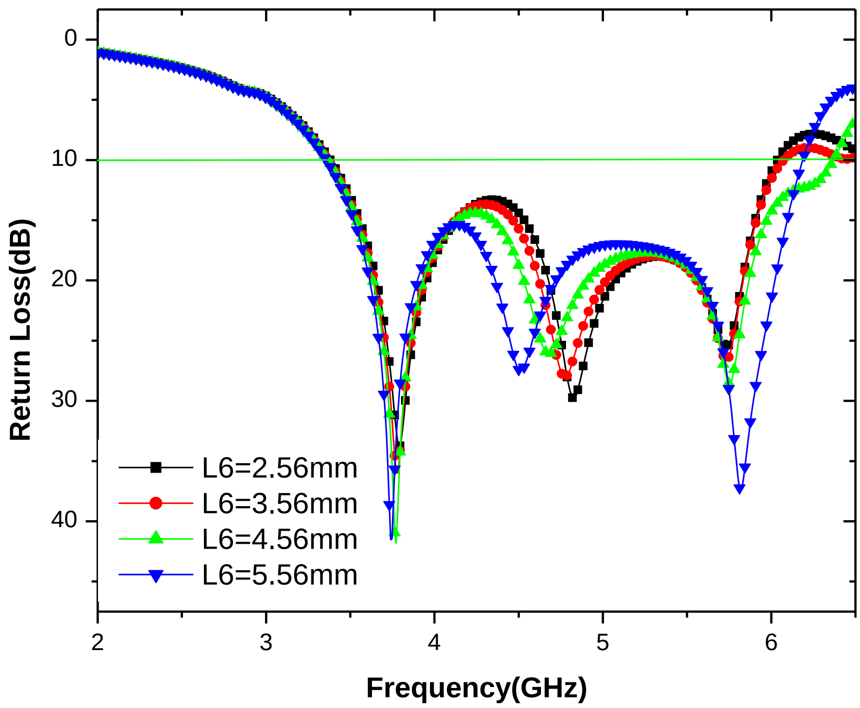

Fig. 3.18 Effects of Variation of Slot Length L_6 on Impedance Bandwidth

3.10.4 Effects without Slot Length L_6

Effects without slot length L_6 on the proposed antenna performance is shown in Fig. 3.19. It has been observed from the results that without slot length (L_6), there is a loss in the bandwidth of proposed antenna with very poor return loss.

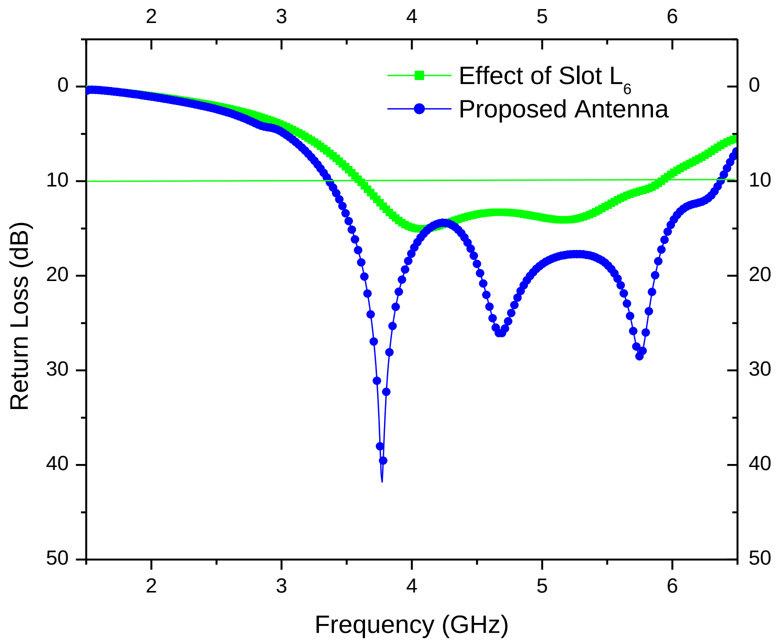

Fig. 3.19 Effects without Slot Length L_6 on Impedance Bandwidth

The effects of all structural parameters variation on performance of the proposed antenna are presented in Table 3.2.

Table 3.2 Effects of Varying Slot Lengths L_1, L_3 and L_6 on Impedance Bandwidth

Parameter	Dimensions (mm)	Resonant-band (GHz)	Bandwidth (GHz)
L_1	14.99	3.54-5.74	2.20
	16.49	3.45-6.34	2.89
	17.99	3.37-6.37	3.0
	19.49	3.29-6.41	3.12
	10.75	3.38-5.95	2.57
	12.25	3.38-6.06	2.68

L_3	13.75	3.37-6.37	3.00
	15.25	3.36-5.07	1.71
L_6	2.56	3.38-6.02	2.64
	3.56	3.38-6.07	2.69
	4.56	3.37-6.37	3.00
	5.56	3.33-6.05	2.72

3.11 Simulated Return Loss

The simulated return loss of the proposed modified antenna with optimized parameters is represented in Fig. 3.19. The simulated result shows that a single wideband impedance bandwidth is observed with three resonant peaks. The simulated result has a wide impedance bandwidth ranging from 3.37 GHz to 6.37 GHz which is able to cover the required bandwidths of the WLAN standard at 5.2 GHz and 5.8 GHz bands, WiMAX standard at 3.5 GHz and 5.5 GHz bands and C-band for satellite communication at 4 GHz ranging from 3.7 GHz - 4.2 GHz. The total impedance bandwidth of modified antenna is 3 GHz.

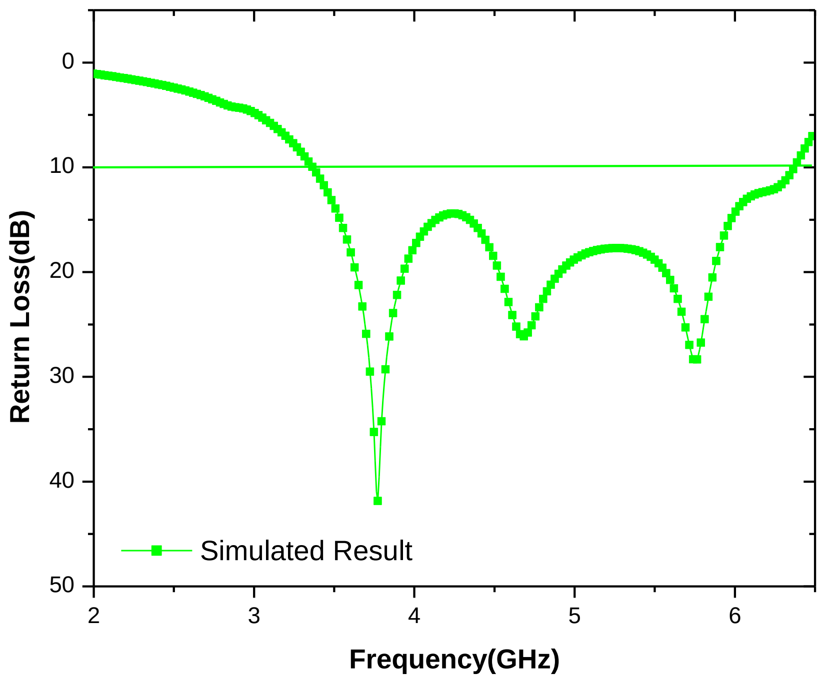

Fig. 3.20 Simulated Return Loss of Modified Antenna

3.12 Measured Return Loss

The same technique is used for the fabrication and measurement of the modified antenna structure as discussed in section 1.6.2 and 1.6.3. The photolithography process is used to fabricate the modified antenna. The photograph of the fabricated prototype with measurement setup is shown in Fig. 3.20.

Fig. 3.21 Photograph of Prototype Antenna

The measured and simulated return loss of the proposed modified antenna is demonstrated in Fig. 3.21. The measured results show that the total bandwidth of prototype antenna is 2.872 GHz. It covers the 5.2 GHz, and 5.8 GHz bands of WLAN standard, and 3.5 GHz, and 5.5 GHz bands of WiMAX standard of heterogeneous wireless communication systems. It can also cover the C-band used for satellite communication from 3.7 GHz to 4.2 GHz. The bandwidth of modified design is still not sufficient to cover the lower frequency band of WLAN standard at 2.4 GHz and WiMAX standard at 2.5 GHz.

We have also compared the measured results with the simulated results obtained from the EM simulator. The simulated and measured results show a satisfactory agreement for modified structure. A similar curve trend is observed for return loss between the measured and the simulated results over the entire resonant frequency band. The experimental return loss has small decrease in the impedance bandwidth with small shift in the frequency towards the lower frequency side. The discrepancy in the result may be due to the slight geometrical error during the fabrication process. The effect of the cable connector is not considered in the simulation process but it is used in the experimental work which acts as a variable load.

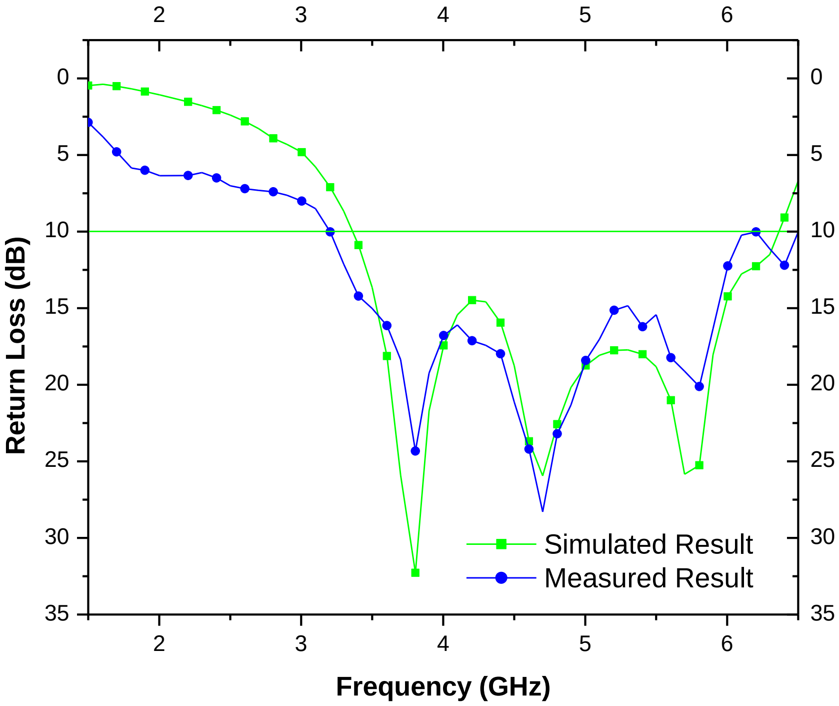

Fig. 3.22 Comparisons of Measured and Simulated Return Loss

3.13 Simulated Gain

The simulated gain of the modified proposed antenna is presented in Fig. 3.22. The antenna has a maximum gain of about 4.85 dBi at 6.22 GHz frequency with gain variations less than 2.5 dBi, whereas the antenna gain is within a range of 2.41–4.85 dBi.

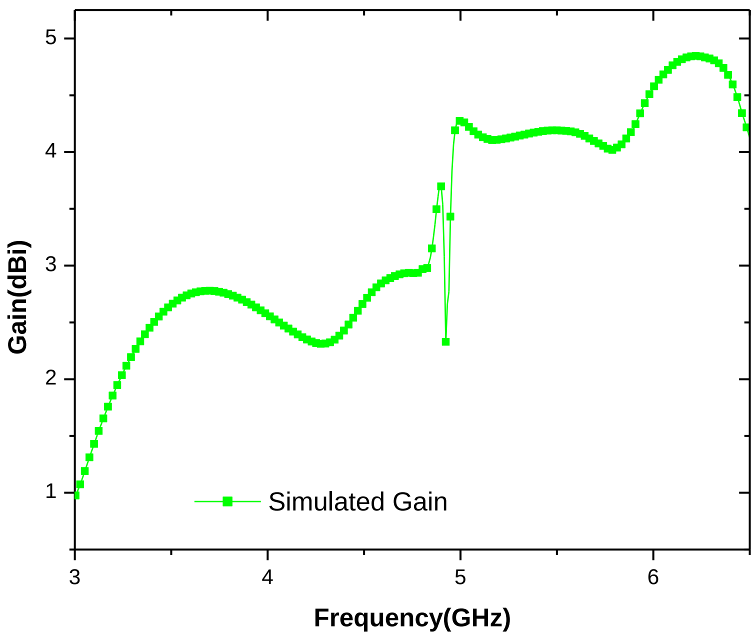

Fig. 3.23 Simulated Gain of the Modified Antenna

3.14 Current Distributions

The current distributions of the modified proposed antenna at two frequencies are revealed in Fig. 3.23. The flow of current is indicated by the arrows. The red colour represents the strong current density whereas blue colour represents the weak current density. It has been observed from the Fig. 3.23 (a) that the surface currents mainly flow along the patch's lower edges and at upper right corner of the patch and a small current distribution along the left arm (L_1) at 4.0 GHz of lower frequency. For the higher resonant mode at 5.75 GHz, most of the surface current is flowing across the left arm (L_1) and also along the slot length L_3 i.e right side of lower part and the small current flow along the other slots of patches like L_4, L_5 and L_6 and also small current flow in the inner part of the rectangular patch as depicted in Fig. 3.23(b).

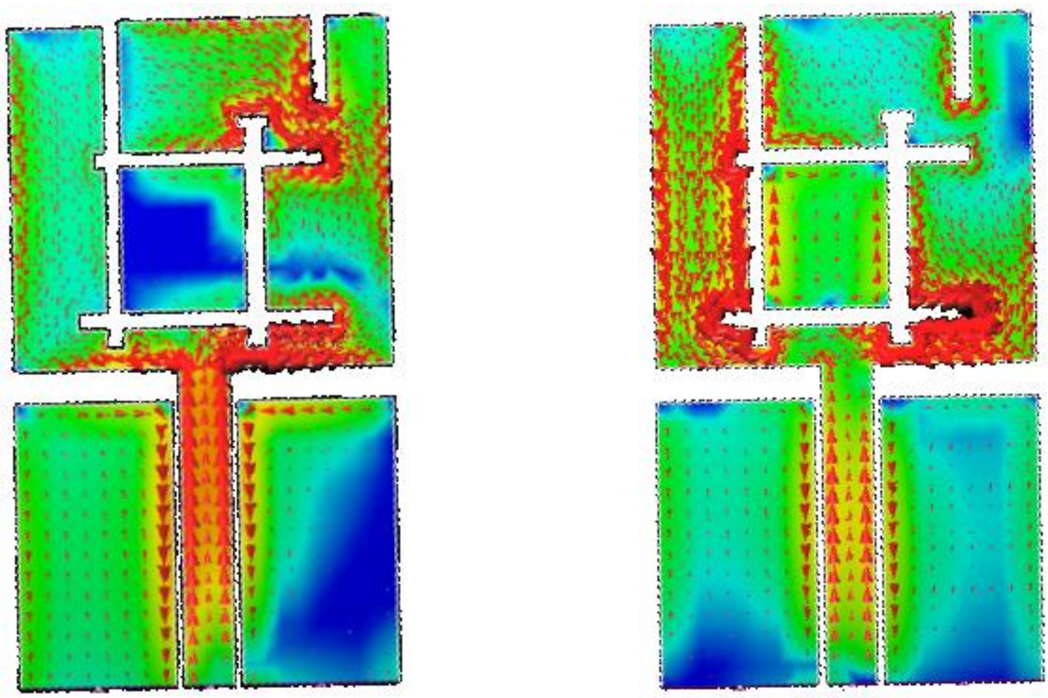

(a) At 4.0 GHz **(b) At 5.75 GHz**

Fig. 3.24 Current Distribution of the Modified Antenna

3.15 2D Radiation Pattern and Radiation Efficiency

The simulated 2D radiation pattern of the proposed modified antenna is presented in Fig. 3.24 at the frequency 5.75 GHz. The radiation patterns obtained in the azimuthal plane are almost close to omni-directional, and those in the elevation plane are looks like a figure of eight shape. The maximum antenna radiation efficiency of the modified design is approximately 90%.

Conclusion

In this chapter, a rectangular shaped monopole antenna with an extended hash shaped slot has been designed and investigated. The first design has two resonant frequencies with wideband operations which satisfies the bandwidth requirements of WLAN/WiMAX applications. This design is modified by inserting a vertical I-shaped slot in the patch to achieve the triple resonant mode operation. The modified proposed antenna has small size as compared to the first design. Both the proposed antennas are not able to cover the lower frequency bands of WLAN standard at 2.4 GHz and WiMAX standard at 2.5 GHz. The design presented in the next the chapter is able to cover all the frequency bands of WLAN and WiMAX standards.

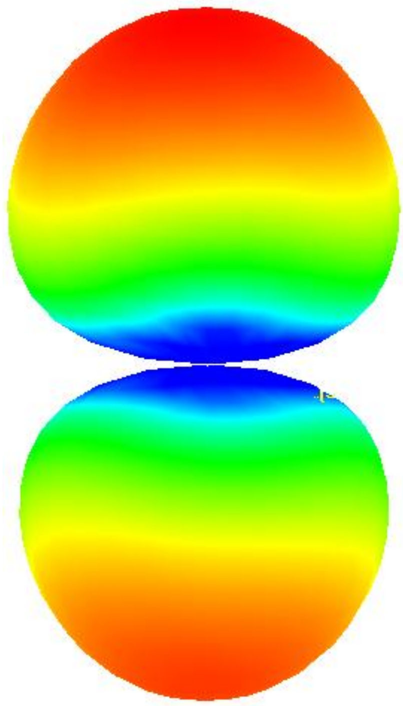

Fig. 3.25 2D Radiation Pattern at 5.75 GHz

CHAPTER-4

DGS BASED MULTIBAND ANTENNA FOR WiFi, WLAN AND WiMAX APPLICATIONS

4.1 Overview

The fast growth in the wireless communication has led to the development of various wireless standards like Wi-Fi, WLAN, WiMAX, UMTS and UWB. Hence, these wireless standards have stimulated the research interest in field of multiband and broadband antennas with compact size. Defected ground structure (DGS) is one of the best and latest technologies used to enhance the properties and quality performance of an antenna. DGS technique generally refers to a defect in the ground plane of microstrip antenna to modify its properties and it facilitates the improvement in the performance of microstrip antennas. It is a unique technique to reduce the antenna size and to increase the impedance bandwidth [139, 140].

Four vertical monopoles are used in proposed antenna to achieve multi-band operation covering Wi-Fi, WLAN and WiMAX standards. The defects are introduced in the ground plane of this antenna to form DGS structure which reduces the size of the antenna. For generating the lower frequency band, the four vertical monopoles antennas are composed of large number of displaced bricks. I-shaped slots are cut in the ground planes to control the flow of current across the antenna surface. The slot sizes are manually optimized to improve the impedance bandwidth across the targeted frequency bands and to reduce the size of antenna.

4.2 Antenna Geometry

Fig. 4.1, illustrate the geometry of the proposed CPW fed antenna for wireless communication systems. FR4 substrate with single sided clad is used for the fabrication of the proposed design with substrate thickness h = 1.6 mm with relative permittivity of 4.4. A CPW feed line is composed of a signal strip of width W_f with two finite ground planes of length Lg, and width Wg placed symmetrically on both sides of the feedline.

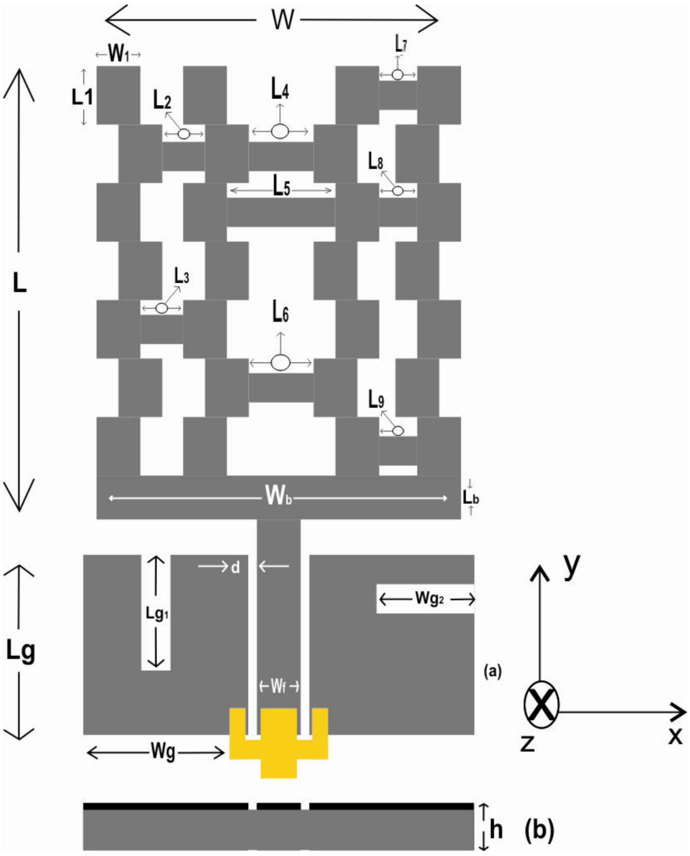

Fig. 4.1 Multiband Antenna Geometry using DGS Technique

The basic T-shaped structure loaded with modified CPW feed is proposed for generating the upper resonant mode. In CPW feed 'I' shaped slots are cut on both sides of ground planes. The four vertical monopoles are placed on top of basic T-shaped structure to obtain the lower resonant mode. Each of the vertical monopole is composed of rectangular shaped bricks of length L_1 and width W_1 place on the top of each other. The zigzag path such created is used to increase the electrical current length and to reduce the size of the proposed antenna. Four vertical monopoles are connected together by the few horizontal strips. These horizontal strips are helpful in merging the diverse frequency bands and to generate a wide band operation in both frequency bands. The eight horizontal strips of variable length are used to connect the vertical monopoles. In order to achieve compact size and better impedance matching, I-shaped (L_{g1}) defect and I-shaped (W_{g2}) defect is inserted along the y-axis and x-axis on both sides of the ground planes of CPW feed, respectively. The overall size of proposed antenna is 28.76 mm × 45.19 mm×1.6 mm.

4.3 Parametric Study

The parametric study of the proposed antenna has been done to achieve the optimum results. In this parametric study, we have varied the values of a single parameter and kept all other parameters as a constant. The effect of different parameters is presented in the following section:

4.3.1 Effects of T shaped and Four Vertical Monopoles

The two different configurations of the proposed antenna are presented in Fig. 4.2. Effects on proposed antenna's performance in terms of return loss is presented in Fig 4.3. It has been observed from the graph that the basic T-shaped antenna with DGS structure is responsible for producing the higher frequency bands. It has also been examined that four vertical monopoles are used to achieve the lower frequency band. The horizontal strips are used to connect the vertical monopoles and to obtain the wideband operation by merging the small frequency bands. These effects are studies in detail in the next two sections 4.3.2 and 4.3.3.

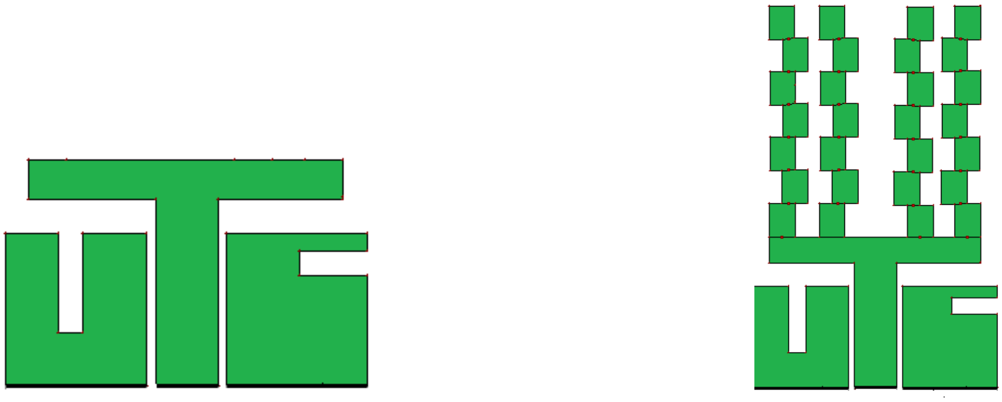

(a) Antenna 1 (b) Antenna 2

Fig. 4.2 Different Configurations of Proposed Antenna

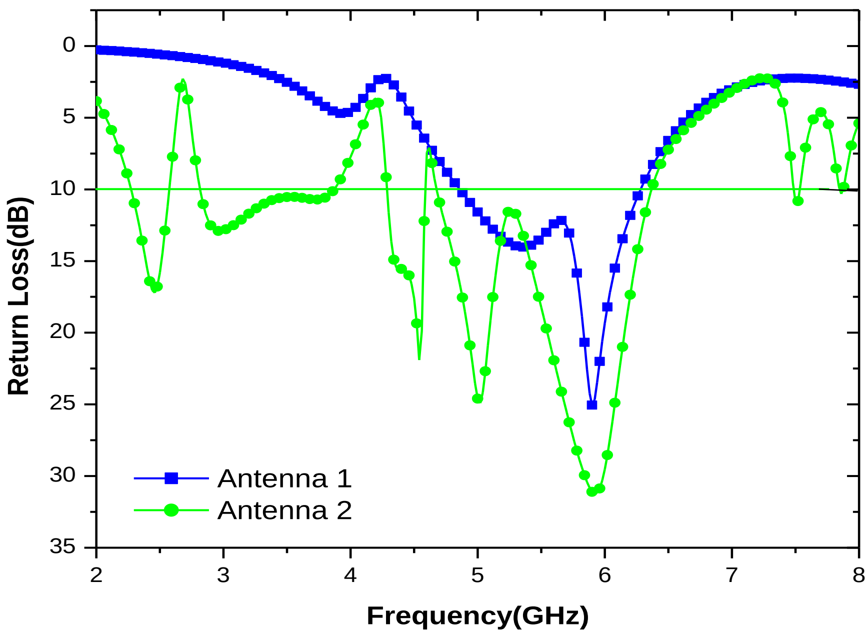

Fig. 4.3 Effects of T-shaped and Four Vertical Monopoles on Return Loss

4.3.2 Effects of Increasing Number of Vertical Monopoles

The four different configurations of the proposed antenna are represented in Fig. 4.4. Fig 4.5 shows the effects of all four vertical monopoles on return loss when they are placed one by one on the basic T-shaped structure. The graphical representation shows that a single vertical monopole (Antenna 1) provides the dual frequency bands with narrow impedance bandwidth. The graphical study shows that when two vertical monopoles are placed on the basic T-shaped structure to generate dual frequency bands. The impedance bandwidth obtained from Antenna 2 configuration is higher as compared to single vertical monopole. It has been observed from graph that placing three vertical monopoles (Antenna 3) provide triple frequency bands but the overall impedance bandwidth is less than as compared to Antenna 2 configuration. The upper frequency band is split into two small bands. All the four vertical monopoles (Antenna 4) are used to provide quad bands. It is clear from the graph that Antenna 4 configuration produces high impedance bandwidth as compared to all other configurations.

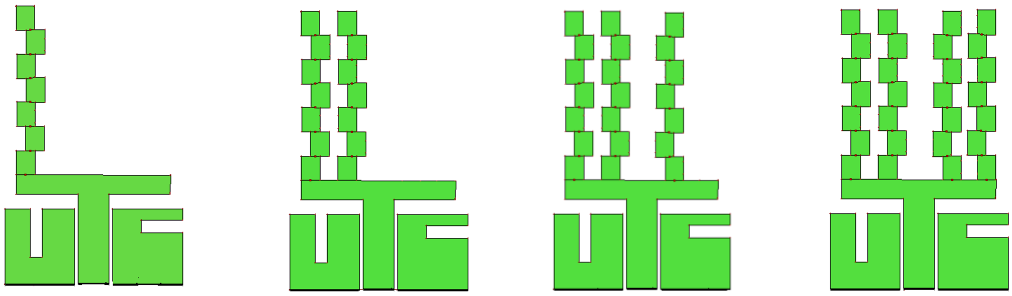

(a) Antenna 1 (b) Antenna 2 (c) Antenna 3 (d) Antenna 4

Fig. 4.4 Different Configurations of Proposed Antenna

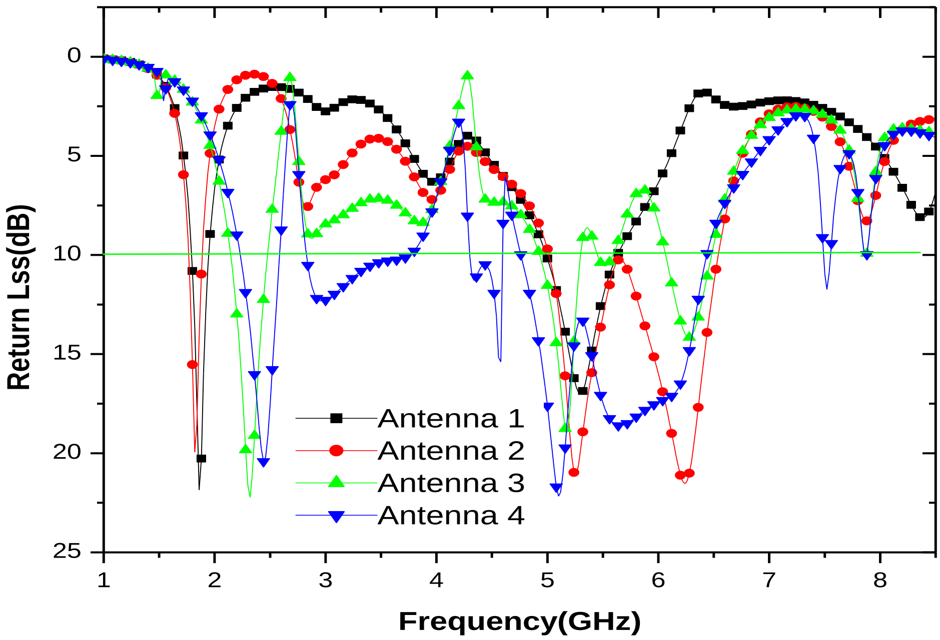

Fig.4.5 Effects of Vertical Monopoles on Return Loss

4.3.3 Effects of Horizontal Strips

Fig. 4.6 shows three different configurations of the proposed antenna with increasing number of horizontal strips. The effects of varying number of horizontal strips on impedance bandwidth of this antenna against frequency are demonstrated in Fig 4.7. The figure shows return loss in case of three antenna configurations after increasing the number of horizontal strips in each case. It has been observed from the graph that separate quad frequency bands are achieved without any horizontal strip (Antenna 1). The horizontal strips L_7, L_8 and L_9 (Antenna 2) are used to connect two right-hand vertical monopoles, which results in merging of the two frequency bands and provide a wideband operation from 4.63 GHz to 6.44 GHz. The horizontal strips L_4, L_5 and L_6 (Antenna 3) are used to connect the two central vertical monopoles, and have impact on the impedance bandwidth. The bandwidth of lower operating band is increased but the upper operating band is split into two bands. Further, improvement in the impedance bandwidth of lower frequency band is achieved by using horizontal strips L_2 and L_3 (Fig. 4.1) and the two upper frequency bands are merged to provide wideband operation.

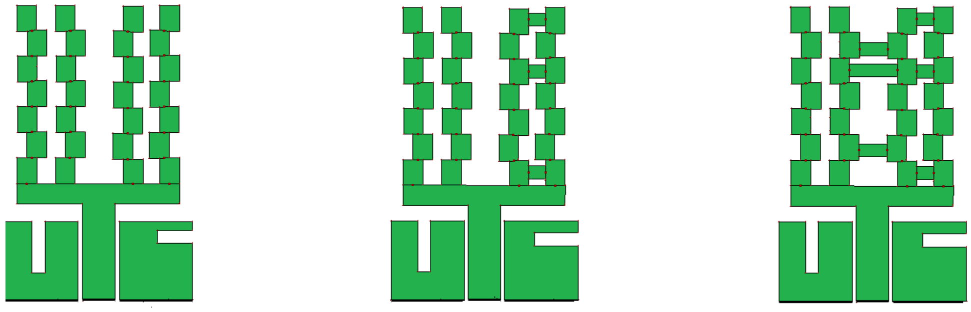

Antenna 1 **Antenna 2** **Antenna 3**

Fig. 4.6 Different Configurations of Monopole Antenna

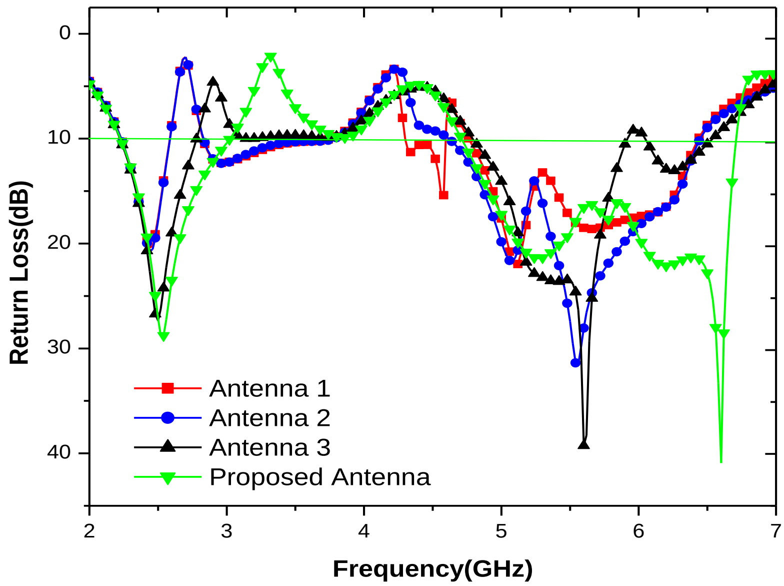

Fig. 4.7 Effects of Horizontal Strips on Impedance Bandwidth

4.3.4 Effects of Inserting Slots in the CPW Ground Plane

Two different configurations with slots inserted in the ground plane and third configuration without slot in ground plane of CPW feed are presented in Fig 4.8. The impact of inserting defects in the ground plane on return loss and bandwidth of the proposed design is depicted in Fig. 4.9. The simulated graph shows that proposed antenna without defects in the ground plane produces only the lower frequency band. It is also concluded from figure that defects in the ground plane have much impact on the high frequency band. It is also examined from graph that when slot is inserted only on the right hand side of the ground plane, then a small band is observed at upper resonating band. But when we include defect only on the left hand side of ground plane of CPW feed, a wide band operation at upper operating band is observed.

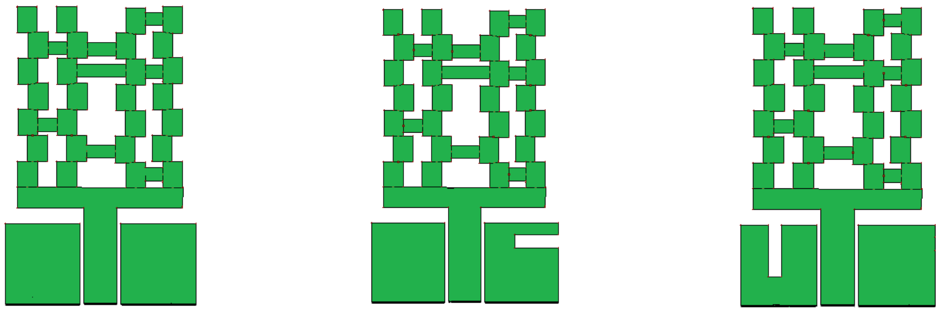

(a) Antenna 1 **(b) Antenna 2** **(c) Antenna 3**

Fig. 4.8 Different Configurations of Proposed Antenna

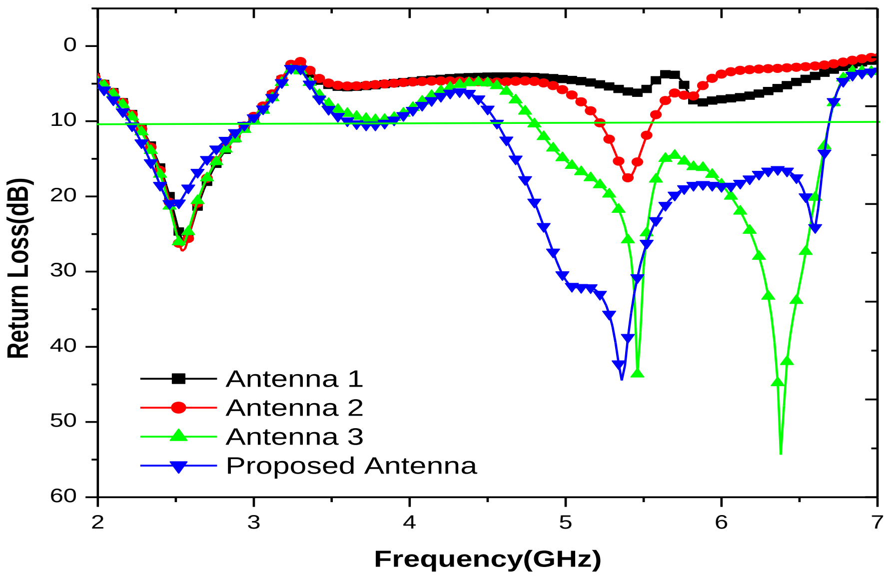

Fig. 4.9 Defects in Ground Plane of Proposed Antenna

4.3.5 Effect of Varying Slot Length in Ground Plane

The impact of varying the length of slots inserted in the ground plane of CPW feed is represented in Fig 4.10. In this configuration, only T shaped structure embedded with varying slots in the ground plane is considered. As we increase the length of the slot, the resonant frequency shifts towards the lower operating side. From the figure, it is clear that DGS based CPW feed antenna helps in miniaturization of the proposed antenna. When the length of slot increase from 4 mm to 6 mm and then further to 8 mm, then the resonant peak frequency shifts towards the lower frequency side.

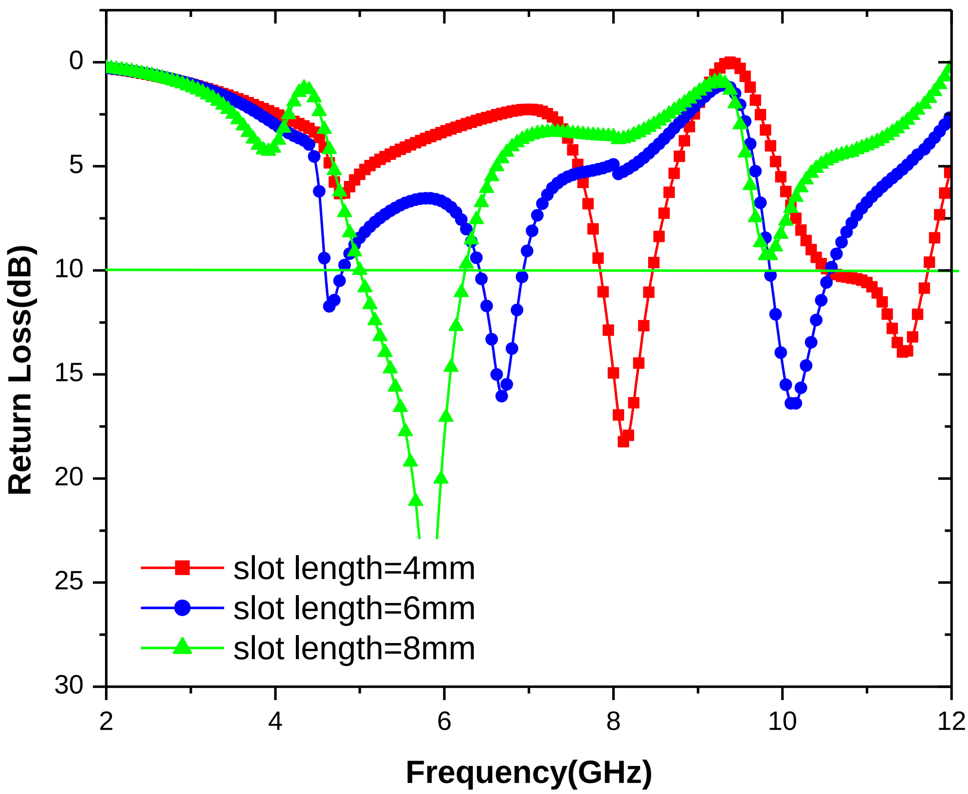

Fig. 4.10 Effects of Varying Slot Length in Ground Plane

4.4 Simulated Return Loss

The simulated return loss of the monopole antenna is depicted in Fig. 4.11 for the optimized parameters. From the graph, it is establish that the proposed antenna has three resonant peaks. The simulated results have impedance bandwidth ranging from 2.232 GHz to 3.12 GHz and 4.712 GHz to 6.81 GHz. It provides wide bandwidth to cover all the required bands of the Wi-Fi standard at 2.4 GHz, WLAN standard at 5.2 GHz and 5.8 GHz, WiMAX standard at 2.5 GHz, 3.5 GHz and 5.5 GHz, and LTE standard at 2.3 GHz frequency band. The optimized geometric parameters of the proposed antenna are presented in Table 4.1.

Table 4.1 Optimized Parameters of Monopole Antenna

Parameters	Diemensions (mm)
L	30.54
W	24.95
L_g	12.3
W_g	11.3
W_f	4.95
L_{g1}	7.9
W_{g2}	6.7
L_1	4
W_1	3
L_2	2.93
L_3	3.0
L_4	4.32
L_5	7.35
L_6	4.33
L_7	2.58
L_8	2.58
L_9	2.58
S_w	2.42
d	0.7

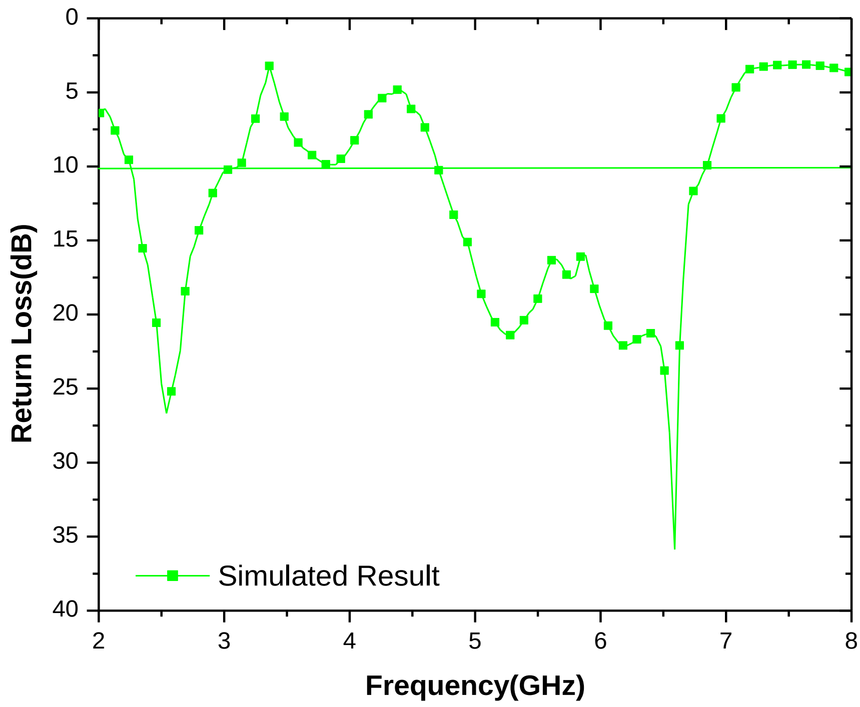

Fig. 4.11 Simulated Return Loss of Monopole Antenna

The same research methodology is used for the fabrication and the measurement of the proposed antenna as presented in the first chapter in section 1.6.5 and 1.6.6.

4.5 Measured Return Loss

The photolithography process is used to fabricate the proposed antenna. The prototype of the fabricated antenna is shown in Fig. 4.12. The return loss of antenna is measured by using Agilent VNA N5071F. The outcomes of the measured results show that a good impedance bandwidth ranging from 2.32 GHz to 3.61 GHz at lower operating band and 4.98 GHz to 7.94 GHz at upper operating band is achieved. For comparison purpose, the simulated and measured results are shown in Fig. 4.13 and a good agreement is seen. Both the curves show similar trends over the entire operating band. The peak resonant frequency is shifted towards higher side and this difference is due to the slight dimensional errors in the fabrication process. The effect of SMA connector is not considered in the simulation process but it was used in the experimental setup and it acts as a load of variable reactance, which affects the return loss of the design.

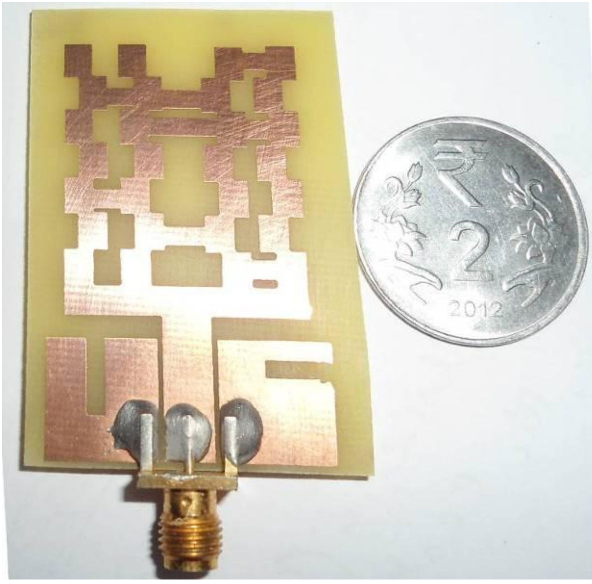

Fig. 4.12 Prototype of the Monopole Antenna

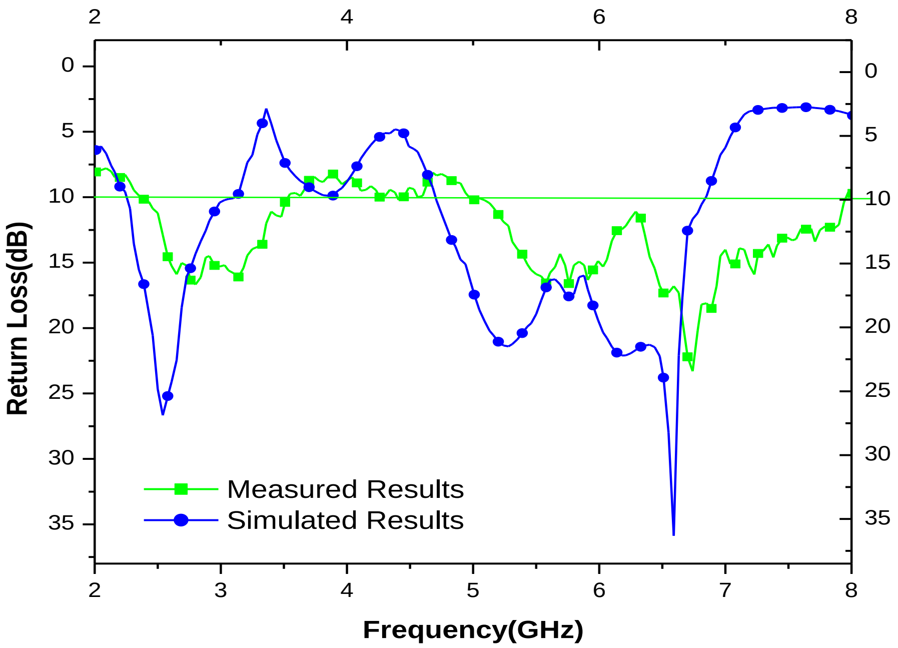

Fig. 4.13 Comparison of Simulated and Measured Return Loss

4.6 Simulated Gain

The simulated gain against frequency of this antenna is shown in Fig. 4.14. The optimum gain is about 3.07 dBi at 2.6 GHz in lower operating band of the proposed antenna. The optimum simulated gain is about 6.79 dBi at 6.6 GHz in the higher operating band.

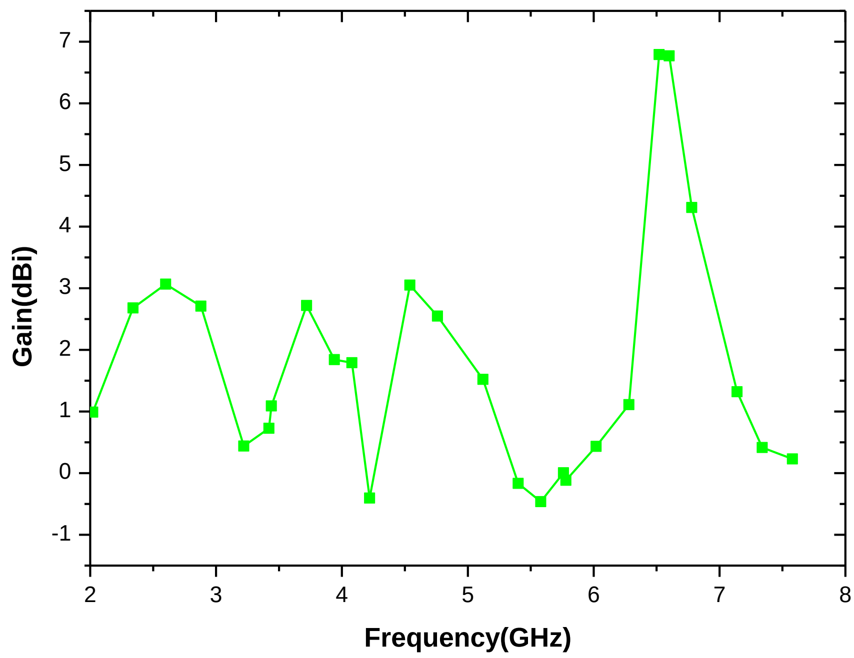

Fig. 4.14 Simulated Gain of the Proposed Antenna

4.7 Current Distributions

The current distributions of the antenna are presented in Fig. 4.15 at resonant frequencies. Arrows indicates the direction of flow of current on the patch surface. The red colour represents the strong current density where as blue colour represents the weak current density. It can be observed from the figure that four vertical monopoles and the defects in the ground plane are mainly responsible for producing lower frequency band as shown in Fig. 4.15 (a) at resonant frequency of 2.6 GHz. The upper operating band produced basically due to T-shaped structure with defects in the ground plane and small current flow around a few horizontal strips as presented in Fig. 4.15 (b) at frequency of 5.58 GHz.

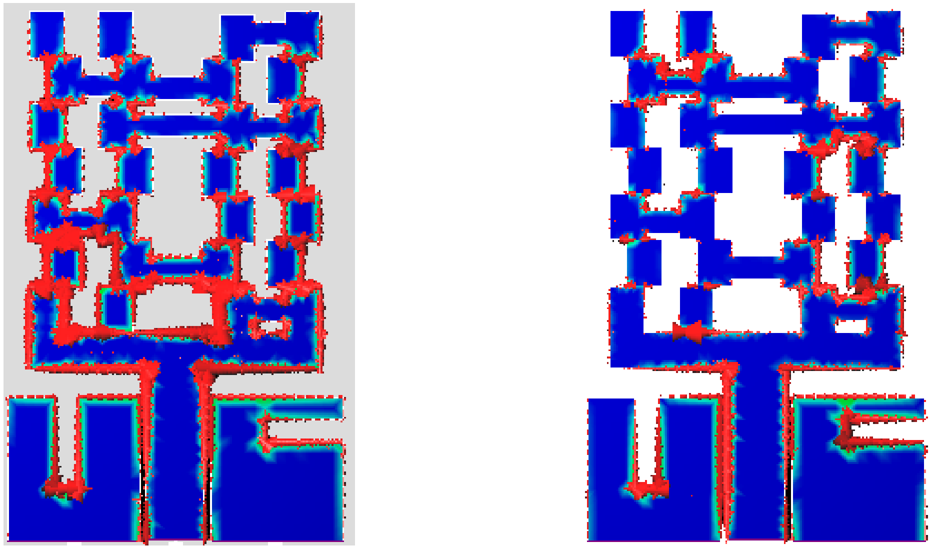

Fig. 4.15 Current Distributions at Frequency (a) 2.6 GHz and (b) 5.58 GHz

4.8 Radiation Pattern and Radiation Efficiency

The simulated and measured normalized radiation patterns of the proposed antenna are presented in Fig. 4.16 at a frequency of 5.7 GHz. The radiation pattern measurement is done inside an anechoic chamber to avoid any interfering EM energy from the surrounding sources. The radiation pattern observed in the azimuthal plane is nearly close to that of omni-directional, and that in the elevation plane looks like figure of eight. The maximum antenna radiation efficiency is approximately 100% at 6.6 GHz as depicted in Fig. 4.17.

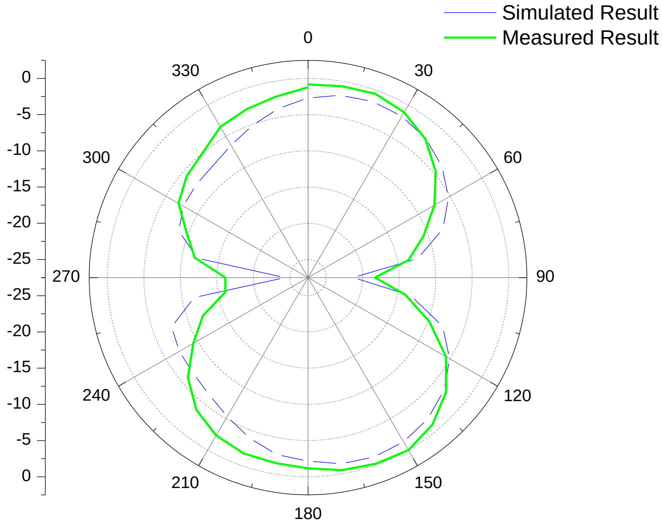

(a) Elevation Plane

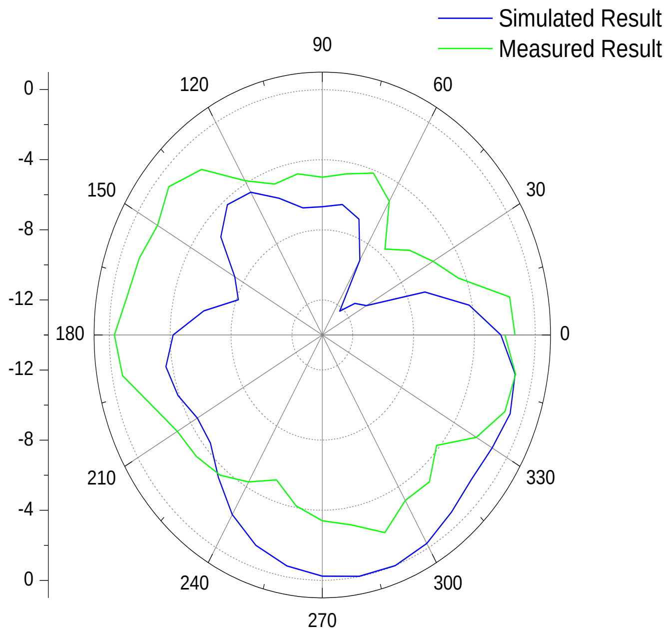

(b) Azimuthal Plane

Fig. 4.16 2D Radiation Pattern of Monopole Antenna at 5.7 GHz

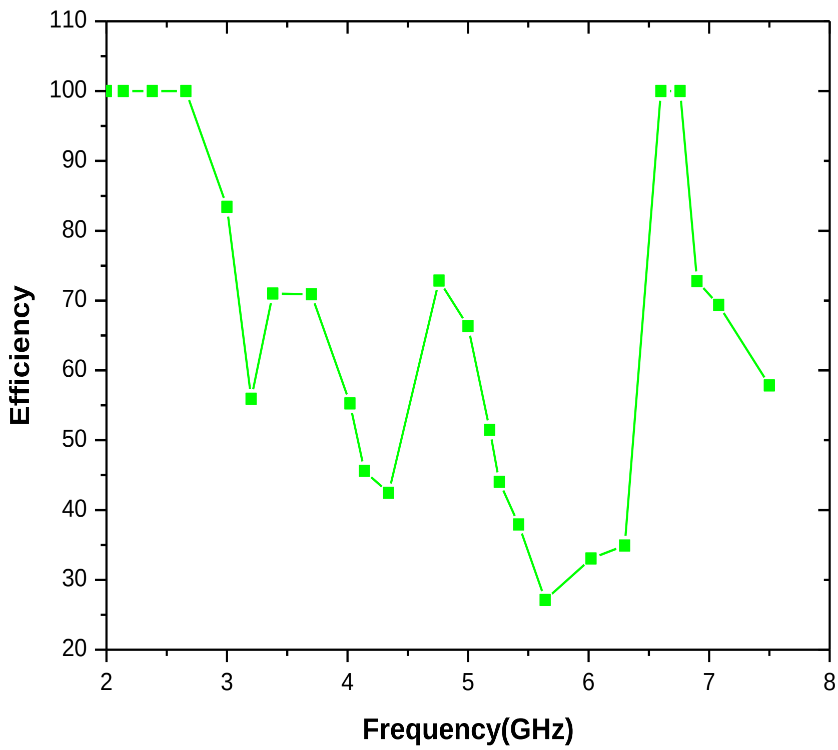

Fig. 4.17 Radiation efficiency of the Proposed Antenna

The summary of optimum results of the proposed antenna is given in the Table 4.2.

Table 4.2 Summary of the Optimum Results

Parameters / Bands	Frequency Band (GHz)	Bandwidth (%)	Max. Gain (dBi)	Max. Efficiency (%)
Lower Band	2.232 - 3.1	29	3.07	100
Upper Band	4.712–6.81	35	6.79	100

Conclusions:

A CPW fed planar monopole antenna based on DGS, comprises of a four vertical monopoles made up of horizontally displaced bricks. This antenna was characterized in terms of the return loss, gain, impedance bandwidth, current distribution, radiation pattern, and radiation efficiency. The proposed structure has been simulated and fabricated on a single sided substrate and tested to verify the design concept. The result of new antenna shows that it satisfies the bandwidth requirements of Wi-Fi/WLAN/WiMAX and LTE standards of heterogeneous wireless communication applications. In the next chapter, a new design is presented that is able to cover all the bands of WLAN/WiMAX/UWB standards.

CHAPTER-5

RECTANGULAR RING WITH INVERTED S AND C SHAPED STRIPS

5.1 Introduction

The purpose of this chapter is to present a microstrip-fed triple band antenna which is suitable for WLAN, WiMAX and UWB applications. UWB technology is probably going to dominate the home networking market. UWB technology gives a boost for wireless connecting devices over short distances and allows sharing of the spectrum with other users. The main advantages provided by UWB technology over Bluetooth are high data speed approximately 100 times than Bluetooth, cheaper and low power consumption.

The commercial application of the frequency band ranges from 3.1 to 10.6 GHz for UWB application. A compact, wideband and multiband antennas are required to integrate the various wireless communication standards into a single unit. The proposed antenna structure has been discussed and reported in the next section.

5.2 Antenna Geometry

A rectangular shaped ring antenna with dimensions of length L and width W has been proposed for WLAN/WiMAX and UWB applications. The geometry of the proposed microstrip line feed antenna is presented in Fig. 5.1 with its optimized parameters. The combination of three inverted 'S' and inverted 'C' shaped strips are used in the rectangular shaped ring antenna to generate the lower frequency bands. All meandering strips used in this antenna are of equal size. The ground plane of width Wg and length Lg is placed on back side of the radiating element of the patch. The overall sizes of antenna are 27.4 mm × 24.75 mm × 1.6 mm and volumetric size is approximately 1 cm^3. The results obtained by using IE3D software is also validated by using FEM based HFSS simulator.

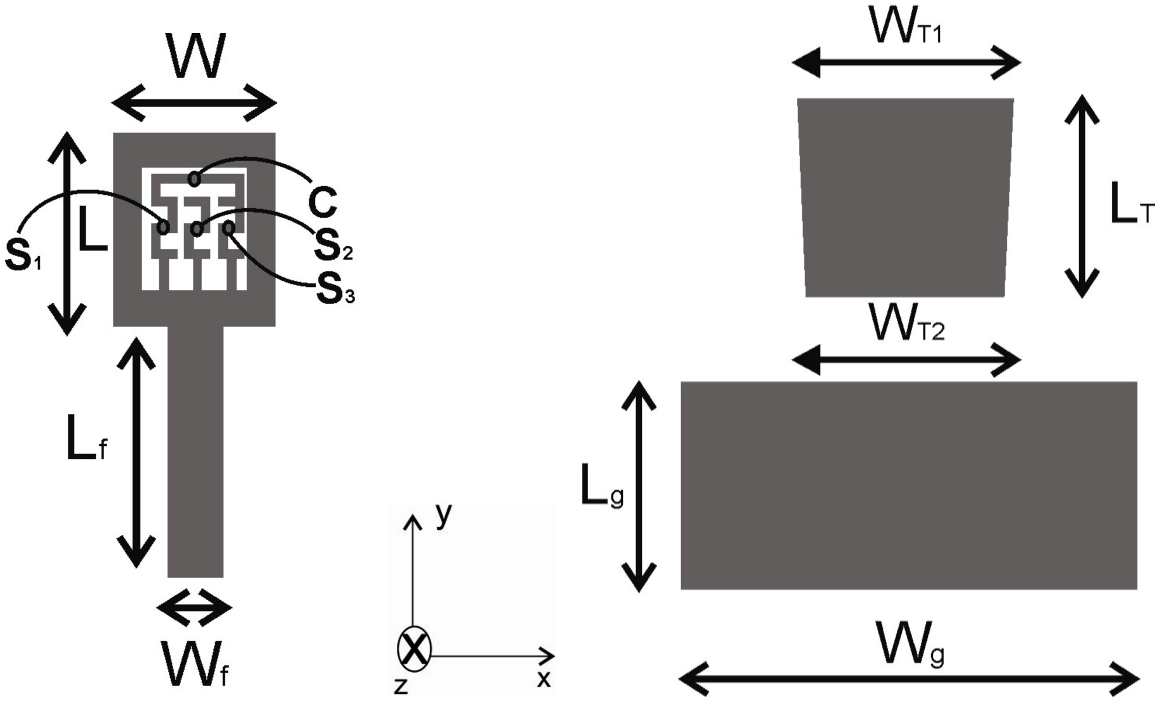

(a) Front View (b) Back View

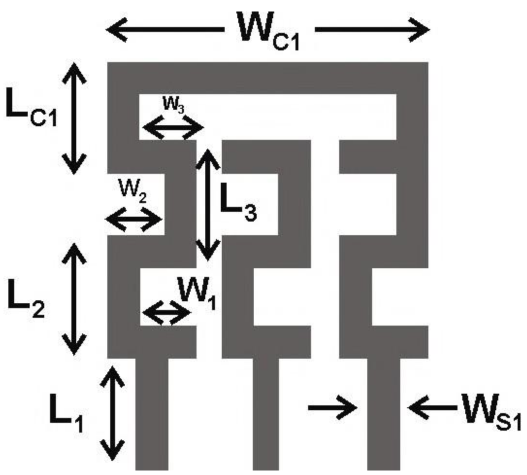

(c) Internal View of inverted 'S' and 'C' shaped strips

Fig.5.1 Geometry of the Rectangular Shaped Ring Antenna

5.3 Parametric Study

The parametric study of the proposed antenna has been done to achieve the optimum results. In this parametric study, we are varying the values of a single parameter while keeping other parameters as a constant. The effect of various parameters on return loss and impedance bandwidth is given in the following section:

5.3.1 Effects of Rectangular Shaped Ring and Basic T-shaped

The geometries of basic T-shaped (Antenna 1) and rectangular shaped ring (Antenna 2) are presented in Fig. 5.2. The effect various geometries on return loss with respect to frequency are presented in Fig 5.3. It has been seen from the figure that Antenna 1 configuration is responsible for producing the upper frequency band and the rectangular shaped ring (Antenna 2) antenna provides triple frequency bands. It has been observed from the results of Antenna 2 that two upper operating bands are nearly similar to bands present in the return loss of antenna and one extra lower frequency band with high bandwidth is also observed. The inverted 'S' and 'C' shaped strips provide the second and third frequency bands and their detailed study is presented in the next section.

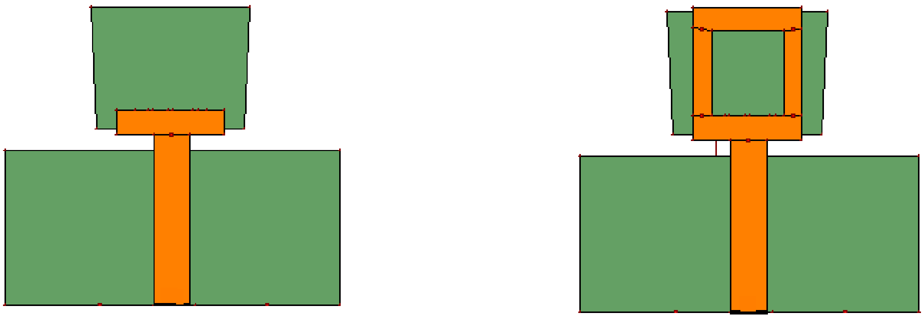

(a) **Antenna 1** (b) **Antenna 2**

Fig. 5.2 Different Geometries of Proposed Antenna

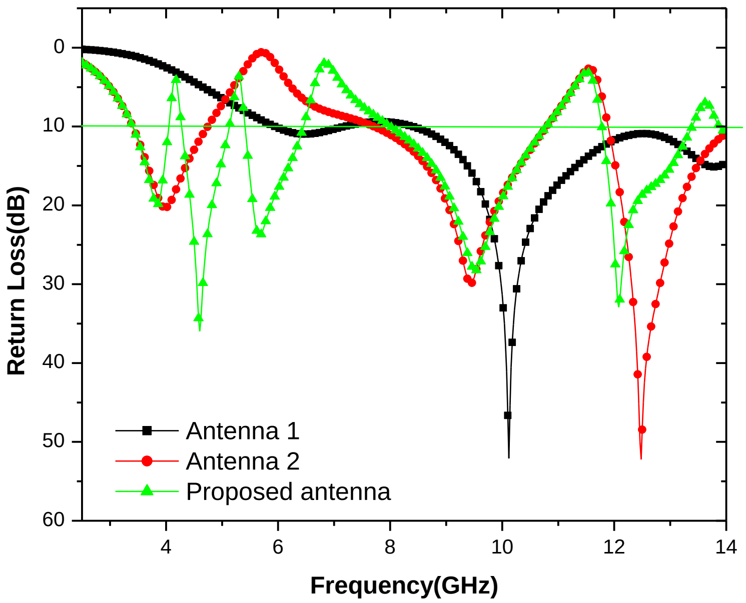

Fig. 5.3 Effects of T-shaped and Ring on Return Loss

5.3.2 Effects of Inverted 'S' Shaped Strip

The different configurations of inserting inverted 'S' shaped strips one by one in the rectangular shaped ring are presented in Fig. 5.4. The effects of three inverted 'S' shaped strips on the impedance bandwidth of proposed antenna are depicted in Fig. 5.5. The rectangular shaped ring antenna embedded with single inverted 'S_1' shaped strip (Antenna 1) is responsible for generating the quad bands. It has also been noticed that there is an improvement in impedance bandwidth due to this configuration. It has been examined from the figure that when inverted 'S_2'(Antenna 2) and 'S_3' shaped strips (Antenna 3) are inserted then there is huge increase in the impedance bandwidth of the proposed design. Due to this configuration, the two upper operating bands are merged together to achieve a wideband operation.

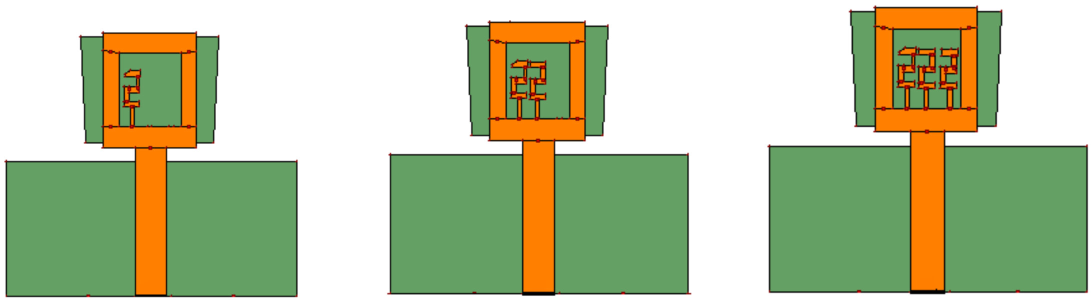

(a) Antenna 1 (b) Antenna 2 (c) Antenna 3

Fig. 5.4 Different Configurations of Proposed Antenna

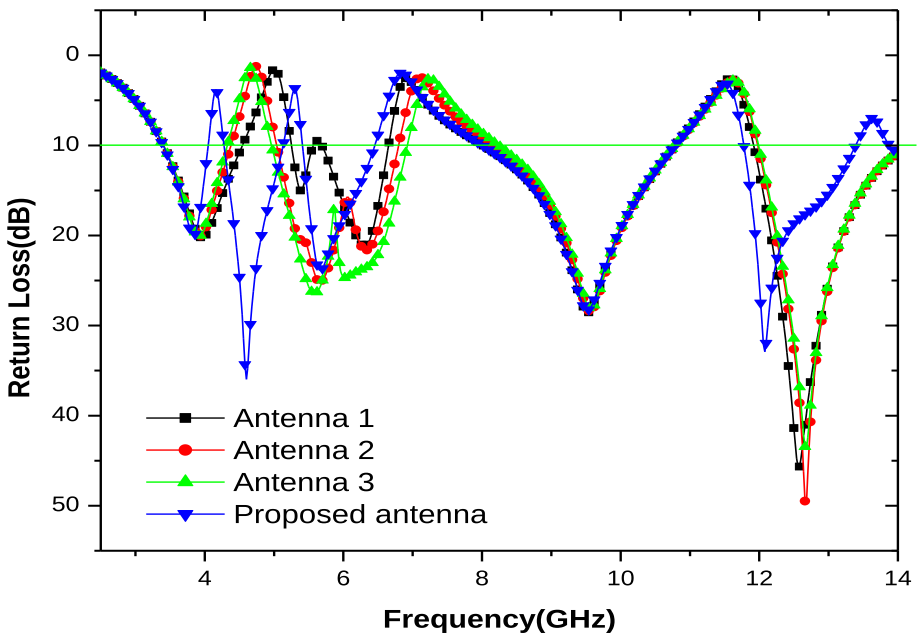

Fig. 5.5 Effects of Three Inverted 'S' Shaped Strips on Return Loss

5.3.3 Effects of Inverted 'C' Shaped Strip

The effect of inserting an inverted 'C' shaped strip over the inverted 'S' shaped strips on the return loss is presented in Fig. 5.6. The proposed configuration is responsible for generating the second frequency band and also results in the improvement of the impedance bandwidth of the antenna.

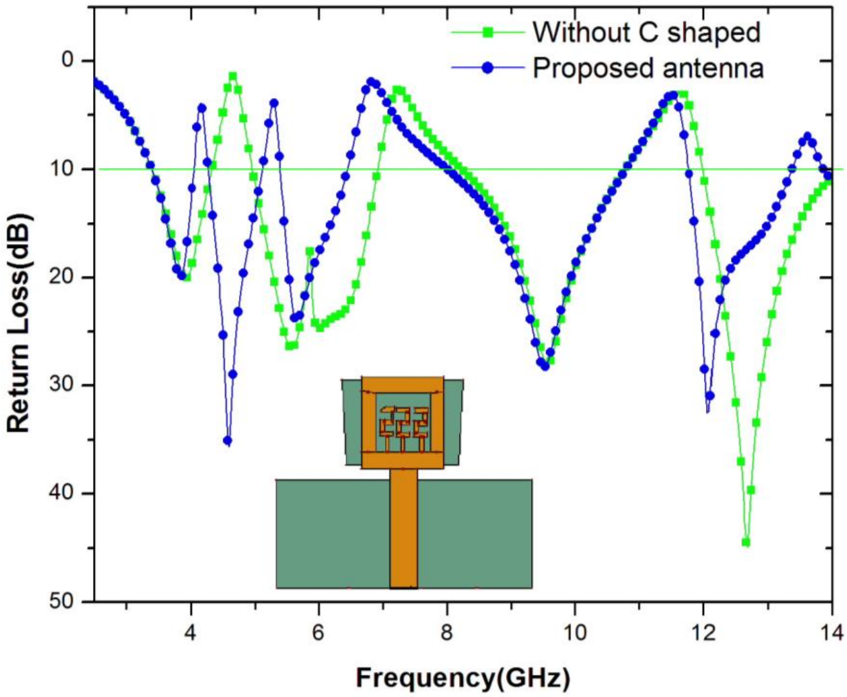

Fig. 5.6 Effects of Inverted 'C' Shaped Strip on Return Loss

5.3.4 Effects of Gap between Radiating Patch and Ground Plane

The configuration showing the varying gap (S_w) of the antenna is depicted in Fig. 5.7. The effects of varying gap (S_w) between ground plane and radiating patch, on the proposed antenna performance is shown in Fig. 5.8. It has been examined that as the value of Sw is decreased from optimized value (1.39 mm), then there is a decrease in the impedance bandwidth of the first, second and fourth frequency bands from the optimum bandwidth and the bandwidth of the third and fifth frequency bands are increased. It is also seen from the figure that by increasing the gap value from optimum value (1.39 mm), there is a small loss in impedance bandwidth of all the frequency bands from optimum impedance bandwidth.

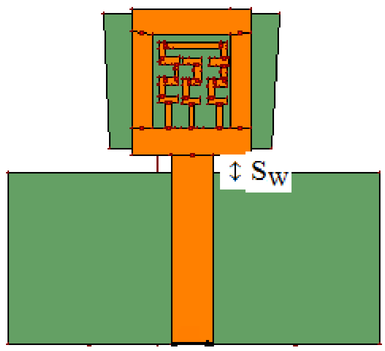

Fig. 5.7 Geometry of Gap between Radiating Patch and Ground Plane

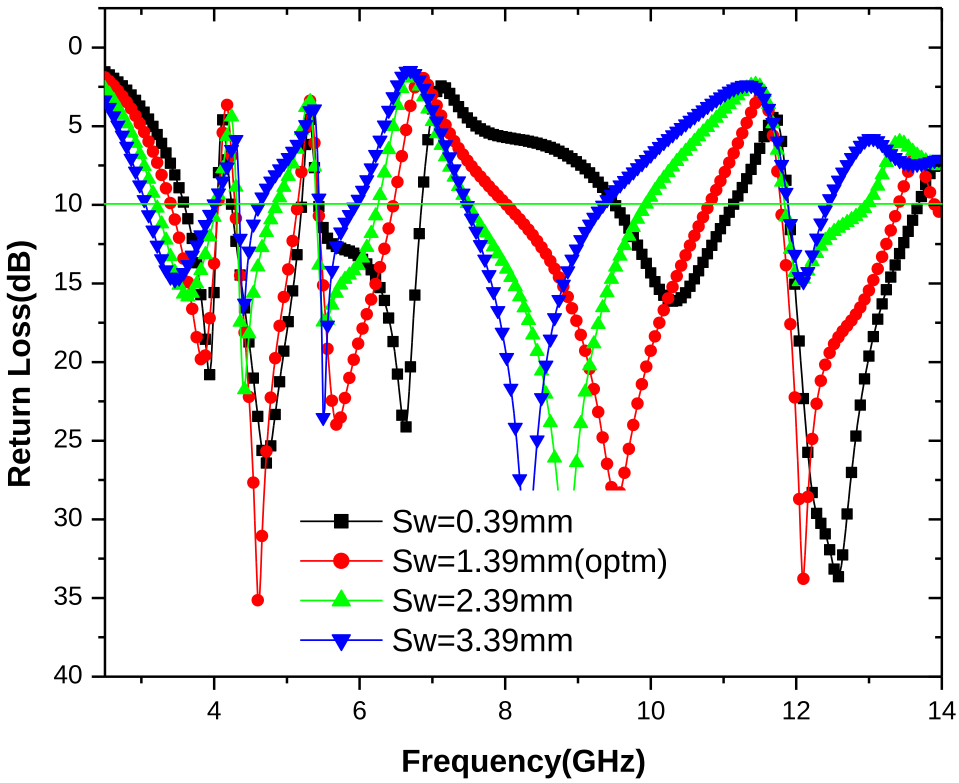

Fig. 5.8 Effects of Gap between Patch and Ground Plane on Return Loss

The optimized dimensions of the proposed RSR antenna are presented in Table 5.1.

Table 5.1: Optimized Parameters of RSR Antenna

Parameters	Diemensions (mm)
L	10.78
W	8.8
L_g	12.58
W_g	27.4
W_f	3
L_1	1.78
W_1	0.9
L_2	1.89
W_2	1.12
L_3	2
W_3	1
L_{C1}	1.37
W_{C1}	5.1
W_{s1}	0.5
W_{T1}	13
W_{T2}	12
L_T	10
g	1.78

5.4 Simulated Return Loss

The simulated return loss for the optimized antenna is obtained by using IE3D simulator and demonstrated in Fig. 5.9. It has been examined that this antenna has five resonant frequencies ranging from 3.416 GHz to 4.032 GHz, 4.312 GHz to 5.124 GHz, 5.3 to 6.44 GHz, and 8.036 GHz to 10.78 GHz and 11.78 GHz to 13.38 GHz. The antenna has a broad bandwidth which covers the required bandwidths of the WLAN standard at 5.2 GHz and 5.8 GHz bands, WiMAX standard at 3.5 GHz and 5.5 GHz bands and partially UWB standard ranging from 3.1GHz to 10.6 GHz with four band notches. The total impedance bandwidth of the multiband antenna is approximately 7.12 GHz.

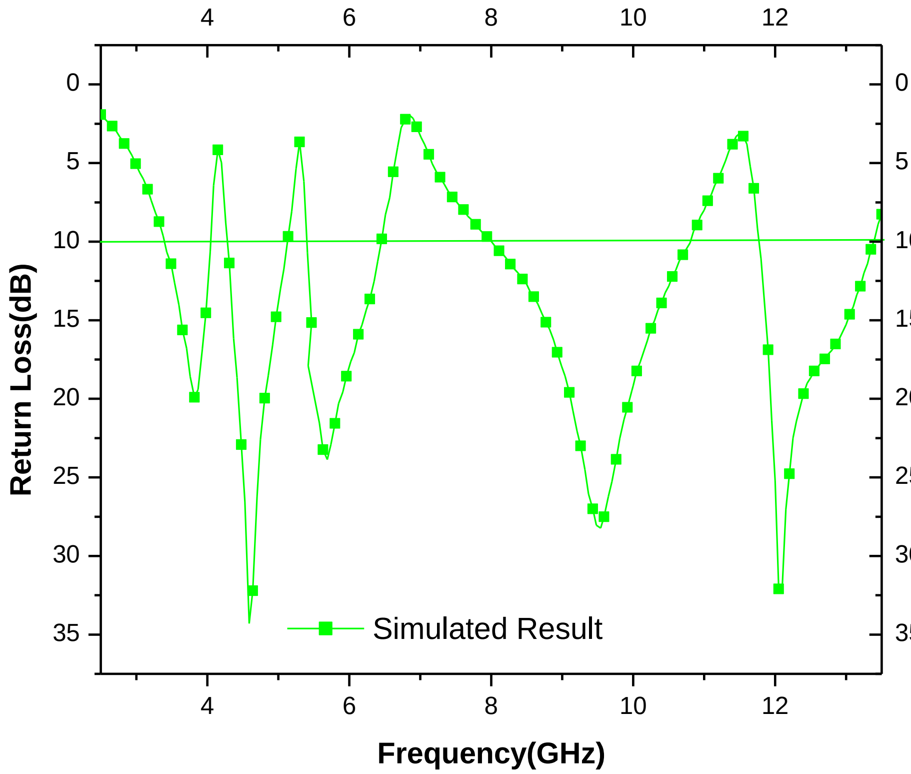

Fig. 5.9 Simulated Return Loss of RSR Antenna

5.4.1 Comparison between IE3D and HFSS Simulated Results

In order to compare the performance of antenna: Zeland IE3D and HFSS simulator are used to model the proposed antenna structure based on different numerical techniques. The comparison of return loss results obtained by using Zeland IE3D and HFSS software is shown in Fig. 5.10. The HFSS simulator also provides five resonant bands ranging from 3.8 GHz to 4.3 GHz, 4.4 GHz to 5.2 GHz, 5.5 GHz to 6.4 GHz, and 8.5 GHz to 10.95 GHz and 12.13 GHz to 13.34 GHz. HFSS simulator result has conformity with return loss obtained from the Zeland IE3D simulator. HFSS simulator is also used to validate the proposed antenna structure. It has been seen from figure that return loss results obtained from HFSS simulator has more precise result than IE3D simulator; HFSS results are also closer to measured results.

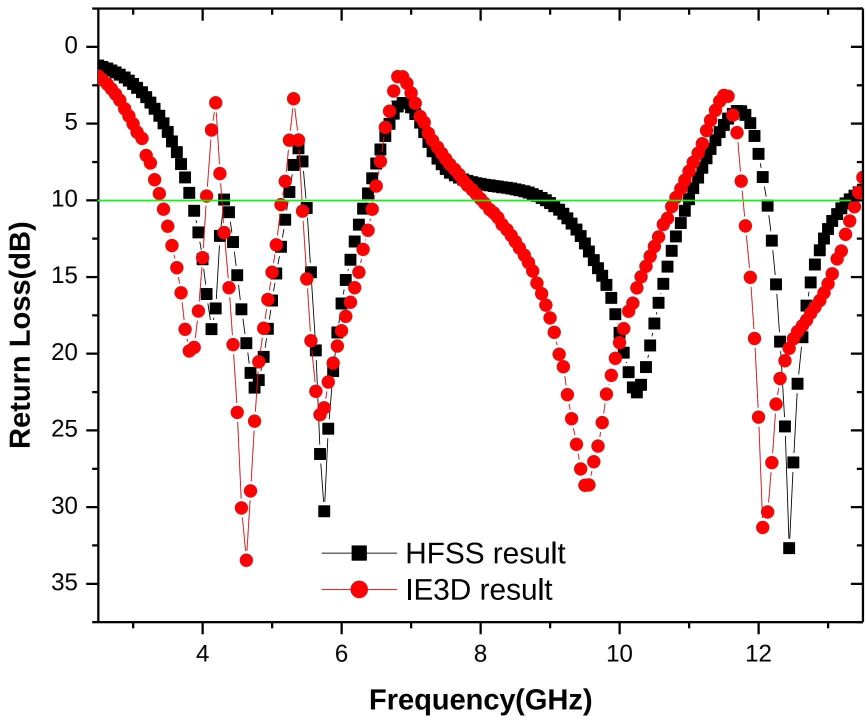

Fig 5.10 Comparison of Return Loss using Zeland and HFSS Simulators

5.5 Measured Return Loss

The prototype of the proposed antenna has been fabricated on FR4 substrate by using photolithography process. The front and back side views of the fabricated antenna are shown in Fig. 5.11(a) and 5.11(b), respectively. The VNA N5071 is used in measurement setup to measure the return loss of the antenna. Before starting the measurement process, the effects of Agilent VNA's system errors are removed by using the calibration technique. The SMA connector is soldered at the edge of the antenna under test (AUT). For measurement of return loss, the low loss 50 ohm coaxial cable is used to connect the AUT with the VNA's port 1. The comparison between IE3D simulated and measured return loss for the proposed antenna is presented in Fig. 5.12. It has been observed from graph that the total five resonant modes are obtained with the fabricated structure. The measured result has penta bands ranging from 3.6 GHz to 4.1 GHz, 4.3 GHz to 5.6 GHz, 5.8 GHz to 6.73 GHz, 7.34 GHz to 10.5 GHz and 12.1 GHz to 12.9 GHz. The proposed antenna can cover the WLAN standard at 5.2 GHz, and

5.8 GHz frequency bands, WiMAX standard at 3.5 GHz, and 5.5 GHz frequency bands, and also covers UWB standard.

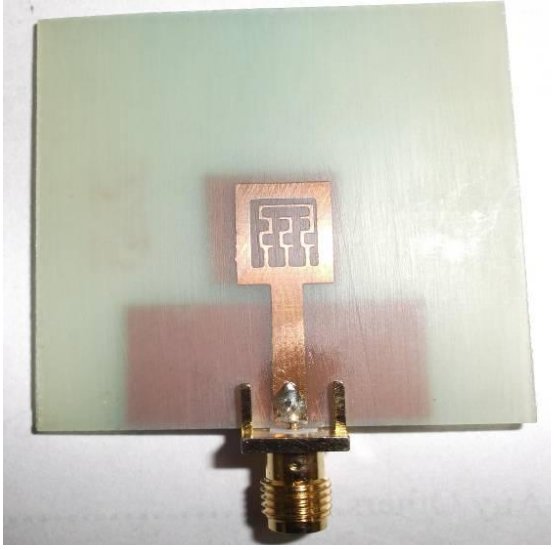

(a) Front View

(b) Back View

Fig. 5.11 Prototype of Fabricated Antenna

By comparing the simulated and measured results a fair agreement is seen over the whole frequency bands. A similar curve style for return loss between the measured and the simulated results has been witnessed over the entire frequency band. In measured result, there is a slight shift in frequency towards higher frequency side with a decrease in the impedance bandwidth. The displacement in the operating band may be due to the slight dimensional errors in the fabrication process. The effect of SMA connector is not considered in the simulation process but it was used in the experimental setup which act as a variable reactance and this loss is in addition to errors in processing. The huge loss in the impedance bandwidth of antenna has been observed in the fifth frequency band.

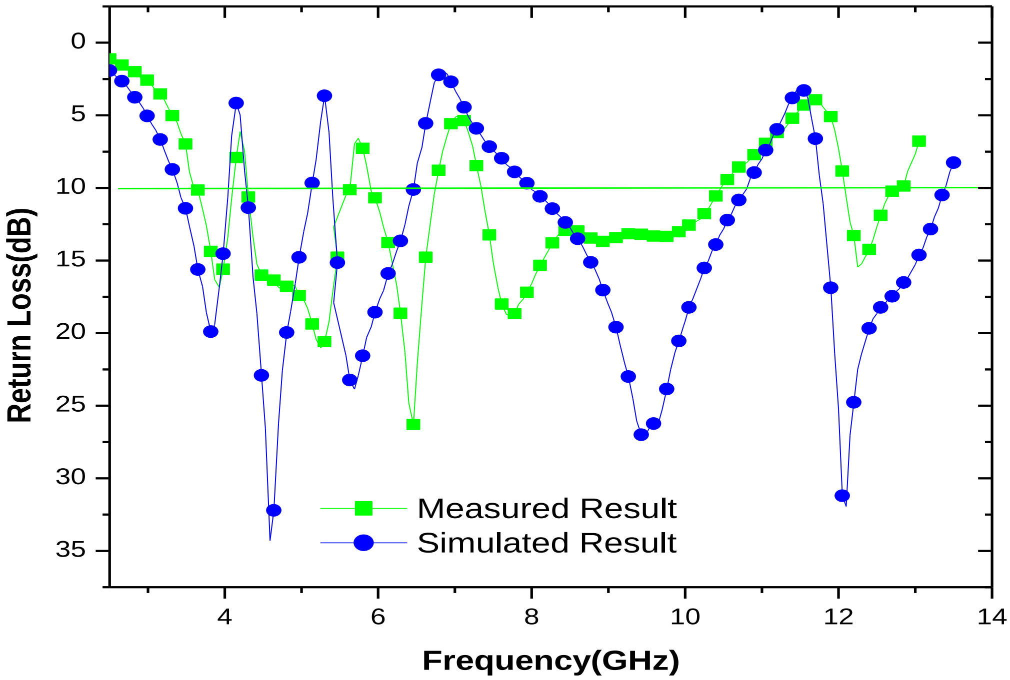

Fig. 5.12 Simulated and Measured Return Loss of Antenna

5.6 Current Distributions

The current distribution on surface of the proposed antenna is presented in Fig. 5.13. It has been observed that the strong current flows along the inverted ‘S_1’, ‘S_3’ and ‘C’ shaped strips and also along the rectangular ring of the antenna as shown in Fig. 5.13 (a) at frequency 3.64 GHz. These portions of the geometry are responsible for generating lower operating bands. The current distribution is presented in Fig. 5.13 (b) at resonant frequency of 5.9 GHz. The graph shows that the weak current flow along the inverted ‘S_2’ strip at frequency 5.9 GHz as compared to a frequency at 3.64 GHz.

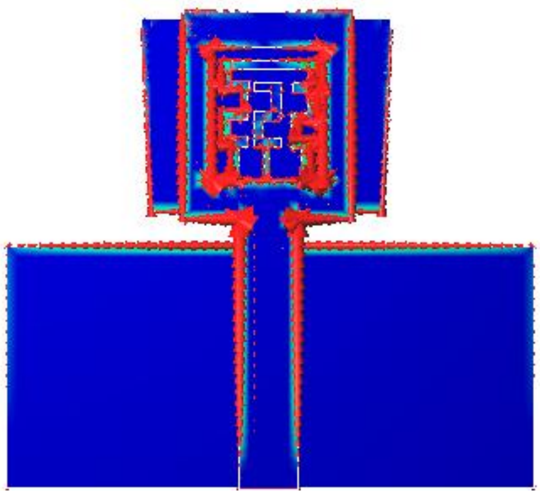

Fig. 5.13 (a) Current Distribution at 3.64 GHz

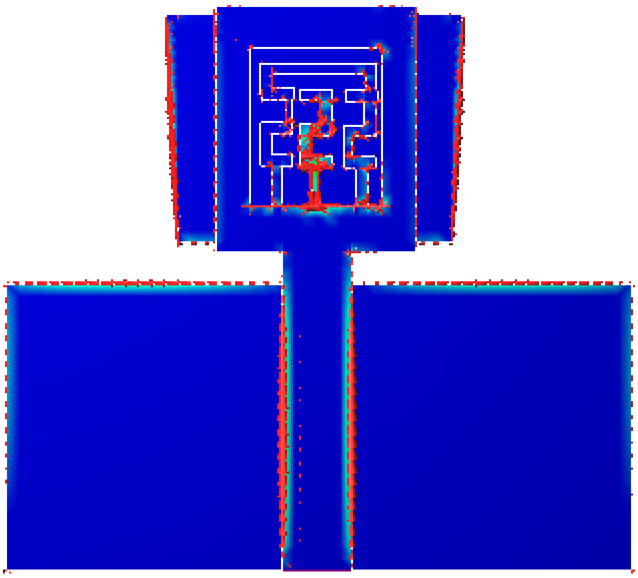

Fig. 5.13 (b) Current Distribution at 5.9 GHz

5.7 2D Radiation Pattern

The simulated 2D radiation patterns of the ring shaped antenna are presented in Fig. 5.14 at the frequency 4.5 GHz (a) Azimuthal Plane and (b) Elevation Plane. The radiation patterns obtained in the azimuthal plane are almost omni-directional antenna, and those in the elevation plane are all similar to figure of eight shape at both the frequencies.

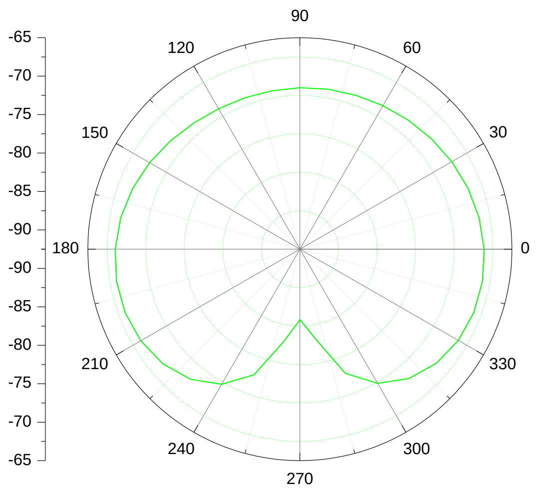

(a) Azimuthal Plane

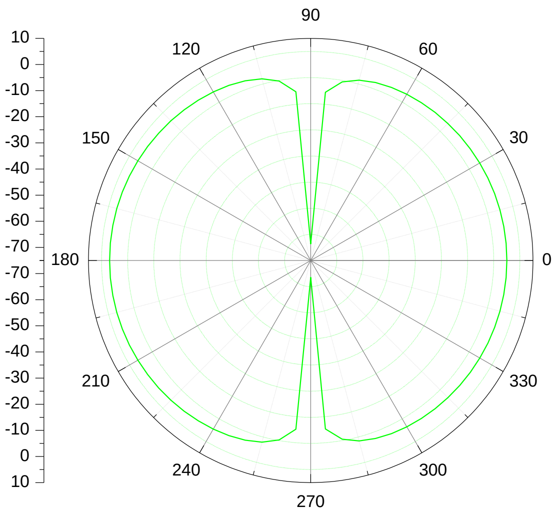

(b) Elevation Plane

Fig. 5.14 Simulated 2D Radiation Pattern

Conclusions

The rectangular-shaped ring antenna loaded with three inverted S and inverted C shaped strip has been proposed for WLAN/WiMAX and UWB applications and provide penta bands. The proposed structure has been simulated and fabricated on a single sided substrate and tested to verify the design concept. A good degree of agreement is observed between the simulated and measured results over the entire operating band. In the next chapter, a new design is proposed which is able to cover all the bands of WLAN, WiMAX and UWB standards with compact size.

CHAPTER-6

MULTIBAND RECTANGULAR SHAPED RING ANTENNA WITH VERTICAL STRIPS

6.1 Overview

A microstrip-fed ring shaped multiband antenna suitable for all the bands of WLAN, WiMAX and UWB standards is presented. The proposed antenna is an excellent candidate for emerging wireless and mobiles units to achieve the objective of multi-band, multi-standards technologies, and applications. The miniaturization of mobile handset is beneficial for customers. It is a serious challenge for antenna engineers. The miniaturization should not sacrifice the antenna performance. The MOM based IE3D simulator is employed for simulation and measurement is done for verification and validation of results. The proposed antenna structure is reported and discussed in detail in the subsequently sections.

6.2 Antenna Geometry

The new antenna structure consists of a rectangular shaped ring antenna embedded with three rectangular vertical strips. The proposed antenna provides a triple band operation with poor return loss. The three vertical strips L_1, L_2 and L_3 are used to improve the impedance bandwidth and provide wideband operation. The layout of the triple band antenna for WLAN/WiMAX/UWB systems is demonstrated in Fig. 6.1. A thick FR4 substrate of height h=1.6 mm, with dielectric constant of 4.4 is used for printing the slotted rectangular shaped patch antenna. The double sided copper clad sheet is used for fabrication of the antenna, on one side of substrate layer has radiating element whereas the back side is used as ground plane. A trapezoidal shaped conductor is used on the back side of radiating element to improve impedance bandwidth.

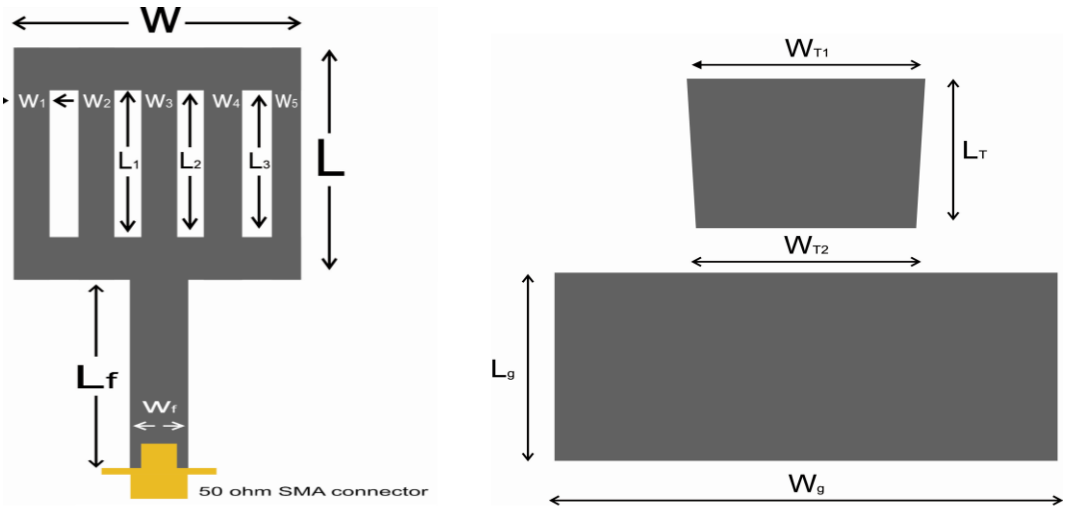

(a) Top View (b) Back View

Fig. 6.1 Geometry of the Rectangular Shaped Ring Antenna

The optimized geometric parameters of the antenna are: length of ring L = 16.47 mm, width of ring W= 11.79 mm, length of ground plane Lg =12.58 mm, width of ground plane Wg=27.39 mm, feed-line width W_f =3 mm, arm length L_1= L_2= L_3= 6.88 mm, strip width W_1 = W_4 =1 mm, strip width W_2 = W_3 = W_5 = 1.1 mm, and spacing between rectangular patch and ground plane S_w =1.4 mm. The optimal diemensions of the trapezoidal plane are: W_{T1} =13 mm, W_{T2}= 12 mm, L_T=10 mm and spacing g=1.78 mm. The overall dimensions of proposed antenna are 27.39 mm × 24.85 mm × 1.6 mm and the total volumetric size of the antenna is 1 cm^3.

6.3 Parametric Study

In the parametric study, one geometry parameter is varied with reference to the optimized value and keeping all the other parameters as constant. The effect on impedance bandwidth of the proposed antenna for different parameters is presented in the next section:

6.3.1 Effects of Basic T, L, U and Rectangular Ring

Fig. 6.2 shows the four different geometries of the proposed antenna. The effects of basic T, L, U and rectangular shaped ring on performance of antenna are presented in Fig. 6.3. The basic T shaped structure (Antenna 1) is responsible for generating single wideband ranging from 4.828 GHz to 9.756 GHz having poor return loss. It has been examined that L shaped structure (Antenna 2) is capable of generating dual frequency band with better return loss as compared to basic T-shaped structure. The U shaped structure (Antenna 3) produces a dualband operation with better return loss and bandwidth of the lower frequency band gets increased as compared to L shaped antenna. It has been seen that rectangular shaped ring (Antenna 4) generates a triple band having poor return loss as compared to the optimized antenna. In order to improve the overall impedance bandwidth, the rectangular shaped arm strips L_1, L_2 and L_3 are used.

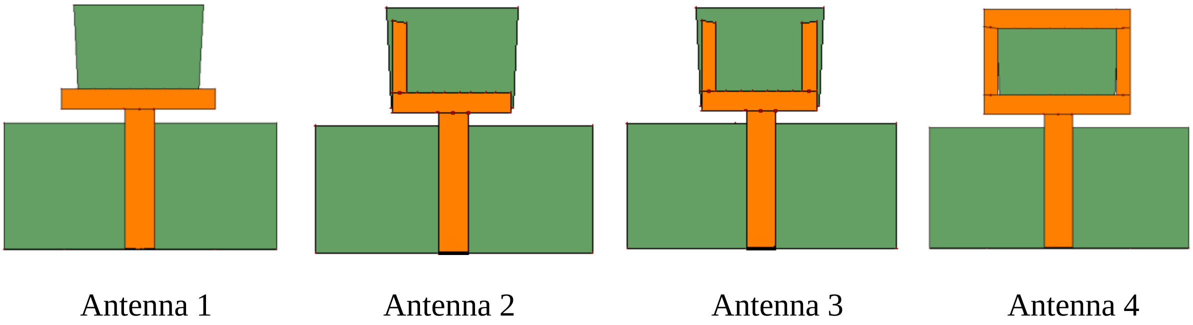

Fig. 6.2 Different Configurations of Proposed Antenna

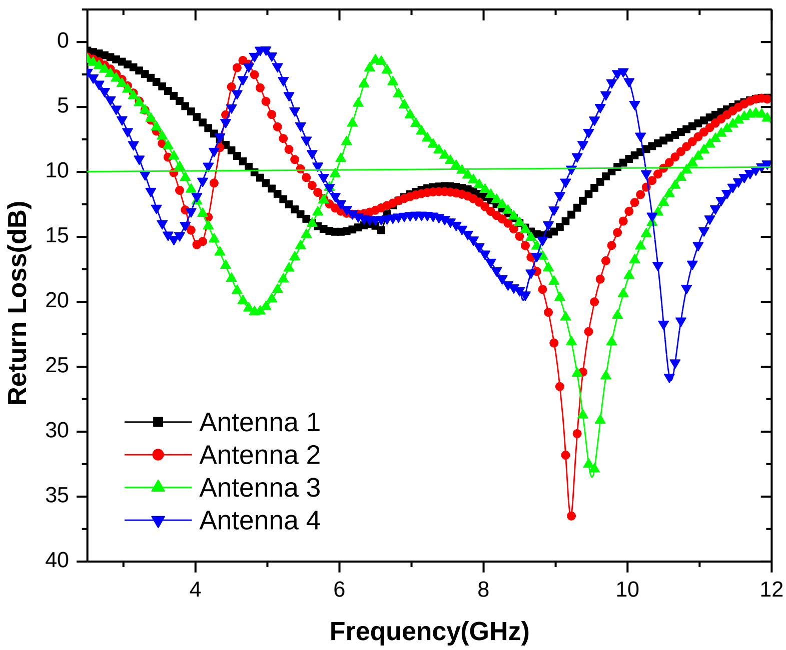

Fig. 6.3 Effects of T, L, U and Ring Strip on Return Loss

6.3.2 Effects of Rectangular Strips L_1, L_2 and L_3

The different configurations of the proposed antenna are presented in Fig. 6.4. The effects of inserting rectangular shaped strips L_1, L_2 and L_3 on antenna's return loss with respect to frequency are represented in Fig. 6.5. It has been noted from the graph that without strips L_1 (Antenna 1), there is a small loss in the bandwidth of the lower frequency band whereas bandwidth of middle and upper frequency bands are increased by a small amount. It is also examined that there is slight shift in peak frequency towards lower frequency in both lower and middle frequency bands. It has also been observed that without strips L_1, L_2 (Antenna 2), the bandwidth of the lower and upper operating bands gets decreased approximately by 45% from the optimum value of the bandwidth. It has also been observed that bandwidth of middle frequency band gets increased by double amount from the optimum value of bandwidth. It has also been seen from the simulation result that without strips L_1, L_2 and L_3, (Antenna 3) the bandwidth of the lower and upper frequency bands gets decreased approximately by 70% and 30% from the optimum value of bandwidth, respectively. The bandwidth of the middle frequency band gets increased by 2.5 times the optimum value of bandwidth.

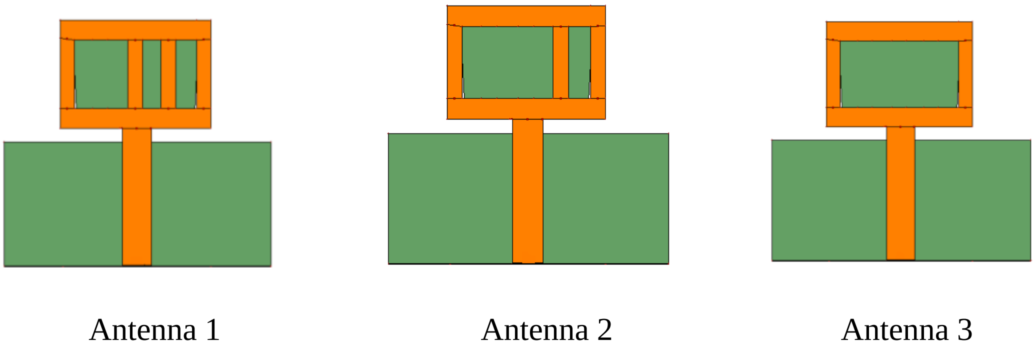

Fig. 6.4 Different Configurations of Proposed Antenna

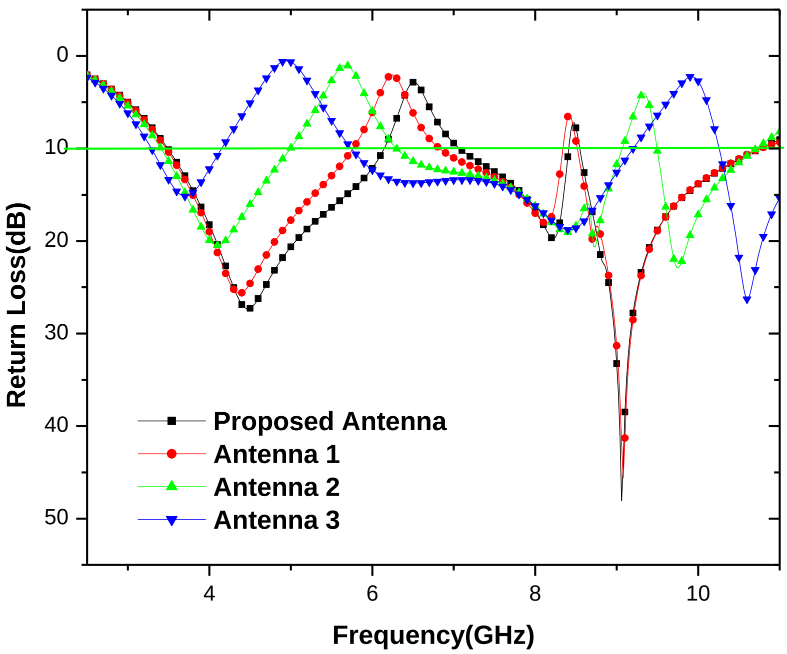

Fig. 6.5 Effects of Vertical Strips L_1, L_2, and L_3 on Impedance Bandwidth

6.3.3 Effects of Gap between Radiating Patch and Ground Plane

The effects of varying gap between ground plane and radiating patch (Sw) on the proposed antenna performance is depicted in Fig. 6.6. It has been seen that as the value of S_w is decreased by 1 mm, there is a decrease in the bandwidth of the upper resonant band by 30% from the optimum value of the bandwidth and two upper frequency bands are merged together to form a single wideband with slight shift in frequency toward higher frequency. It is also observed that further decrease in the value of S_w, there is a loss in bandwidth by 70% of lower frequency band and 45% of upper frequency band, respectively from optimum value of the impedance bandwidth. It is also concluded that by increasing the value of S_w, there is a slight decrease in bandwidth of the lower and middle frequency bands but the upper frequency band is largely affected.

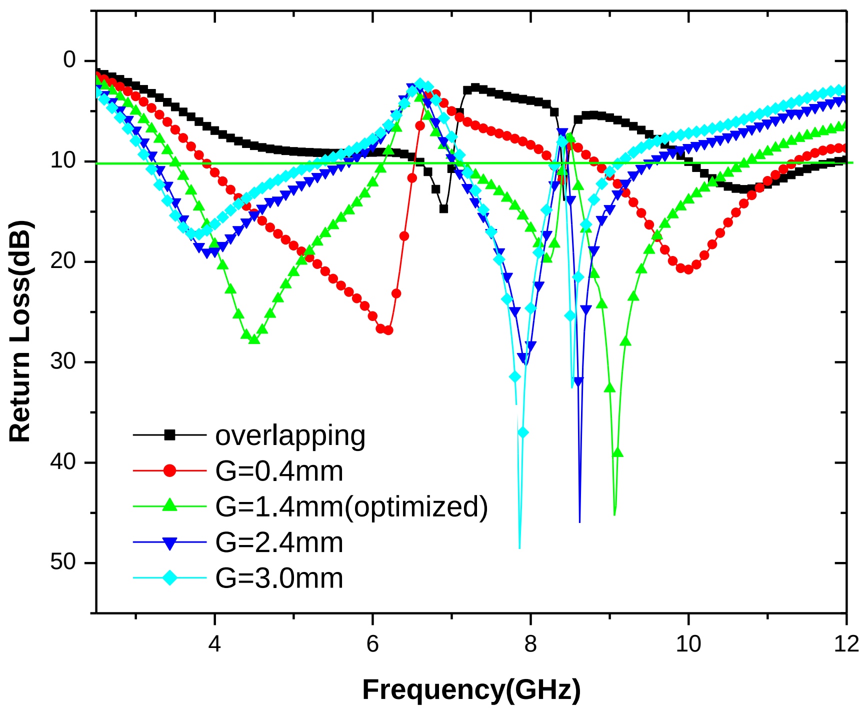

Fig. 6.6 Effects of Gap S_w on Impedance Bandwidth

6.4 Simulated Return Loss

The simulated return loss of the antenna for optimized parameters is presented in Fig. 6.7. It has been observed from the simulated result that has lower operating band ranges from 3.5 GHz to 6.14 GHz, middle operating band from 7.1 GHz to 8.4 GHz and upper frequency band from 8.56 GHz to 10.76 GHz, respectively. It is able to cover the required bands of WLAN standard at 5.2/5.8 GHz and WiMAX standard at 3.5/5.5 GHz and also covers UWB standard from 3.1 GHz to 10.6 GHz band. The total impedance bandwidth of the proposed antenna is 6.14 GHz. The band notch has been observed in graph from 6.15 GHz to 7 GHz frequency band.

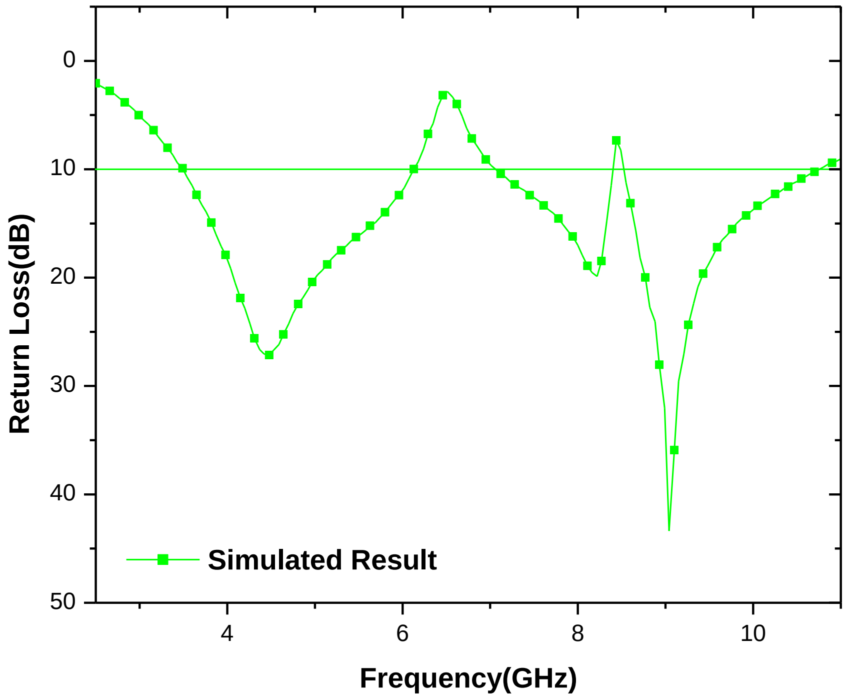

Fig. 6.7 Simulated Return Loss of Proposed Antenna

6.5 Measured Return Loss

The double sided copper clad substrate is used for the fabrication of the proposed antenna. The same research methodology is used for designing, fabricating and testing the proposed antenna. The photograph of the fabricated antenna is shown in Fig. 6.8. The Agilent VNA N5071 is used to measure the S-parameters of the proposed antenna. The calibration technique is used to remove the effects of the system errors. The SMA connector is soldered at the edge of the proposed antenna. For the measurement of impedance bandwidth parameter, low loss coaxial cable is used to connect the AUT with the VNA’s port 1. The simulated and measured return loss of rectangular shaped ring antenna is presented in Fig. 6.9 for comparison. The proposed antenna’s measured result has provided a broad dualband operation. The measured result has lower operating band ranges from 3.82 GHz to 5.96 GHz and upper operating band from 6.84 GHz to 10.1 GHz, respectively. The two upper frequency bands are observed in the simulated result but these bands are merged to form a single wideband in the measured result. The measured result covers all the bands of WLAN standard, and WiMAX standard and UWB standard of heterogeneous wireless communication systems.

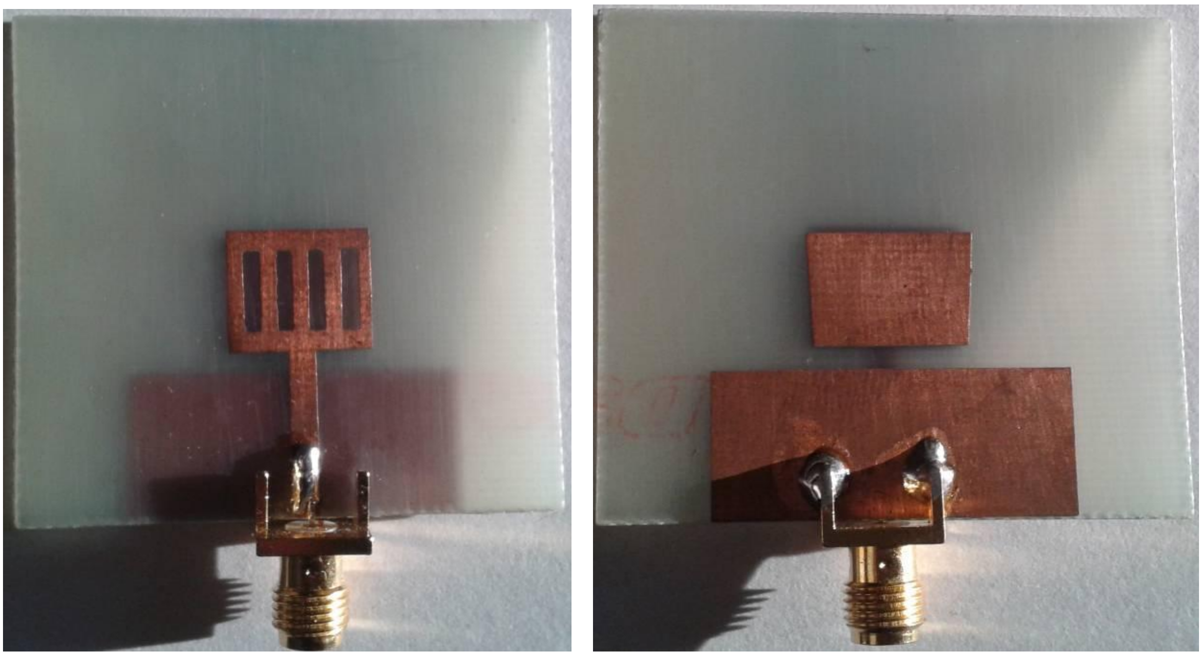

(a) Top View (b) Back View

Fig. 6.8 Photograph of Fabricated Prototype

A good degree of conformity is observed between the simulated and measured results. A similar curve trend for return loss between the measured and the simulated results is observed over the whole frequency band. The measured results show a slight shift in the frequency towards lower frequency band thereby causing loss in the overall bandwidth. The antenna diemensional parameters are changed during the fabrication process which produces the errors in the measured results and also due to extra adaptor used during measurement process between calibration end and proposed antenna. The SMA connector is responsible for shift in the frequency band and decrease in the impedance bandwidth.

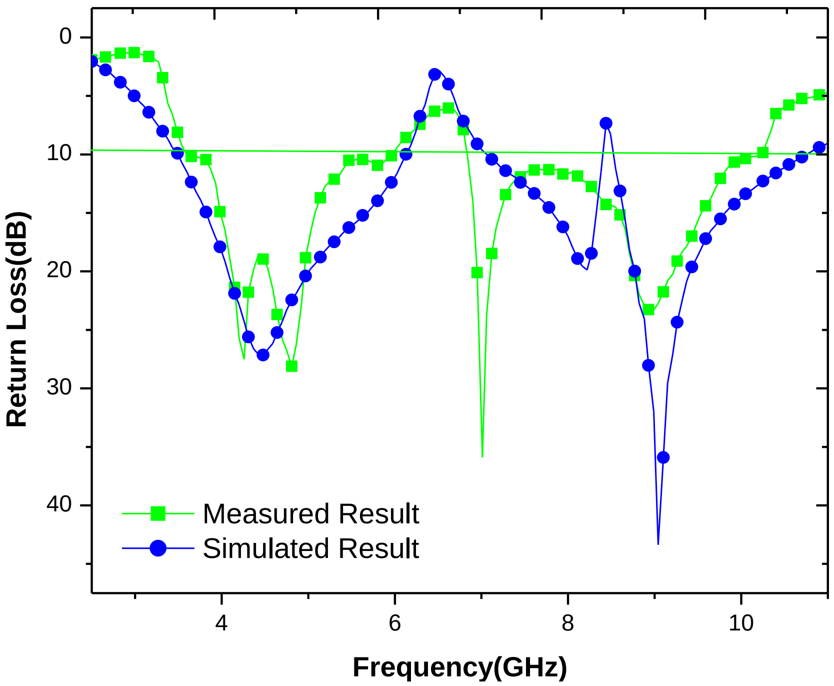

Fig. 6.9 Simulated and Measured Return Loss of the Proposed Antenna

6.6 Current Distributions

The current distributions of the proposed antenna are presented in Fig. 6.10. The current distribution at frequency 4.5 GHz of lower frequency band shows that small current flows along the rectangular strips especially along upper end of rectangular shaped ring and strong current flows along feedline of the proposed antenna as shown in Fig. 6.10 (a). It can be examined from the graph that arm lengths L_1, L_2 and L_3 are mainly responsible for producing the middle frequency band and also improvement in the bandwidth of the proposed antenna. Fig. 6.10 (b) shows that at frequency 7.4 GHz, the strong current flows along the arm lengths L_1, L_2 and L_3, and feedline and boundaries of the ground plane.

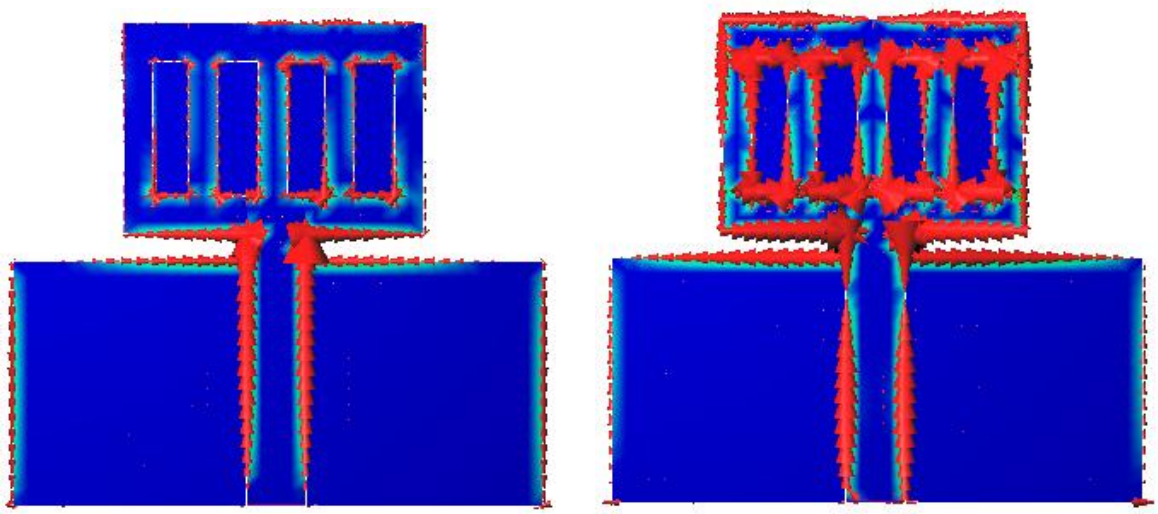

Fig. 6.10 Current Distribution at Frequency (a) 4.5 GHz (b) 7.4 GHz

6.7 Radiation Pattern

The simulated radiation patterns of multiband antenna embedded with rectangular shaped arm strips are demonstrated in Fig. 6.11 at 4.88 GHz frequency. The simulated radiation patterns of the proposed antenna in the azimuthal plane (x-y) and elevation plane (y-z) are shown in Fig. 6.11 (a) and Fig. 6.11 (b), respectively. The omni-directional radiations patterns are obtained in the azimuthal plane and those in the elevation plane are all similar to figure of eight shape. The peak antenna radiation efficiency is approximately 70%.

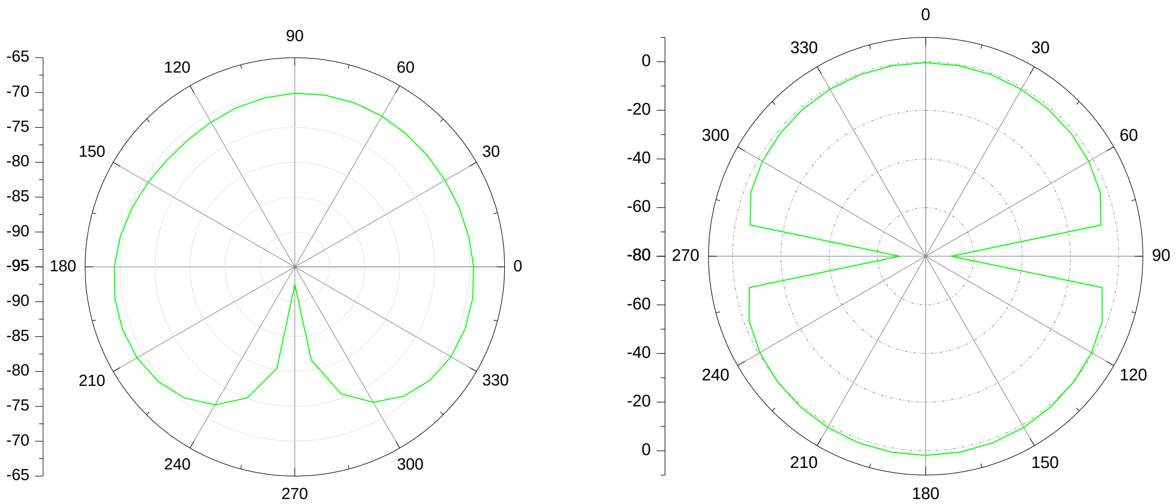

(a) Azimuthal Plane (b) Elevation Plane

Fig. 6.11 Radiation Pattern at 4.88 GHz Frequency

Conclusion

A new triple band rectangular shaped ring antenna inserted with rectangular shaped vertical arms has been proposed and is found to be suitable for WLAN/WiMAX and UWB applications. The simulated results provide triple band with wideband operation. The antenna has been optimized using parametric study. Finally, the optimized antenna is fabricated and tested. Both the measured and simulated curves show similar trends over the entire operating band. The antenna remains compact in size of 1 cm^3 with multiband operation which is suitable for heterogeneous wireless communication systems.

CHAPTER-7

CONCLUSIONS AND FUTURE SCOPE

7.1 Conclusions

This chapter brings the thesis to a close by summarizing the results obtained from simulation or numerical as well as experimental investigations conducted on antenna parameters of various new proposed antenna structures. The multiband antenna research, motivation and objective of the thesis have been discussed initially. The literature review on multiband antenna clearly convinces the importance of this work and novelty of work presented. Further, literature review is presented on different dual band, triple band and multiband antennas for Wi-Fi, WLAN, WiMAX and UWB technologies and applications. It also presents the gap in the present study and motivation for the present work. It is concluded that a lots of research is going on in field of multiband and broad band antenna design for Wi-Fi/WLAN/WiMAX and UWB applications. The selection of materials and research methodology employed for calculation of antenna design parameters, simulation and experimental investigations have been explained in detail. In this work, five multiband antennas are proposed, simulated, fabricated and tested for next generation heterogeneous wireless communication systems.

In first design, the rectangular shaped multiband antenna embedded with 'hash shaped slots' has been proposed for WLAN/WiMAX applications. The simulation impedance bandwidth of proposed antenna has two resonant frequencies with wideband operation. It provides two broadband ranging from 3.4 GHz - 4.132 GHz for lower frequency band and 4.312- 6.028 GHz for upper frequency band, respectively. The parametric study is conducted to understand the effect of the different parameters on the return loss of the antenna. The measured result shows that single wideband operating bandwidth is observed. The comparisons between the measured and simulated results show a satisfactory agreement over the whole operating band. The optimum simulated gain of this antenna is 5.51 dBi at 4.85 GHz frequency. The current distribution is also observed at different frequencies to study the behavior of radiating structure. The first design is modified by inserting I-shaped slot from the top of the patch to achieve three resonating modes with higher bandwidth. The modified antenna design provides the triple resonant frequencies which satisfy the requirements of WLAN/WiMAX systems.

In third design, the proposed antenna is composed of four vertical monopoles with CPW feed and defect in the ground plane has been proposed to achieve multi-band operation and which satisfy the bandwidth requirements of Wi-Fi, WLAN and WiMAX applications. The size of antenna is reduced by inserting the I-shaped defects in the ground plane. The simulated impedance bandwidths ranging from 2.232 GHz to 3.1 GHz and 4.712 GHz - 6.81 GHz. The measured result shows that dual-band operation has been obtained and also a fair agreement with the simulated result. The measured impedance bandwidths range from 2.32 GHz to 3.61 GHz at lower frequency band and 4.98 GHz to 7.94 GHz at upper frequency band, respectively. The measured result shows a good conformity with the simulated result. A comprehensive parametric study has been conducted to optimize the performance of the proposed antenna. The proposed antenna has a peak gain of about 6.79 dBi at 6.5 GHz frequency. The gain and impedance bandwidth and radiation pattern of the proposed antenna meets the requirements of next generation heterogeneous wireless communication systems.

In the fourth proposed antenna design is based on rectangular shaped ring embedded with three inverted ‘S’ and inverted ‘C’ shaped strips which generates the penta-band or multiband operation. The simulated impedance bandwidth of proposed antenna ranging from 3.416 GHz to 4.032 GHz, 4.312 GHz to 5.124 GHz, 5.3 GHz to 6.44 GHz, 8.036 GHz to 10.78 GHz and 11.78 GHz to 13.38 GHz. It has a broader bandwidth to cover the required bandwidths of the WLAN standard, WiMAX standard and UWB standard. The parametric study is conducted to understand the working of this antenna. The optimum antenna radiation efficiency is approximately 70%. The fabrication and testing of the proposed antenna is done to verify the design concept.

In the fifth design, rectangular shaped ring antenna based on microstrip feed has been presented. This proposed antenna is an answer to the recent demand of multi-function or multiband antenna for heterogeneous wireless communication systems. The simulated impedance bandwidths ranging from 3.5 GHz to 6.14 GHz for lower frequency band and 8.56 GHz to 10.76 GHz for middle frequency band and 7.09 GHz to 8.4 GHz for upper frequency band, respectively. The proposed antenna has a broad impedance bandwidth to cover the required bandwidths of the WLAN standard at 5.2 GHz and 5.8 GHz, WiMAX standard at 3.5 GHz and 5.5 GHz. The proposed antenna also covers the required bandwidth of the UWB standard band from 3.1 GHz to 10.6 GHz with band notch frequency at 6.15 GHz to 7 GHz. The optimum antenna radiation efficiency is approximately 80%. The fabrication and testing of the proposed antenna is done to verify the design concept.

Table No. 7.1: Performance evaluation Proposed Design with Literature

Design/Ref Parameters	Proposed Design 1	Proposed Design 3	Proposed Design 4	Proposed Design 5	Ref [64]	Ref [65]
Bandwidth (GHz)	3.4 - 4.132 4.31-6.028	2.232-3.12 4.712-6.81	3.416-4.082 4.312-5.124 5.3-6.44 8.036-10.78 11.78-13.38	3.5 – 6.14 7.1-8.4 8.56-10.76	2.368-2.563	2.38 - 2.51 5.10-5.88
Gain (dBi)	2.2-3.1 2.4-5.51	3.07 6.79	Low gain	Low gain	2.4 Low gain	2.04-2.58 Low gain
Bands Covered	WLAN 5.2/5.8 WiMAX3.5/5.5	WLAN/ WiMAX	WLAN/WiMAX/ UWB	WLAN/WiMAX/ UWB	WLAN 2.4 GHz but not able to cover higher bands	WLAN 2.4/5.2/ 5.8

Design/Ref Parameters	Ref [75]	Ref [76]	Ref [77]	Ref [80]	Ref [96]	Ref [104]
Bandwidth (GHz)	2.28 – 2.79 4.89 -5.32 5.71-6.17	2.36 -2.51 4.8-6.5	2.26-2.62 4.36-6.28	2.4	2.3-2.7	2.36-2.51 3.38-3.72 4.79-6.24
Gain (dBi)	Gain is not mentioned	1.47-1.57 3.31-3.94	1.3 at 2.44 GHz 2.8 at 5.32 GHz	Poor gain	Poor gain	0.64 1.87 3.74
Bands Covered/ Comments	Partially cover upper frequency bands of WLAN	Poor return loss in lower frequency band of WLAN	WLAN Poor gain	WLAN 2.4 GHz but no upper bands	WiMAX 2.5 GHz but not able to cover 3.5/5.5 GHz	WLAN 2.4/5.2/ 5.8 WiMAX 3.5/5.5 GHz

In conclusion, this thesis had met the objective of designing, simulating, fabricating and testing of triple band and multiband microstrip antenna for next generation heterogeneous wireless communication systems. However, there are still important areas that require further work and some of them will be illustrated in the next section.

7.2 Future Scope

Though an exhaustive study on multiband antenna design has been carried out in this work, still there is enough scope for improvement and further research. Some such works are briefly mentioned below:

1. The gain and efficiency of the antenna presented in this work are analyzed and found to be relatively small. Hence, it needs to be improved by using different techniques.
2. The design optimization of a triple band and multiband patch antenna has been implemented by using Particle Swarm Optimization (PSO) technique. This is interfaced with standard electromagnetic simulator (IE3D) using Matlab software. The performances of the PSO-IE3D combined antenna designs have better impedance bandwidth than the single tool used in this work.
3. The multiband fractal antenna can be designed by using the new fractal geometry like v-koch, Sierpinski gasket etc.
4. Neural network approach can be used to optimize the proposed design to achieve the better results and also used to validate the design concept.

REFERENCES

[1] Eko Tjipto Rahardjo, Fitri Yuli Zulkifli and Desi Marlena, "Multiband Microstrip Antenna Array for WiMAX Application," *in Proc. of APMC Conference*, ISBN: 978-1-4244-2641-6, 2008.

[2] T.S. Rappaport, *Wireless Communications*, *Principles and Practice.* Prentice Hall, 1996.

[3] Ehab Esam Dawood Al-Rawachy, "Design of Microstrip Patch Antenna for IEEE 802.16-2004 Applications," PhD dissertation, University Tun Hussein Onn Malaysia, April, 2011.

[4] Rohith K. Raj, "Development and Analysis of a Compact Dual-Band Coplanar Antenna," PhD dissertation, Cochin University of Science and Technology, Cochin, August, 2007.

[5] J. Schiller, *Mobile Communications.* Addison Wesley, 2000.

[6] Peter Lindberg, "Wideband Active and Passive Antenna Solutions for Handheld Terminals," PhD dissertation, Faculty of Science and Technology, Uppsala University, Feb., 2007.

[7] Z. Liu, P. Hall, and D. Wake, "Dual-Frequency Planar Inverted-F Antenna," *IEEE Transactions on Antennas and Propagation*, Vol. 45, No. 10, pp. 1451–1458, Oct. 1997.

[8] H. Bing, C. He and L. Jiang, "Performance Analysis of Vertical Handover in a UMTS-WLAN Integrated Network," *in Proc. IEEE International Symposium on Personal, Indoor and Mobile Radio Communication Proceedings, China*, 2003, pp. 187-191.

[9] R. Katz and M. Stemm, "Vertical Handoffs in Wireless Overlay Networks," *Mobile Network Application*, Vol. 3, No. 4, pp. 335–350, 1998.

[10] Syed Shameem, M. Sridhar, V. Vamsi Krishna, and S. Inthiyaz, "Design of Single Feed Multi-Frequency Patch Antenna," *Global Journal of Computer Application and Technology*, Vol. 1, Issue-4, pp. 796-805, 2011.

[11] Kin Lu Wong, *Planar Antenna for Wireless Communication.* Hoboken, New Jersey: John Wiley & Sons, Inc., 2003.

[12] Kush Agarwal, Nasimuddin, And Arokiaswami Alphones, "RIS-Based Compact Circularly Polarized Microstrip Antennas," *IEEE Transactions on Antennas and Propagation*, Vol. 61, No. 2, pp. 547-554, Feb. 2013.

[13] Hattan F. Abutarboush, "Fixed and Reconfigurable Multiband Antenna," PhD dissertation, Brunel University, London, United Kingdom, July 2011.

[14] Avtar Singh, "A Digital Signal Processor Based Hand-Held Multichannel, Multiple-Subject Biotelemetry System," *NASA Ames Report NCC2*-5112, 1995.

[15] Wen Chung Liu, Chao-Ming Wu and Yang Dai, "Design of Triple Frequency Microstrip Fed Monopole Antenna using Defected Ground Structure," *IEEE Transaction on Antennas and Propagation*, Vol. 59, Issue-7, pp. 2457 – 2463, 2011.

[16] B. T. P. Madhav, Vgkm Pisipati, N. V. K Ramesh, Habibulla Khan and P. V. Datta Prasad, "Planar Inverted-F Antenna on Liquid Crystal Polymer Substrate for PCS, UMTS, Wibro Applications," *ARPN Journal of Engineering and Applied Sciences*, Vol. 6, No. 4, April 2011.

[17] Rashid Ahmad Bhatti, Young Sin Shin, Ngoc-Anh Nguyen, and Seong-Ook Park, "Design of a Novel Multiband Planar Inverted-F Antenna for Mobile Terminals," *IEEE Proceedings of IWAT 2008, Chiba, Japan*, 2008.

[18] Available on http://en.wikipedia.Org/wiki/return_loss

[19] C. A. Balanis, *Antenna Theory: Analysis and Design*. Second Edition, John Wiley and Sons, 1997.

[20] Ramesh Garg, Prakash Bharti, Inder Bahl and Apisak Ittipiboon, *Microstrip Antenna Design Handbook.* London: Artech House Publishers, 2001.

[21] Available on: www.cisco.com/en/us/prod/collateral/wireless/ps7183/ps469/ prod_ whte _paper0900Aecd806a1a3e.pdf

[22] Available on: http://www.absoluteastronomy.com/topics/standing_wave_ratio

[23] Warren L. Stutzman, William A. Davis, *Antenna Theor.* Wiley Encyclopedia of Electrical and Electronics Engineering, Dec., 1999, DOI: 10.1002/047134608X. W1206.

[24] G.A. Deshamps, "Microstrip Microwave Antenna," *Presented At 3rd USAF Symposium Antenna*, 1953.

[25] J. Q. Howell, "Microstrip Antennas," *in Proc. IEEE APS International Symposium Digest*, 1972, pp. 177- 180.

[26] R. E. Munson, “Conformal Microstrip Antenna and Microstrip Phased Arrays,” *IEEE Trans. Antenna Propagation*, Vol. AP-22, pp. 74-77, 1974.

[27] Mohammad S. Sharawi, “Use of Low Cost Patch Antennas in Modern Wireless Technology,” *in Proc. IEEE International Conference*, 2006.

[28] H. Gutton, and G. Baissinot, “Flat Aerial for Ultra High Frequencies,” *French Patent* No.-703113, 1955.

[29] L. Lewin, “Radiation from Discontinuities in Stripline,” *IEEE Proceedings*, Vol. 107C, 1960, pp. 163-170.

[30] H. D. Weinschel, “Cylindrical Array of Circularly Polarized Microstrip Antenna,” *in Proc. IEEE Antenna Propagation Soc. International Symposium*, 1975, pp. 177-180.

[31] A. Derneryd, “A Theoretical Investigation of the Microstrip Antenna,” *Tech. Report PT-00929, Physical Science Laboratory, Las Cruce*, 1979.

[32] P.K. Agrawal, and M.C. Bailey, “An Analysis Technique for Microstrip Antennas,” *IEEE Transaction on Antennas Propagation*, Vol. AP. 25, pp.756-759, 1977.

[33] E.H. Newman and P. Tulyathan, “Analysis of Microstrip Antenna using Moment Method,” *IEEE Transaction Antenna Propagation*, Vol. AP-29, No. 1, pp. 47-53, Jan., 1981.

[34] Y. T. Lo, D. Solomon, and W. F. Richards, “Theory and Experiment for Microstrip Antennas,” *IEEE Transaction on Antennas Propagation*, Vol. AP-27, pp. 137-145, Mar. 1979.

[35] K. R. Caver and E. L. Coffey, “Theoretical Investigation of the Microstrip Antenna,” *Tech. Report PT-00929, Physical Science Laboratory, Las Cruce*, NM, 1979.

[36] P. Hammer, D. Van Bouchaute, D. Verschraeven, and A. Vande Capelle, “A Model for Calculating the Radiation Field of Microstrip Antenna,” *IEEE Transaction on Antennas Propagation*, Vol. AP-27, No. 2, pp. 267-270, Mar. 1979.

[37] C. M. Butler, “Analysis of Coax-Fed Circular Microstrip Antenna,” *In Proc. Workshop Printed Circuit Antenna Tech., New-Mexico State University, Las Cruce*, Oct. 1979, pp.13.

[38] J. W. Mink, “Circular Ring Microstrip Antenna Elements,” *Dig. International Symposium Antennas Propagation Society, Quebee City, Canada*, June 1980.

[39] L. C. Shen, “The Elliptical Microstrip Antenna with Circular Polarization,” *IEEE Transaction on Antennas Propagation*, Vol. AP-29, pp. 95-99, 1981.

[40] R. Chadha and K.C Gupta, “Green's Function for Circular Sectors, Annular Rings, and Annular Sectors in Planar Microwave Circuits,” *IEEE Transaction on Microwave Theory and Technique*, Vol. MTT-29, pp. 252-257, 1974.

[41] Girish Kumar and K.P. Ray, Broadband Microstrip Antennas. Boston, London: Artech House Inc., 2003.

[42] Vivekananda Lanka Subrahmanya, “Pattern Analysis of the Rectangular Microstrip Patch Antenna,” PhD dissertation, Electrical Engineering, University College of Boras School of Engineering, Boras, 2009.

[43] R. Saluja, A.L. Krishna, P.K. Khanna and D. Sharma, “Analysis of Bluetooth Patch Antenna with Different Feeding Techniques using Simulation and Optimization,” *IEEE International Conference on Recent Advances in Microwave Theory and Application*, Print ISBN:978-1-4244-2690-4, pp. 742-744, 2008.

[44] Available on: Http://Lib.Znate.Ru/Docs/Index-149720.Html?Page=4

[45] C.P. Wen, “Coplanar Waveguide: A Surface Strip Transmission Line Suitable for Non-Reciprocal Gyro-Magnetic Device Application,” *IEEE Transaction, MTT-17*, pp. 1087-1090, 1969.

[46] Davinder Parkash and Rajesh Khanna, “Multiband Antenna Structure for Heterogeneous Wireless Communication Systems Using DGS Technique” *International Journal of Microwave and Wireless Technologies, 2013*, Doi: 10.1017/S1759078713001104.

[47] Mihai Ghenghea, Angela Darie, and Ion Bogdan, “Matlab Based Teaching Tools for Antennas and Propagation,” *Asociatia Generala A Inginerilor Din Romania*, 2012.

[48] S. S. Yavalkar, R. T. Dahatonde, Dr. S. S. Rathod, Dr. S. B. Deosrkar, “Parametric Study for Rectangular Microstrip Patch Antennas,” *IOSR Journal of Electronics and Communication Engineering (IOSR-JECE)*, P- ISSN: 2278-8735. Volume 5, Issue 2, pp. 49-53, Apr. 2013.

[49] Zakir Ali Vinod Kumar Singh Shahanaz Ayub, “Broad Band Slotted Stacked Microstrip Antenna for Wireless Applications,” *International Journal of Advanced Research in Computer Science and Software Engineering*, Volume 2, Issue 2, pp. 1-4, February 2012.

[50] G. Senser, L. Aladan, M. Kuzuoglu, “Use of Matrix Padé Approximation in the Analysis of Irregularly Shaped Patch Antennas with Multiport Network Model,” *in*

Proc. International Conference on Electromagnetics in Advanced Applications, ICEAA '09, 2009.

[51] Ranjit Kumar, Ranjit, Research Methodology, A Step By Step Guide for Beginners. 3rd Ed., Sage Publications Ltd., 2011.

[52] Available on:www.zeland.com

[53] Available on:www.ansoft.com

[54] Available on:www.agilent.com

[55] Q. Ni, L. Romdhani, T. Turletti, "A Survey of Qos Enhancements for IEEE 802.11 Wireless LAN," *Wiley Journal of Wireless Communications and Mobile Computing* Vol. 4, no. 5, pp. 547–566, 2004.

[56] S.G. Glisic, Advanced Wireless Networks: 4G Technologies. Wiley Publishing, 2005.

[57] IEEE 802.11a-1999, "IEEE Standard for Local and Metropolitan Area Networks Specific Requirements – Part 11:" *Wireless LAN Medium Access Control (MAC) and Physical Layer (PHY) Specifications High Speed Physical Layer in the 5 GHz Band*, 1999.

[58] IEEE 802.11g-2003, "IEEE Standard for Local and Metropolitan Area Networks Specific Requirements – Part 11:" *Wireless LAN Medium Access Control (MAC) and Physical Layer (PHY) Specifications Amendment 4: Further Higher Data Rate Extension In The 2.4 GHz Band*, June 27, 2003.

[59] Atheros Communication, 'Super G Maximizing Wireless Performance,' Www.Super-G.Com/Atheros_Superg_Whitepaper.Pdf, 2004

[60] J. Geier, Wireless LAN's. Second Edition, SAMS Publishing House, 2002.

[61] Available on: Http://www.wimax.com/commentary/news/wimax_industry_news/news2-20-2006mw2

[62] Available on:http:en.wikipedia.org/wiki/wimax/wimax

[63] Available on:http:en.wikipedia.org/uwb/ultra-wideband

[64] Saou-Wen Su and Fa-Shian Chang, "A Bent, Shorted, Planar Monopole Antenna for 2.4 GHz WLAN Applications," *Microwave and Optical Technology Letters*, Vol. 51, No. 2, pp. 455-457, February 2009.

[65] Kyung-Sup Kwak and Sun-Ho Choi, "Horseshoe-Shaped Antenna for Dual-Band WLAN Communications with Multi-L Slots," *Microwave and Optical Technology Letters*, Vol. 51, No. 2, pp. 463-465, February 2009.

[66] Meng-Ju Chiang, Sen Wang, and Chun-Chieh Hsu, “Compact Multi-Frequency Slot Antenna Design Incorporating Embedded Arc-Strip,” *IEEE Antennas and Wireless Propagation Letters*, Vol. 11, pp. 834-837, 2012.

[67] Chun-Cheng Lin, Chih-Yu Huang, and Guan-Han Chen, “Obtuse Pie-Shaped Quasi-Self-Complementary Antenna for WLAN Applications,” *IEEE Antennas and Wireless Propagation Letters*, Vol. 12, pp. 353-355, 2013.

[68] Long Zheng and Guangming Wang, “Design of Triple-Frequency Folded Slot Antenna for 2.4/3.5/5.2/5.8-GHz WLAN Applications,” *Progress in Electromagnetics Research Letters*, Vol. 43, pp. 115-123, 2013.

[69] W. Ren, “Compact Dual-Band Slot Antenna for 2.4/5 GHz WLAN Applications,” *Progress in Electromagnetics Research* B, Vol. 8, pp. 319–327, 2008.

[70] Siddik Cumhur Basaran and Yunus E. Erdemli, “A Dual-Band Split-Ring Monopole Antenna for WLAN Applications,” *Microwave and Optical Technology Letters*, Vol. 51, No. 11, pp. 2685-2588, November 2009.

[71] W.-C. Liu, “Optimal Design of Dualband CPW-Fed G-Shaped Monopole Antenna for WLAN Application,” *Progress In Electromagnetics Research, PIER* 74, pp. 21–38, 2007.

[72] Yue Song, Yong Chang Jiao, Tian Ling Zhang, Zi Bin Weng, and Fu Shun Zhang, “Compact Multiband Printed Antenna for Wireless Applications,” *Microwave and Optical Technology Letters*, Vol. 51, No. 3, pp. 669-671, March 2009.

[73] Wen-Chung Liu, “Broadband Dual-Frequency CPW-Fed Antenna with a Cross Shaped Feeding Line for WLAN Application,” *Microwave and Optical Technology Letters*, Vol. 49, No. 7, pp. 1739-1744, July 2007.

[74] Xiaowei Zhang , Jingyun Zhang, Runbo Ma, Xinwei Chen and Wenmei Zhang, “Compact Dual-Frequency Linear Antenna with Partial Ground Plane,” *International Journal of Electronics*, Vol. 96, No. 12, pp. 1309–1315, December 2009.

[75] Xiaodi Song, “Small CPW-Fed Triple Band Microstrip Monopole Antenna for WLAN Applications,” *Microwave and Optical Technology Letters*, Vol. 51, No. 3, pp. 747-749, March 2009.

[76] Yue Song, Yong-Chang Jiao, Hui Zhao, Zheng Zhang, Zi-Bin Weng, and Fu-Shun Zhang, “Compact Printed Monopole Antenna for Multiband WLAN Applications,” *Microwave and Optical Technology Letters*, Vol. 50, No. 2, pp. 365-367, February 2008.

[77] T.H. Kim and D.C. Park, “CPW-Fed Compact Monopole Antenna for Dual-Band WLAN Applications,” *Electronics Letters*, Vol. 41, No. 6, March 2005.

[78] Saou-Wen Su, Jui-Hung Chou, and Yung-Tao Liu, “A One-Piece Flat-Plate Dipole Antenna for Dual-Band WLAN Operation,” *Microwave and Optical Technology Letters,* Vol. 50, No. 3, pp. 678-680, March 2008.

[79] Mahesh P. Abegaonkar, Yatinder Chhikara, Ananjan Basu and Shibon Koul, “Tapered-CPW Fed Printed Triangular Monopole Antenna,” *Eucap 2006,in Proc. First European Conference on Antennas and Propagation,* 2006.

[80] Zied Harouni, Lotfi Osman, and Ali Gharsallah, “Efficient 2.45 GHz CPW Patch Antenna Including Harmonic Rejecting Device for Wireless Power Transmission,” *IEEE 8th International Multi-Conference On Systems, Signals and Devices*, 2011.

[81] Y.-J. Wu, J.-W. Fan, and B.-H. Sun, “Dual-Band Omni-Directional Antenna for WLAN Application,” *Microwave and Optical Technology Letters,* Vol. 50, No. 5, pp. 1328-1330, May 2008.

[82] Jian-Hui Gu, Shun-Shi Zhong, Ling-Long Xue, and Zhu Sun, “Dual-Band Monopole Antenna with L-Shaped Strips for 2.4/5 GHz WLAN Applications,” *Microwave and Optical Technology Letters,* Vol. 50, No. 11, pp. 2830-2833, November 2008.

[83] Yue Song, Yong Chang Jiao, Xiao Ming Wang, Zi Bin Weng, and Fu Shun Zhang, “Compact Coplanar Slot Antenna Fed By Asymmetric Coplanar Strip for 2.4/5 GHz WLAN Operations,” *Microwave and Optical Technology Letters*, Vol. 50, No. 12, pp. 3080-3083, December 2008.

[84] Tae-Hyun Kim and Dong-Chul Park, “Compact Dual-Band Antenna with Double L-Slits for WLAN Operations,” *IEEE Antennas and Wireless Propagation Letters*, Vol. 4, pp. 249-252, 2005.

[85] Zheng Zhang, Yong Chang Jiao, Yue Song, Tian Ling Zhang, Shu Man Ning, and Fu Shun Zhang, “A Modified CPW-Fed Monopole Antenna with very Small Ground for Multiband WLAN Applications,” *Microwave and Optical Technology Letters,* Vol. 52, No. 2, pp. 463-465, February 2010.

[86] C. M. Wu, “Dual-Band CPW-Fed Cross-Slot Monopole Antenna for WLAN Operation,” *IET Microwave Antennas Propagation*, Vol. 1, Issue-2, pp. 542–546, 2007.

[87] Jia-Yi Sze, Chung-I G. Hsu, and Sheng-Chin Hsu, "Design of a Compact Dual-Band Annular-Ring Slot Antenna," *IEEE Antennas and Wireless Propagation Letters*, Vol. 6, pp. 423-426, 2007.

[88] A. K. Arya, A. Patnaik, and M. V. Kartikeyan, "Microstrip Patch Antenna with Skew-F Shaped DGS for Dual Band Operation," *Progress in Electromagnetics Research M*, Vol. 19, pp. 147-160, 2011.

[89] J.-Y. Sze, T.-H. Hu and T.-J. Chen, "Compact Dual-Band Annular-Ring Slot Antenna with Meandered Grounded Strip," *Progress in Electromagnetics Research*, *PIER* 95, pp. 299-308, 2009.

[90] J. G. Joshi, Shyam S. Pattnaik, and S. Devi, "Metamaterial Embedded Wearable Rectangular Microstrip Patch Antenna," *International Journal of Antennas and Propagation*, Volume 2012, Article ID 974315, 2012.

[91] Wen-Shan Chen and Yu-Chen Chang, "CPW-Fed Printed Monopole Antenna with Branch Slits for WiMAX Applications*," Microwave and Optical Technology Letters*, Vol. 50, No. 4, pp. 952-954, April 2008.

[92] Peng-Yu Lai and Kin-Lu Wong, "Capacitively Fed Hybrid Monopole Slot Chip Antenna for 2.5/3.5/5.5 GHz WiMAX Operation in the Mobile Phone," *Microwave and Optical Technology Letters*, Vol. 50, No. 10, pp. 2689-2694, October 2008.

[93] Jui-Han Lu and Bing-Jhang Huang, "Planar Compact Slot Antenna with Multi-Band Operation for IEEE 802.16m Application," *IEEE Transactions on Antennas and Propagation*, Vol. 61, No. 3, pp. 1411-1413, March 2013.

[94] Wen-Shan Chen and Yen-Hao Yu, "The Design of Printed Rhomb Shaped Antenna with Slits for WiMAX Systems," *Microwave and Optical Technology Letters*, Vol. 49, No. 10, pp. 2503-2508, October 2007.

[95] Wen-Shan Chen, Yu-Chen Chang, and Fa-Shian Chang, "Novel Design of Printed Monopole Antenna for WiMAX Application," *Microwave and Optical Technology Letters*, Vol. 49, No. 8, pp. 1806-1809, August 2007.

[96] Nan Chang, "Circularly Polarized Antenna For 2.3–2.7 GHz WiMAX Band," *Microwave and Optical Technology Letters*, Vol. 51, No. 12, pp. 2921-2923, December 2009.

[97] J. P. Geng, J. J. Li, R. H. Jin, S. Ye, X. L. Liang and M. Z. Li, "The Development of Curved Microstrip Antenna with Defected Ground Structure," *Progress in Electromagnetics Research*, *PIER* 98, pp. 53-73, 2009.

[98] Qing-Xin Chu and Liang-Hua Ye, “Design of Compact Dual-Wideband Antenna with Assembled Monopoles,” *IEEE Transactions on Antennas and Propagation*, Vol. 58, No. 12, pp. 4063-4066, December 2010.

[99] Lin Dang, Zhen Ya Lei, Yong Jun Xie, Gao Li Ning, and Jun Fan, “A Compact Microstrip Slot Triple-Band Antenna for WLAN/WiMAX Applications,” *IEEE Antennas and Wireless Propagation Letters*, Vol. 9, pp. 1178-1181, 2010.

[100] Bin Yuan, Peng Gao, Shuang He, Liang Xu, and Hai Tao Guo, “A Novel Triple-Band Rectangular Ring Antenna with Two L-Shaped Strips for WiMAX and WLAN Applications,” *Progress in Electromagnetics Research* C, Vol. 40, pp. 15-24, 2013.

[101] Liang Dong, Zhiya Zhang, Guang Fu, and Meng Su, “A Compact Microstrip Slot Antenna with a Pair of Inverted L-Strips and Elliptical-Arc-Shaped Stub for WLAN/WiMAX Applications,” *Progress in Electromagnetics Research C*, Vol. 40, pp. 131-141, 2013.

[102] Jing Pei, An-Guo Wang, Shun Gao, and Wen Leng, “Miniaturized Triple-Band Antenna with a Defected Ground Plane For WLAN/WiMAX Applications,” *IEEE Antennas and Wireless Propagation Letters*, Vol. 10, pp. 298-301, 2011.

[103] Yogesh Kumar Choukiker and Santanu Kumar Behera, “Compact Sectoral Fractal Planar Monopole Antenna for Wideband Wireless Applications,” *Microwave and Optical Technology Letters*, Vol. 56, No. 5, pp. 1073-1076, May 2014.

[104] Hong Chen, X. Yang, Y. Z. Yin, S. T. Fan, and J. J. Wu, “Tri-Band Planar Monopole Antenna with Compact Radiator for WLAN/WiMAX Applications,” *IEEE Antennas and Wireless Propagation Letters*, Vol. 12, pp. 1440-1443, 2013.

[105] Y. Song, Y.-C. Jiao, G. Zhao, and F.-S. Zhang, “Multiband CPW-Fed Triangle-Shaped Monopole Antenna for Wireless Applications,” *Progress in Electromagnetics Research, PIER 70*, pp. 329–336, 2007.

[106] Lin C. Tsai, “Design of Triple-Band T–U Shaped CPW-Fed Slot Antennas,” *Microwave and Optical Technology Letters*, Vol. 56, No. 4, pp. 844-848, April 2014.

[107] Deepti Das Krishna, M. Gopikrishna, C. K. Anandan, P. Mohanan, and K. Vasudevan, “CPW-Fed Koch Fractal Slot Antenna for WLAN/WiMAX Applications,” *IEEE Antennas and Wireless Propagation Letters*, Vol. 7, pp. 389-392, 2008.

[108] Ayman A. R. Saad, Elsayed E. M. Khaled, and Deena A. Salem, “Wideband Slotted Planar Antenna with Defected Ground Structure,” *PIERS Proceedings, Suzhou, China*, September 2011, pp. 1092-1097.

[109] Wen-Chung Liu, Chao-Ming Wu, and Nien-Chang Chu, “A Compact CPW-Fed Slotted Patch Antenna for Dual-Band Operation,” *IEEE Antennas and Wireless Propagation Letters*, Vol. 9, pp.-110-113, 2010.

[110] Junjun Wang and Xudong He, “Analysis and Design of a Novel Compact Multiband Printed Monopole Antenna,” *International Journal of Antennas and Propagation*, Volume 2013, Article ID 694819.

[111] Chien-Yuan Pan, Tzyy-Sheng Horng, Wen-Shan Chen, and Chien-Hsiang Huang, “Dual Wideband Printed Monopole Antenna for WLAN/WiMAX Applications,” *IEEE Antennas and Wireless Propagation Letters,* Vol. 6, pp. 149-151, 2007.

[112] Pingan Liu, Yanlin Zou, Baorong Xie, Xianglong Liu, and Baohua Sun, “Compact CPW-Fed Tri-Band Printed Antenna with Meandering Split-Ring Slot for WLAN/WiMAX Applications,” *IEEE Antennas and Wireless Propagation Letters*, Vol. 11, pp. 1242-1244, 2012.

[113] Y.-C. Lee and J.-S. Sun, “Compact Printed Slot Antennas for Wireless Dual and Multi-Band Operations,” *Progress in Electromagnetics Research*, *PIER 88,* pp. 289–305, 2008.

[114] T. Shanmuganantham, K. Balamanikandan, and S. Raghavan, “CPW-Fed Slot Antenna for Wideband Applications,” *International Journal of Antennas and Propagation*, Volume 2008, Article ID 379247, 2008.

[115] Liang-Hua Ye and Qing-Xin Chu, “Compact Dual-Wideband Antenna for WLAN/WiMAX Applications,” *Microwave and Optical Technology Letters*, Vol. 52, No. 6, pp. 1228-1231, June 2010.

[116] Shan Shan Huang, Jun Li, and Jian Zhong Zhao, “Design of a Compact Triple-Band Monopole Planar Antenna for WLAN/WiMAX Applications,” *Progress in Electromagnetics Research C*, Vol. 48, pp. 29-35, 2014.

[117] Hsien-Wen Liu, Chia-Hao Ku, and Chang-Fa Yang, “Novel CPW-Fed Planar Monopole Antenna for WiMAX/WLAN Applications,” *IEEE Antennas and Wireless Propagation Letters*, Vol. 9, pp. 240-243, 2010.

[118] Qiu-Yi Zhang and Qing-Xin Chu, “Triple-Band Dual Rectangular Ring Printed Monopole Antenna for WLAN/WiMAX Applications,” *Microwave and Optical Technology Letters*, Vol. 51, No. 12, pp. 2845-2847, December 2009.

[119] Huiqing Zhai, Zhihui Ma, Yu Han, and Changhong Liang, “A Compact Printed Antenna for Triple-Band WLAN/WiMAX Applications,” *IEEE Antennas and Wireless Propagation Letters,* Vol. 12, pp. 65-68, 2013.

[120] Y. Y. Cui, Y.Q. Sun, H. C. Yang, and C. L. Ruan, “A New Triple-Band CPW-Fed Monopole Antenna for WLAN and WiMAX Applications,” *Progress in Electromagnetics Research M,* Vol. 2, pp. 141–151, 2008.

[121] Hong Chen, Ying-Zeng Yin, and Jian-Jun Wu, “Compact Tri-Band Meandered Ring Monopole Antenna with Two Embedded Strips For WLAN/WiMAX Applications,” *Progress in Electromagnetics Research Letters*, Vol. 45, pp. 63-67, 2014.

[122] Mohsen Koohestani, and Mohsen Golpour, “Compact Rectangular Slot Antenna with a Novel Coplanar Waveguide Fed Diamond Patch for Ultra Wideband Applications,” *Microwave and Optical Technology Letters*, Vol. 52, No. 2, pp. 331-334, February 2010.

[123] S. S. Karimabadi and A. R. Attari, “Compact and Ultra Wideband Printed Elliptical Monopole Antenna with Modified-Shape Ground Plane,” *Microwave and Optical Technology Letters*, Vol. 51, No. 11, pp. 2604-2607, November 2009.

[124] Anil Kr Gautam, Swati Yadav, and Binod Kr Kanaujia, “A CPW-Fed Compact UWB Microstrip Antenna,” *IEEE Antennas and Wireless Propagation Letters*, Vol. 12, pp. 151-154, 2013.

[125] M. Meloui, I. Akhchaf, M. Bassouh, M. Nabil Srifi and M. Essaaidi, “A Compact Multi-Band Antenna for Multi-Standard Wireless and Mobile Communication Technologies,” *International Journal of Microwave and Optical Technology*, Vol.7, No. 1, 2012.

[126] Kuiwen Xu, Zhongbo Zhu, Huan Li, Jiangtao Huangfu, Changzhi Li, and Lixin Ran, “A Printed Single-Layer UWB Monopole Antenna with Extended Ground Plane Stubs,” *IEEE Antennas and Wireless Propagation Letters*, Vol. 12, pp. 237-2240, 2013.

[127] K.P. Ray and S. Tiwari, “Ultra Wideband Printed Hexagonal Monopole Antennas,” *IET Microwave and Antennas Propagation,* Vol. 4, Issue 4, pp. 437–445, 2010.

[128] H. Wang and H. Zhang, “A CPW-Fed Ultra-Wideband Planar Inverted Cone Antenna,” *Progress in Electromagnetics Research C*, Vol. 12, pp. 101-112, 2010.

[129] Wen-Tsan Chung, Ching-Her Lee, and Chow-Yen-Desmond Sim, “Compact Monopole Antenna Design for WLAN/UWB Applications,” *Microwave and Optical Technology Letters*, Vol. 51, No. 12, pp.-2874-2878, December 2009.

[130] Sang Yong Park, Seon Jeong Oh, and Jong Kweon Park, “Dual-Band Antenna for WLAN/UWB Applications,” *Microwave and Optical Technology Letters*, Vol. 52, No. 10, pp.-2188-2191, October 2010.

[131] Ji Hae Kim, Jung Nam Lee, and Jong Kweon Park, “Triple-Band Antenna with Slots for PCS/WLAN/UWB Applications,” *Microwave and Optical Technology Letters*, Vol. 52, No. 11, pp. 2540-2544, November 2010.

[132] Ali Foudazi, Hamid Reza Hassani, and Sajad Mohammad Ali Nezhad, “Small UWB Planar Monopole Antenna with Added GPS/GSM/WLAN Bands,” *IEEE Transactions on Antennas and Propagation*, Vol. 60, No. 6, pp. 2987-2992, June 2012.

[133] Kwok L. Chung, T. H. Mak, and W. Y. Tam, “A Modified Two-Strip Monopole Antenna for Wi-Fi and WiMAX Applications,” *Microwave and Optical Technology Letters*, Vol. 51, No. 12, pp. 2884-2887, December 2009.

[134] Sudhanshu Verma, and Preetam Kumar, “Printed Egg Curved Slot Antennas for Wideband Applications,” *Progress in Electromagnetics Research B*, Vol. 58, pp. 111-121, 2014.

[135] Bahadir S. Yildirim, Bedri A. Cetiner, Gemma Roquet, and Luis Jofre, “Integrated Bluetooth and UWB Antenna,” *IEEE Antennas and Wireless Propagation Letters*, Vol. 8, pp. 149-152, 2009.

[136] Mehdi Rahanandeh, Amir Saman Noor Amin, Matin Hosseinzadeh, Pejman Rezai, and Mohammad Sadegh Rostami, “A Compact Elliptical Slot Antenna for Covering Bluetooth/WiMAX/WLAN/ITU,” *IEEE Antennas and Wireless Propagation Letters*, Vol. 11, pp. 857-860, 2012.

[137] R. Zaker, Ch. Ghobadi, and J. Nourinia, “A Modified Microstrip-Fed Two-Step Tapered Monopole Antenna for UWB and WLAN Applications,” *Progress in Electromagnetics Research, PIER 77*, pp. 137–148, 2007.

[138] Sumana Kumari and Nisha Gupta, "Multi-Segment MPA with T-Feed For Multi-Band Wireless Communication," *International Journal Of Electronics*, Vol. 99, No. 4, pp. 491-501, April 2012.

[139] Macro A. Antoniades, and George V. Eleftheriades, "A Compact Multiband Monopole Antenna with a Defected Ground Plane," *IEEE, Antennas and Wireless Propagation Letters*, Vol.7, pp. 2008.

[140] A. K. Arya, A. Patnaik, and M. V. Kartikeyan, "Microstrip Patch Antenna with Skew-F Shaped DGS for Dual Band Operation," *Progress in Electromagnetics Research M*, Vol. 19, pp. 147-160, 2011.